HYDROGEN AND POLY-BETA HYDROXY BUTYRIC ACID PRODUCTION AND EXPRESSION ANALYSES OF RELATED GENES IN *RHODOBACTER CAPSULATUS* AT DIFFERENT ACETATE CONCENTRATIONS

A THESIS SUBMITTED TO
THE GRADUATE SCHOOL OF NATURAL AND APPLIED SCIENCES
OF
MIDDLE EAST TECHNICAL UNIVERSITY

BY

BURCU ÖZSOY

IN PARTIAL FULFILLMENT OF THE REQUIREMENTS
FOR
THE DEGREE OF MASTER OF SCIENCE
IN
BIOLOGY

FEBRUARY, 2012

Approval of the thesis:

HYDROGEN AND POLY-BETA HYDROXY BUTYRIC ACID PRODUCTION AND EXPRESSION ANALYSES OF RELATED GENES IN RHODOBACTER CAPSULATUS AT DIFFERENT ACETATE CONCENTRATIONS

submitted by **BURCU ÖZSOY** in partial fulfillment of the requirements for the degree of **Master of Science in Biology Department, Middle East Technical University** by,

Prof. Dr. Canan Özgen _____
Dean, Graduate School of **Natural and Applied Sciences**

Prof. Dr. Musa Doğan _____
Head of Department, **Biology**

Prof. Dr. Ufuk Gündüz _____
Supervisor, **Biology Dept.**, **METU**

Assist. Prof. Dr. Gökhan Kars _____
Co-supervisor, **Biology Dept., Selçuk University**

Examining Committee Members:

Prof. Dr. Meral Yücel _____
Biology Dept., METU

Prof. Dr. Ufuk Gündüz _____
Biology Dept., METU

Prof. Dr. İnci Eroğlu _____
Chemical Engineering Dept., METU

Assoc. Prof. Dr. Ayşegül Gözen _____
Biology Dept., METU

Assist. Prof. Dr. Gökhan Kars _____
Biology Dept., Selçuk University

Date: 10.02.2012

I hereby declare that all information in this document has been obtained and presented in accordance with academic rules and ethical conduct. I also declare that, as required by these rules and conduct, I have fully cited and referenced all material and results that are not original to this work.

Name, Last name: Burcu Özsoy

Signature :

ABSTRACT

HYDROGEN AND POLY-BETA HYDROXY BUTYRIC ACID PRODUCTION AND EXPRESSION ANALYSIS OF RELATED GENES IN *RHODOBACTER CAPSULATUS* AT DIFFERENT ACETATE CONCENTRATIONS

Özsoy, Burcu

M.Sc., Department of Biology
Supervisor: Prof. Dr. Ufuk Gündüz
Co-supervisor: Assist. Prof. Dr. Gökhan Kars

February 2012, 141 pages

Hydrogen, which is a clean energy source, is one of the alternatives for fossil fuels. Biological hydrogen production is one of the hydrogen production methods. *Rhodobacter capsulatus* is a photosynthetic bacterium that produces hydrogen via photofermentation. *R. capsulatus* can also synthesize some valuable by-products such as Poly-beta- hydroxy butyric acid (PHB), which is a biodegradable bioplastic.

In a two stage biohydrogen production system, which is combination of dark fermentation and photofermentation, dark fermentor effluents are used for photofermentation by *R.capsulatus*. Dark fermentor effluents usually contain high amount of acetate. High amount of acetate may decrease the efficiency of hydrogen

production by causing high amount of PHB production. Therefore, it is significant to determine optimum acetate concentration for photofermentation.

In this study, the effects of acetate concentration on hydrogen and PHB production by *R.capsulatus* were investigated by growing bacteria at various acetate concentrations (10 mM-65 mM). In addition, gene expression analysis was performed to investigate the effects of acetate at transcriptional level. For this purpose, expression levels of the genes that encode nitrogenase which is the enzyme that catalyzes hydrogen production and PHB synthase, which is the key enzyme of the PHB synthesis pathway, are examined.

Optimum acetate concentration for photofermentation with high hydrogen yield and low PHB amount was determined to be in the range 25 mM-50 mM. *nifD* expression was found to be high at optimum acetate concentrations and *phaC* expression was found to be the highest at 65 mM.

Keywords: *Rhodobacter capsulatus,* biohydrogen, poly-β-hydroxybutyric acid, nifD, phaC

ÖZ

FARKLI ASETAT KONSANTRASYONLARINDA *RHODOBACTER CAPSULATUS'UN* POLY- BETA HİDROKSİ BÜTİRİK ASİT VE HİDROJEN ÜRETİMİ VE İLGİLİ GEN İFADELERİNİN İNCELENMESİ

Özsoy, Burcu

M.Sc., Biyoloji Bölümü
Tez Yöneticisi: Prof. Dr. Ufuk Gündüz
Ortak Tez Yöneticisi: Yrd. Doç. Dr. Gökhan Kars

Şubat 2012, 141 sayfa

Temiz bir enerji kaynağı olan hidrojen fosil yakıtlarına alternatif bir enerji kaynağı olmaktadır. Biyolojik hidrojen üretimi hidrojen üretim yöntemlerinden biridir. *Rhodobacter capsulatus* photofermentasyon yoluyla hidrojen üreten fotosentetik bir bakteridir. Aynı zamanda parçalanabilir bir biyoplastik olan Poly-beta-hidroksi bütirik asit (PHB) gibi yararlı yan ürünler de üretebilmektedir.

Karanlık fermentasyon ve fotofermentasyon aşamalarından oluşan iki aşamalı hidrojen üretim sistemlerinde, karanlık fermentasyon çıktısı olan atık su fotofermentasyon için kullanılmaktadır. Karanlık fermantasyon atık suları genellikle yüksek düzeyde asetat içermektedir. Asetat PHB sentezi için iyi bir kaynak olduğundan yüksek düzeydeki asetat PHB üretimini artırarak hidrojen üretim verimini düşürebilir.

Bu yüzden, fotofermentasyon için optimum asetat konsantrasyonunun belirlenmesi önemlidir.

Bu çalışmada, *R.capsulatus* hücreleri farklı asetat konsantrasyonlarında üretilerek asetat konsantrasyonunun hidrojen ve PHB üretimine etkisi hem fizyolojik hem de gen ifade düzeyinde incelenmiştir. Nitrojenaz hidrojen üretiminde, PHB sentaz is PHB üretiminde rol alan temel enzimlerdir. *R.capsulatus*'da *nifD* nitrojenaz enziminin alt birimlerinden birini kodlayan, *phaC* ise PHB sentaz enzimini kodlayan genlerdir. Bahsi geçen bu genler gen ifadesi analizleri için uygun görülmüştür.

Elde edilen bulgulara göre düşük PHB ve yüksek hidrojen üretimi olabilmesi için optimum asetat konsantrasyonu 25-50 mM olarak belirlenmiştir. *nifD* geninin optimum asetat konsantrasyonlarında iyi ifade edildiği, *phaC* ifade düzeyinin ise 65 mM'da en yüksek olduğu görülmüştür.

Anahtar kelimeler: *Rhodobacter capsulatus,* biyohidrojen, Poly-beta hidroksi bütirik asit, nifD, phaC

To my family,

ACKNOWLEDGEMENTS

I would like to express my deepest gratitude to my supervisor Prof. Dr. Ufuk Gündüz for her guidance and advice throughout this study. I also would like thank to Prof. Dr. Meral Yücel and Prof. Dr. İnci Eroğlu for their helpful support during this study.

I am deeply grateful to Assist. Prof. Dr. Gökhan Kars for his continual guidance, advice and support throughout the study. I also would like to thank to Assist. Prof. Dr. Başar Uyar and Dr. Ebru Özgür for their helpful comments.

I also feel great appreciation to examining committee member Assoc. Prof. Dr. Ayşegül Gözen for her participation and for her valuable comments.

I would like to show my gratitude to Pelin Sevinç, Nilüfer Afşar, Endam Özkan and Gülşah Pekgöz for their support, friendship and valuable suggestions throughout the study. I am grateful to my dear friends Gülistan Tansık, Tuğba Keskin and Zelha Nil for their support, friendship and suggestions. I would like to give my special thanks to Ahu İzgi and Çağrı Urfalı for their friendship and support. I also thank to Lab 206 members: Yaprak Dönmez, Esra Kaplan, Neşe Çakmak, Aktan Alpsoy, Murat Erdem, Okan Tezcan, Çiğdem Şener, Rouhollah Khodadust, Gözde Ünsoy. I would also like to thank to members of METU Biohydrogen group: Gökçe Avcıoğlu, Dominic Deo Androga, Muazzez Gürgan, Efe Boran, Görkem Baysal, Begüm Peksel and Emrah Sağır for their help. I would like to give my special thanks to Sevilay Akköse for answering all my questions whenever I need help and for allowing me to use the primer designed by her.

I am deeply grateful to my close friends Kübra Gürtaş and Nejla Yıldırım for their valuable friendship throughout my life.

Lastly, I owe my deepest gratitude to my mother Ayşıl Özsoy, my father Feyzi Özsoy and my brother Aykut Özsoy for their endless love, care and for their patience throughout this study. This thesis would not have been possible without their support. I would like to give my special thanks to my dear sister-in-law Aysu Özsoy for her kindness and suggestions.

This study was supported by 6th frame European Union Project ”Hyvolution”, and BAP project with number of BAP-07-02-2010-00-01.

TABLE OF CONTENTS

LIST OF TABLES

TABLES

LIST OF FIGURES

FIGURES

LIST OF ABBREVIATIONS

A	Irradiated area (m^2)
Acetyl-CoA	Acetyl Coenzyme A
ATP	Adenosine triphosphate
BP	Biebl and Pfenning
cDNA	Complementary DNA
CO_2	Carbondioxide
CO	Carbonmonoxide
DEPC	Diethylpyrocarbonate
DBI	Density of band intensity
EtBr	Ethidium bromide
e	Constant (2.718282)
Fd	Ferrodoxin
FID	Flame ionization detector
Fe	Iron
GC	Gas chromatography
gdw	Gram dry weight
H_2	Hydrogen
$H_{max,e}$	Experimental maximum cumulative hydrogen production (mmoles)
$H_{max,m}$	Maximum cumulative hydrogen production obtained from Modified Gompertz Model (mmoles)
HPLC	High Performance Liquid Chromatography
k_0	Rate constant for zero order reaction
k_1	Rate constant for first order reaction
k_2	Rate constant for second order reaction
mmole	Millimole
mM	Millimolar

n	Order of the reaction
nifD	Nitrogen fixation gene D
NCBI	National Center of Biotechnology Information
OD	Optical density
PCR	Polymerase Chain Reaction
phaC	PHA synthase gene
PHA	Polyhydroxyalkonate
PHB	Poly-β-hydroxy butyric acid
PNS	Purple non-sulfur bacteria
PS	Photosystem
r	Extent of the fit
R^2	Coefficient of determination value
R.capsulatus	*Rhodobacter capsulatus*
R.palustris	*Rhodobacter palustris*
R.rubrum	*Rhodospirillum rubrum*
R. sphaeroides	*Rhodobacter sphaeroides*
R.eutropha	*Ralstonia eutropha*
RT-PCR	Reverse Transcriptase – Polymerase Chain Reaction
TCA	Citric Acid Cycle
$X_{0,e}$	Experimental initial bacteria concentration (gdw/L)
$X_{o,m}$	Maximum bacterial concentration obtained by Logistic Model (gdw/L)
$\lambda_{,e}$	Experimental lag time (h)
$\lambda_{,m}$	Lag time obtained from Modified Gompertz Model (h)
μ	Specific growth rate
16S rRNA	16S ribosomal RNA

CHAPTER 1

INTRODUCTION

1.1 Hydrogen Energy

Fossil fuels supply 80 % of world energy requirement (Das and Veziroğlu, 2001). However, it is believed that inadequate fossil fuel resources will be consumed in the future (Hallenbeck et al., 2009). Therefore an alternative energy source is required to fulfill future energy need. Furthermore, cleaner energy sources should be found since fossil fuels are harmful to the environment (Das and Veziroğlu, 2001). In combustion of fossil fuels, greenhouse gasses (CO_2, CH_4, N_2O etc.) and many other pollutants (SO_x, CO, heavy metals etc) are released (Das and Veziroğlu, 2001, Momirlan and Veziroğlu, 2002). Therefore, alternative energy sources, which are renewable and environmentally friendly, must be found for the world's future. Hydrogen, the lightest and plentiful element in the universe, is considered to be future energy source. It is regarded as a clean non-polluting fuel since water is the main product when it is burned (Das and Veziroğlu, 2001). Among the many hydrogen production methods, photobiological hydrogen production, which is hydrogen production by biological systems, is accepted as potentially environmentally production method since it is renewable using the primary energy source, sunlight and does not release carbon dioxide during combustion (Asada and Miyake, 1999).

1.2 Hydrogen Production Methods

Apart from being clean and alternative future energy carrier, hydrogen has many areas of useage. For instance, it can be used as the fuel for direct combustion in an internal combustion engine or as the fuel for a fuel cell (Das and Veziroğlu, 2008). In addition to those, hydrogen is mainly used in petroleum refining and petrochemical industries for ammonia and methanol synthesis (Kothari et al., 2008).

Hydrogen can be produced mostly from fossil fuels, water and biomass (Dasand Veziroğlu, 2001). The major resources of presently used hydrogen production methods and their percentages are given in Figure 1.1.

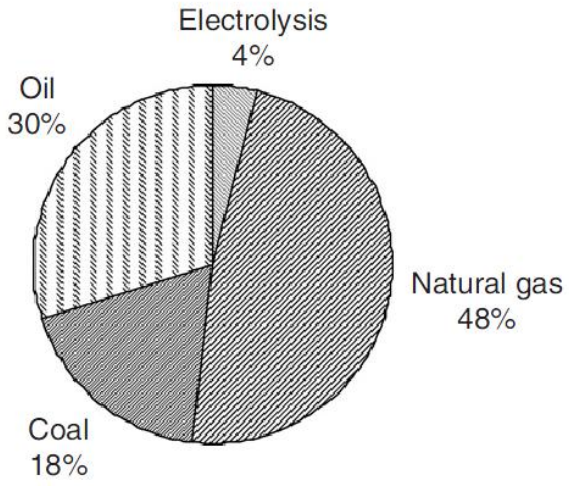

Figure 1.1 Percentages of the major resources of hydrogen production methods (Kothari et al., 2008).

Most of the hydrogen is produced by steam reforming of natural gas which is extensively methane (Kothari et al., 2008; Momirlan and Veziroğlu, 2002). The reforming of natural gas is a process that produces a gas stream which consists of hydrogen, CO and CO_2 (Holladay et al., 2009). There is a big disadvantage of this process, which is the release of large amounts of CO_2 into the atmosphere (Kothari et.al.2008). Partial oxidation of hydrocarbons is one of the other methods that uses fossil fuels. In this method, hydrocarbons are converted to hydrogen by incomplete combustion of them with oxygen (Holladay et al., 2009). At the end of the reaction, not only CO_2 but also CO is produced which is a crucial disadvantage of the method (Kothari et.al., 2008). Hydrogen is also produced by gassification of coal which is based on partial oxidation of it to a mixture of hydrogen and CO_2 (Holladay et al., 2009; Kothari et.al., 2008).

Additionally, hydrogen is produced by splitting water into hydrogen and oxygen. There are three main methods that seperates water into its simplest forms. The first one is electrolysis in which water is splitted by an electric current passing through two electrodes. The second one is the thermolysis in which heat is used to decompose water in to hydrogen and oxygen. The third one is the photoelectrolysis which uses sunlight to seperate water into hydrogen and oxygen (Holladay et al., 2009). Electrolysis of water is one of the most utilized industrial processes (Momirlan and Veziroğlu, 2002).

In addition to those processes, hydrogen is produced from biomass which can be animal wastes, crop residues, agricultural wastes, corn, tree residues etc. Hydrogen production methods from biomass include: the thermochemical processes which are gassification and pyrolysis; hydrogen production by biological systems (Holladay et al., 2009). The first one pyrolysis is performed by heating biomass at a high temperature in the absence of air to convert it into liquid oil, charcoal and gaseous

compounds. The second one gassification is conducted by gasifying biomass at high temperatures in the presence of oxygen so that biomass particles are subjected to partial oxidation forming charcoal and gaseous products (Ni et al., 2006).

Hydrogen production methods like steam reforming, partial oxidation, water electrolysis and biomass gassification have achieved maturity and have commercially been used while some of the methods are at the research and development stage. (Holladay et al., 2009; Momirlan and Veziroğlu, 2002) (Table 1.1).

Table 1.1 The stage of the major hydrogen production methods. "R" and "D" represents research and development, respectively (Momirlan and Veziroğlu, 2002).

Production process	Status
Steam reforming of natural gas	Mature
Catalytic decomposition of natural gas	Mature
Partial oxidation of heavy oil	Mature
Coal gasification	R and D—Mature
Steam-iron coal gasification	R and D
Water electrolysis	Mature
Thermochemical cycles (pure)	R and D
Thermochemical cycles (hybrid)	R and D
Photochemical processes	Early R and D
Photoelectrochemical processes	Early R and D
Photobiological processes	Early R and D

These commercial methods are energy intensive because they are conducted at high temperatures and pressures (Das and Veziroğlu, 2001). For instance, the non-catalytic partial oxidation of hydrocarbon takes place with flame temperatures of 1300-1500°C to ensure complete conversion (Holladay et al., 2009). Furthermore, these methods are not environmentally friendly since they are generally based on utilization of fossil fuels. On the other hand, biological hydrogen production is a less

energy intensive and an environmentally friendly hydrogen production method (Das and Veziroğlu, 2001).

1.2 Biohydrogen

Biohydrogen production is catalyzed by microorganims in an aqueous environment at ambient temperatures and atmospheric pressure (Das and Veziroğlu, 2008). Although hydrogen yield and production rate is not well enough for practical application, it has many advantages compared to conventional methods (Hallenbeck and Ghosh, 2009). To begin with, in contrast to current hydrogen production technologies, biohydrogen is cheap because it does not require high electricty cost or a metal catalyst. Moreover, other hydrogen production technologies mainly depend on carbon-based nonrenewable energy sources therefore they are not sustainable (Brentner et al., 2010). There are mainly four types biohydrogen production methods. In addition, there are integrated methods which are combinations of two or more biohydrogen production methods. These methods will be explained in detail below. Moreover, an overview of the four main hydrogen production methods including advantages and disadvantages in given in Table 1.2.

Table 1.2 Overview of Biohydrogen Methods Including Organisms, Reactions, Key enzymes, Pros and Cons. Adapted from Brentner et al. (2010).

Mechanism	Organisms	Key enzymes	Pros	Cons
Direct biophotolysis	Green algae, Cyanobacteria	Hydrogenase	H_2 produced from sunlight and water	O_2 sensitivity, bioreactor design challenges to maximize utilization of sunlight, low H_2 production efficiency
Indirect biophotolysis	Cyanobacteria	Hydrogenase nitrogenase	Heterocysts seperate H_2 production from O_2 – evolution within organisms	Bioreactor design challenges to maximize utilization of sunlight
Photofermentation	Purple-nonsulfur bacteria	Nitrogenase	Utilizes energy from sunlight to convert small organic acids or waste organic compounds to H_2 and CO_2	Bioreactor design challenges to maximize utilization of sunlight
Dark Fermentation	Anaerobic bacteria	Dehydrogenases, (fumarate) reductases, hydrogenases	High H_2 production, utilizes waste streams, mixed culture friendly	Many byproducts, intensive biogas seperation to retireve H_2, incomplete substrate utilization/low yields

1.3.1 Biophotolysis

In this method, hydrogen is produced by the microorganisms which seperate water into hydrogen and oxygen by using the absorbed light energy. Green algae and blue green algae (Cyanobacteria) are the organisms that produce hydrogen via direct and indirect biophotolysis.

1.3.2.1 Direct Biophotolysis

Green algae and cynanobacterium which carry out plant-type photosynthesis produce hydrogen via direct photolysis (Hallenbeck and Ghosh, 2009). In this process, light energy absorbed by photosystem (PS) I and II helps to transfer electrons from oxidized water to ferrodoxin. Reduced ferrodoxin serves as an electron donor to hydrogenase that catayzes the reversible reaction which is the conversion of protons (H^+) to molecular hydrogen (Eroğlu and Melis, 2011). The reaction is represented as:

$$2H^+ + 2FD^- \leftrightarrow H_2 + 2FD \qquad (1.1)$$

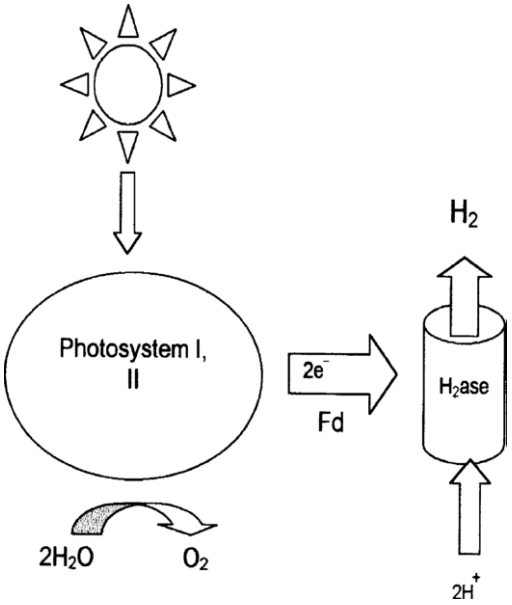

Figure 1.2 The scheme of hydrogen production by direct biophotolysis (Hallenbeck and Benemann, 2002).

Problem of this process is the inhibiton of hydrogenase by O_2, which is produced as a by-product of function of PS II (Eroğlu and Melis, 2011). Therefore, hydrogen production via direct biophotolysis can operate for a short period of time until the accumulated O_2 inactivates the hydrogenase. This problem can be overcome by removing oxygen by purging inert gasses to the reaction mixture or by using O_2 absorbers such as glucose oxidase (Eroğlu and Melis, 2011; Hallenbeck and Benemann, 2002). Another approach is the direction of the cell's own mitochondrial respiration to consume O_2 (Eroğlu and Melis, 2011).

1.3.2.2 Indirect Biophotolysis

In indirect biophotolysis, which is mainly performed by filamentaous cyanobacteria, photosynthetic processes are seperated from hydrogen production temporally or

spatially (Brentner et al., 2010). Filamentaous cyanobacteria may develop into structurally modified and functionally specialized cells, which can perform nitrogen fixation catalyzed by nitrogenase. These specialized cells are called heterocysts. They do not require photosynthetic apparatus as they are fed by neighbouring photosynthetic cells. So during nitrogen fixation in which hydrogen is produced as an obligatory side product, oxygen sensitive nitogenase of heterocysts, is not inhibited by the generated oxygen (Levin at al., 2004; Brentner at al., 2010).

There are also non-heterocystous cynanobacteria which can seperate O_2 and H_2 production in time (temporal seperation) (Dasgupta et al., 2010). The scheme of indirect biophotolysis is given in Figure 1.3.

Cynaobacteria species also posses uptake hydrogenase which catalyze oxidation of hydrogen that is produced by nitrogenase and bi-directional hydrogenases which is capable of both oxidizing and synthesizing H_2 (Levin at al., 2004). Uptake hydrogenases lower hydrogen efficiency so genetic manipulations are done to overcome this problem.

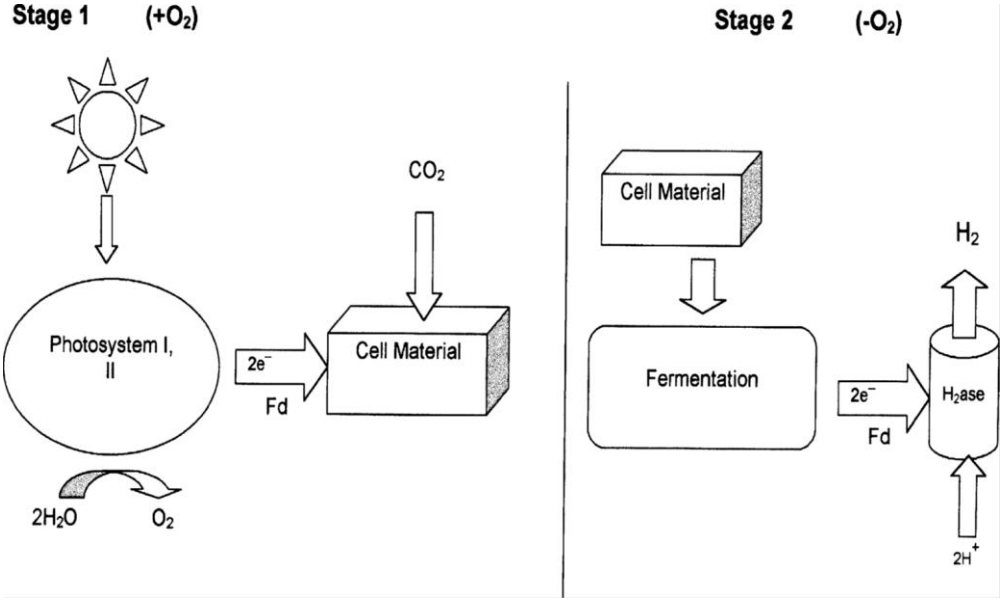

Figure 1.3 The scheme of hydrogen production by indirect biophotolysis (Hallenbeck and Benemann, 2002).

1.3.2 Dark Fermentation

Anaerobic bacteria can produce hydrogen when they are grown under anaerobic conditions and in the dark on carbohydrate- rich substrates (Levin et al.,2004).

When anaerobic bacteria grow on organic substrates, these substrates are broken down by oxidation to provide building blocks and energy for cell growth. The oxidation produces electrons which are removed in order to preserve electrical neutrality. Under anoxic conditions protons act as electron acceptors and are reduced to molecular hydrogen (H_2). In fermentation processes, initial reaction is the conversion of glucose to pyruvate by glycolysis. Then pyruvate is oxidized to acetyl-coA which is converted to acetyl phosphate resulting in formation of ATP and acetate. Oxidation of pyruvate to acetyl-CoA requires reduction of ferrodoxin. Hydrogenase oxidizes reduced ferrodoxin producing Fd(ox) and releasing electrons to produce molecular hydrogen (H_2) (Das and Veziroğlu, 2008).

The scheme of dark fermentation is given in Figure 1.4.

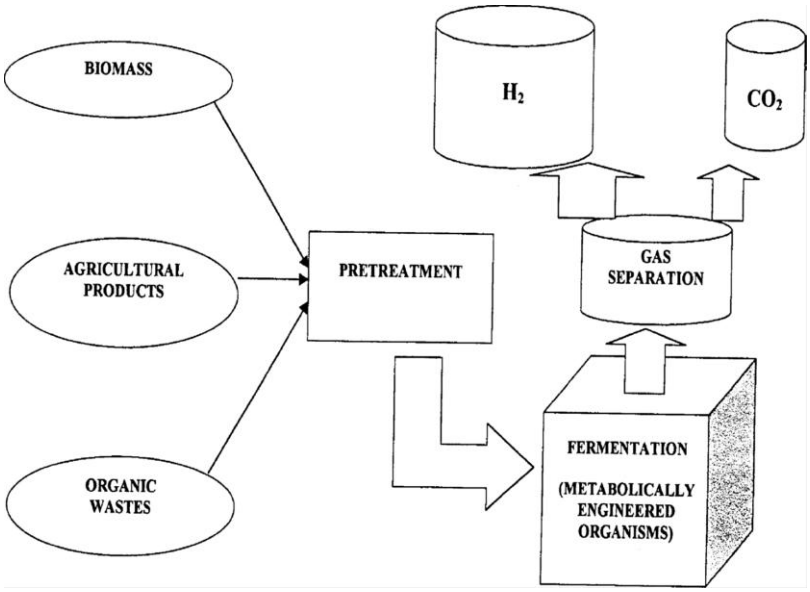

Figure 1.4 The scheme of hydrogen production by dark fermentation (Hallenbeck and Benemann, 2002).

The overall reaction of the process is shown in the equations 1.2 and 1.3.

$$\text{Pyruvate} + \text{CoA} + 2\text{Fd (ox)} \rightarrow \text{acetyl-CoA} + 2\text{Fd} + CO_2 \quad (1.2)$$

$$2\,H^+ + \text{Fd} \rightarrow H_2 + \text{Fd (ox)} \quad (1.3)$$

Preferred carbon sources for fermentation processes are carbohydrates, primarily glucose, which predominantly give rise to acetic acid and butyric acids together with H_2 and CO_2 (Das and Veziroğlu, 2008). The reactions are shown in equations 1.4 and 1.5.

$$C_6H_{12}O_6 + 2H_2O \rightarrow 2CH_3COOH + 2CO_2 + 4H_2 \quad (1.4)$$

$$C_6H_{12}O_6 + 2H_2O \rightarrow CH_3CH_2COOH + 2CO_2 + 2H_2 \quad (1.5)$$

Anaerobic bacteria that produce hydrogen during fermentation are divided into two groups which are strict and facultative anaerobes. *Clostridium* and *Desulfovibrio* belong to strict anaerobes; *Enterobacter, Citrobacter, Klebsiella, Escherichia coli* and *Bacillus* belong to facultative anaerobes (Lee et al.,2010)

One of the advantages of hydrogen production by dark fermentation is the high production rate compared to other biological hydrogen methods (Das and Veziroğlu, 2008; Lee et al., 2010). Another advantage is that fermenting bacteria can use complex forms of organic substrates such as cellulose, food wastes etc. for hydrogen production (Lee et al., 2010).

The most prominent disadvantage of the system is the low hydrogen yield (Hallenbeck and Benemann, 2002; Das and Veziroğlu, 2008; Lee et al., 2010). Based on known fermentation reactions, the theoritical maximum hydrogen yield is only 4 mole H_2/mole glucose (Lee et al., 2010). This is thought to be a natural consequence since fermentations have been optimized by evolution to produce cell biomass other than hydrogen (Hallenbeck and Benemann, 2002). Additionally, in contrast to other biohydrogen methods in which pure hydrogen gas is produced, in dark fermentation mixed biogas, which contains mainly H_2 and CO_2 but also lesser amounts of methane, carbonmonoxide and/or hydrogen sulfide, are produced (Levin et al.,2004). Therefore, a seperation step is required to recover evolved H_2 (Brentner et al.,2010).

1.3.3 Photofermentation

Photofermentation is a mechanism found in a diverse group of photosynthetic bacteria. It is well characterized in purple nonsulfur (PNS) bacteria which produce hydrogen under anaerobic and nitrogen-deficient conditions using light energy and organic substrates as carbon sources. The reaction of hydrogen production from an organic acid is as follows:

$$CH_3COOH + 2H_2O + \text{light energy} \rightarrow 4\ H_2 + 2CO_2 \qquad (1.6)$$

The key enzyme of the process is nitrogenase which is expressed in bacteria that grow on nitrogen deficient conditions. Purple non-sulfur bacteria also posses uptake hydrogenases which convert produced hydrogen to protons and electrons (Brentner et al., 2010; Levin et al., 2004). The scheme of photofermentation is shown in Figure 1.5.

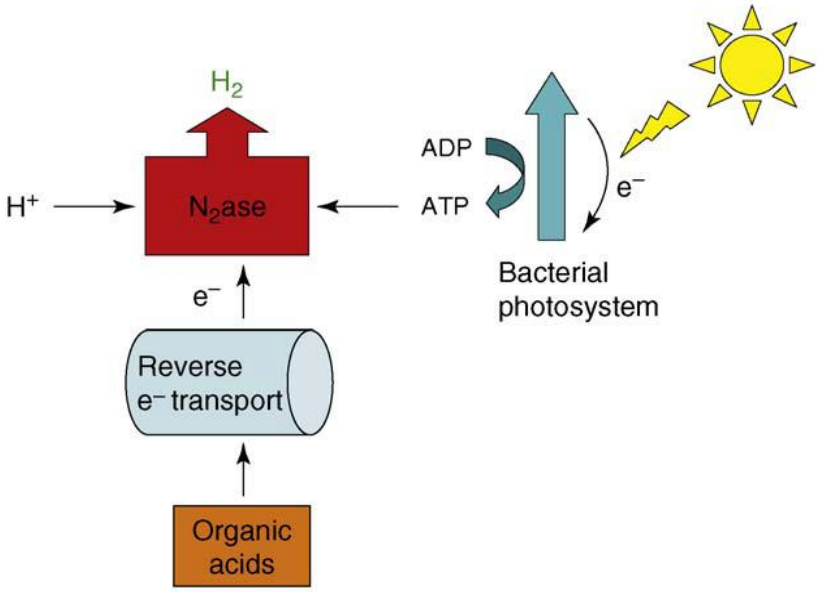

Figure 1.5 The scheme of hydrogen production by photofermentation (Hallenbeck and Ghosh, 2009).

Hydrogen production by PNS bacteria has many advantages over other hydrogen production methods (Das and Veziroglu, 2001; Basak and Das, 2007). The major advantages are listed below:

- high substrate to product conversion yields,
- lack of O_2 evolving activity which causes problem of inactivation of hydrogen producing system in different biological systems (cyanobacteria and green algae),
- ability to use wide spectrum of light,
- ability to consume organic substrates derivable from wastes. Therefore it is also applicable for wastewater treatment.

Hydrogen production by PNS bacteria and properties of them will be explained in detail later.

1.3.4. Integrated Systems

Although biohydrogen is advantageous compared to conventional methods each biological hydrogen production method has its own disadvantages (Table 1.2). In order to overcome challenges of one process, integrated systems can be conducted by combining two or more biological processes. The most common integrated system is the combination of dark fermentation and photofermentation (Brentner et al., 2010). In the first step, in which dark fermentation takes place, a mix of H_2 and CO_2 is produced as anerobic bacteria break down carbohydrates and forms organic acids. In the second step, where photofermentation is conducted, purple non-sulfur bacteria produce H_2 by using light energy and decomposing organic acids that was formed in the first reactor (Brentner et al., 2010). The scheme of the system is given in Figure 1.6.

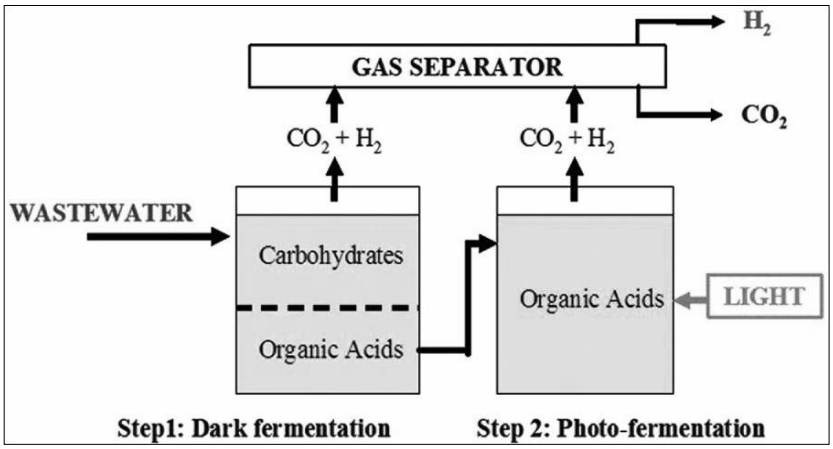

Figure 1.6 The scheme of an integrated system (Hallenbeck et al., 2009).

The therotical yield of integration of these two processes could be 12 moles of hydrogen per mole of glucose. The overall reactions in an integrated system of dark fermentation and prhotofermentation are given in equations 1.7 and 1.8. Small

organic acids are the intermediate metabolites that link the two processes (Eroğlu and Melis, 2011).

Dark fermentation stage:

$$C_6H_{12}O_6 + 2H_2O \rightarrow 2CH_3COOH + 2CO_2 + 4H_2 \quad (1.7)$$

Photofermentation stage:

$$2CH_3COOH + 4H_2O \rightarrow 4CO_2 + 8H_2 \quad (1.8)$$

In this way, complete decompositon of carbohydrates to H_2 and CO_2 is achieved. It was impossible by anaerobic bacteria to break down these small organic acids to H_2 since conversion of them is not an energetically favorable and cannot be achieved by their fermentative metabolism. On the other hand, photosynthetic bacteria are able to overcome the free energy barrier in the consumption of organic acids by utilizing sunlight energy. Additionally, by combining these two processes, light energy demand of photosynthetic bacteria is diminished (Melis and Melnicki, 2006; Das and Vezioğlu, 2001).

Large amounts of small organic acids such as acetate, butyrate, lactate, malate may be accumulated in the dark fermentor effluents depending on the bacterial species and the nutrients used in the fermentation. Abundance of the organic acids may be such that even rate of growth is inhibited which also limits the yield of H_2 production (Melis and Melnicki, 2006).

1.3.4.1 The Hyvolution Project

The Hyvolution Project was an European Union 6th framework integrated project. The full title of it is "nonthermal production of pure hydrogen from biomass". The overall scheme of HYVOLUTION project is demonstrated in Figure 1.7.

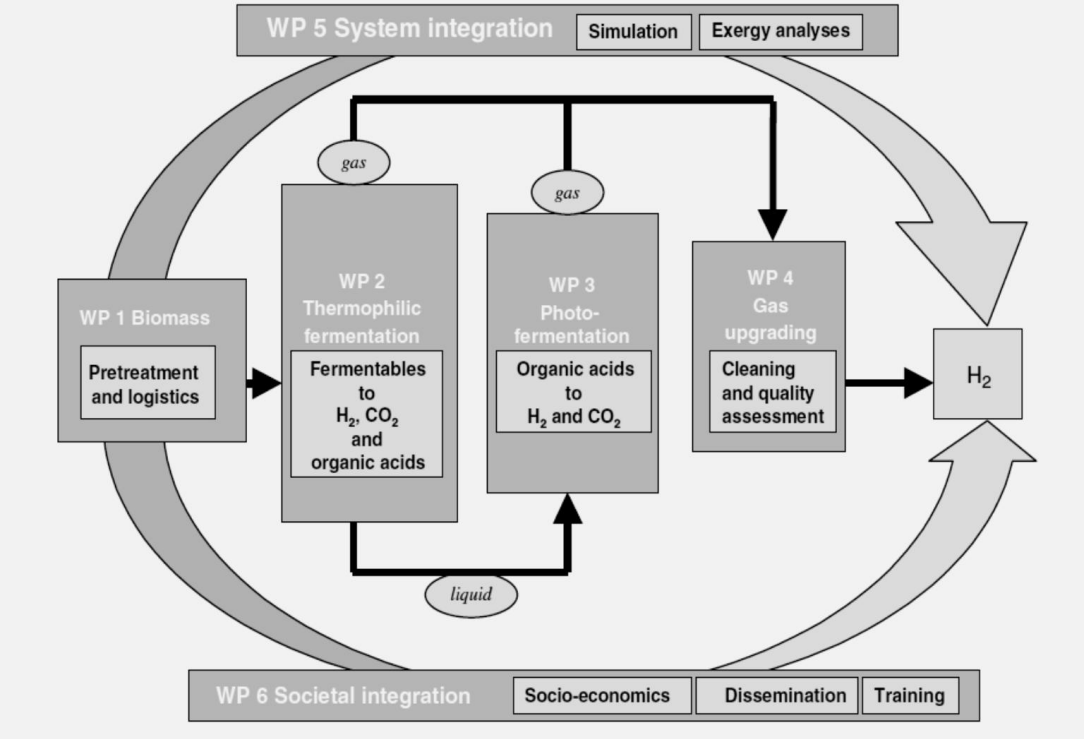

Figure 1.7 The overall scheme of HYVOLUTION project (Claassen and Vrije, 2006).

In this project, development of a two stage bioprocess for the cost-effective production of pure hydrogen from multiple biomass feedstocks was aimed. The first stage of the bioprocess was the thermophilic fermentation of different feedstocks to H_2, CO_2 and organic acids. In the second stage the dark fermenter effluents were used in photofermentation in which organic acids were converted to more hydrogen and CO_2 (Claassen and Vrije, 2006).

METU Biohydrogen group was a member of the project and the coordinator of work package 3 (WP3). The main aim of WP3 was to optimize hydrogen production by photofermentation of organic acids with high yields and also to construct a prototype photobioreactor.

1.3.5 Microbial Electrolysis Cells (MECs)

The MEC is a new technology which is combination of bacterial metabolism with electrochemistry to achieve H_2 production. Anode-respiring bacteria for instance from genera of *Geobacter, Shewanella* are attached to the anode where they oxidize simple organic compounds such as acetate, ethanol, lactate, butyrate and propionate and they tranfer the generated electons in the anode to the conductive solid. Then via an external electrical circuit electrons reach the cathode where they react with H_2O to produce H_2 which evolves out of the cathode compartment. Main challenges of this system are requirement for an external energy supply to increase the energy of the generated electrons and low H_2 production rate (Lee et al., 2010).

1.3 The General Characteristics of Purple Non-Sulfur (PNS) Bacteria

The purple non-sulfur (PNS) bacteria are group of gram negative, photorophic purple bacteria which do not form intracellular elemental sulfur globules and do not grow at both alkaline and highly saline conditions (Imhoff et al., 1984). In nature, they are found in freshwater, marine habitats as well as in moist soils and sediments.

The cells are rod shaped, ovoid, spherical or spiral shaped. Some of them are motile some of them are nonmotile. Motile forms have polar, subpolar or peritrichous flagella (Imhoff, 2006). PNS bacteria cultures are in yellowish to greenish and deep

brown color when they are grown anaerobically under illumination but in the presence of oxygen their color turns to red. The red color change is acused by the conversion of carotenoids to ketocarotenoids (Pellerin and Gest,1983).

Most PNS bacteria, particularly freshwater species, are inhibited by sulfide even at low concentrations. However, some species are able to resist to this toxic compound and use it as photosynthetic electron donor. For instance, *Rhodomicrobium vannielii* can tolerate 2-3 mM sulfide concentrations. In contrast, growth of *Rhodobacter capsulatus* is completely inhibited at 2 mM and growth of *Rhodopseudomonas palustris* is inactivated at sulfide concentrations as low as 0.5 mM (Imhoff, 2006).

PNS bacteria can grow as photoheterotrophs, photoautotrophs or chemoheterotrophs by switching from one mode to another depending on the conditions. For instance, in presence of organic acids, under anaerobic conditions and illumination, they can grow photoheterophically and produce hydrogen (Basak and Das, 2007). Some species are sensitive to oxygen whereas other species can grow under oxic conditions in dark (Imhoff, 2006). Most of the PNS bacteria can utilize different organic carbon sources such as acetate and pyruvate. They can also use intermediates of the tricarboxylic acid cycle. Acetate is assimilated by virtually all PNS bacteria. Neverthless, acetate assimilation pathways may differ among the species. Most of these bacteria posses the two key enzymes of the glyoxylate cycle, which are isocitrate lyase and malate synthase, and assimilate acetate via this pathway. However, it is certain there is variance in acetate assimilation among the PNS bacteria (Imhoff, 2006). For instance, it is known that acetate is assimilated via citramalate cycle and ethylmalonyl-coA pathway in *R.capsulatus* and R.*sphaeroides,* respectively (Kars and Gündüz, 2010). PNS bacteria are also capable of performing anoxygenic photosynthesis while growing under anoxic conditions in the light. They have only one photosystem which does not have enough power to split water. In other words, they carry out anoxygenic photosynthesis since they do not posses

photosystem II unlike cyanobacteria and green algae (Imhoff, 2006; Sasikala et al., 1991).

Rhodobacter capsulatus is a gram negative PNS bacterium which belongs to α subdivision of *Proteobacteria*. The taxonomy of *R.capsulatus* is given in Table 1.3.

Table 1.3 Taxonomy of *R.capsulatus* (Sevinç, 2010).

Super Kingdom	***Prokaryota***
Kingdom	*Monera*
Sub Kingdom	*Eubacteria*
Phylum	*Gracilicutes*
Class	*Photosynthetic eubacteria*
Order	*Rhodospirillates*
Family	*Rhodospirillaceae*
Genus	*Rhodobacter*
Species	*capsulatus*

It is rod shaped with cell diameter of 0.5-1.2 μm and it divides by binary fission. Microscopic picture of *R.capsulatus* is shown in Figure 1.8.

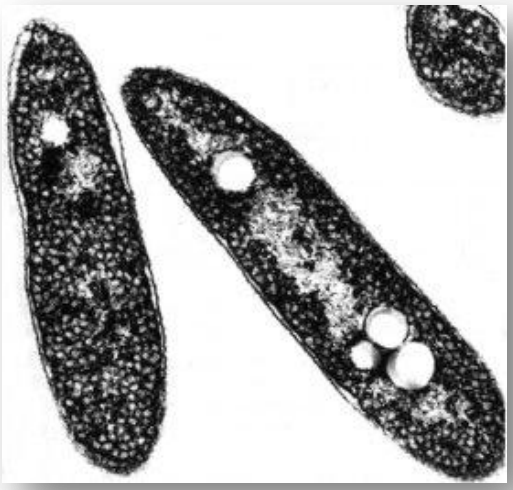

Figure 1.8 The microscopic picture of *R.capsulatus.* (http://www.iet.uni-duesseldorf.de/Frameseiten/Photobiotechnologyand topframenav.htm7)

1.6 Hydrogen Production by PNS Bacteria

R.capsulatus and other PNS bacteria produce hydrogen in the absence of oxygen, by consuming organic compounds and using light energy. The culture media should be limited on nitrogen sources in order to force the bacteria to remove excess energy and reducing power by producing hydrogen (Koku et al., 2002). Although PNS bacteria can utilize variety of carbon sources such as acetate, lactate, malate, glucose, few of them are preferred substrates for hydrogen production by photofermentation. Efficient hydrogen production takes place when they are grown on simple organic acids such as lactate, malate other than sugars (Kars and Gündüz, 2010; Koku et al., 2002).

In PNS bacteria, during photofermentation as a result of catabolism of organic compounds electrons are released and then they are transferred to the electron carriers in the membrane, which are nicotinamide adenine dinucleotide (NAD) and ferrodoxin. Meanwhile, photosynthetic apparatus, which is composed of transmembrane proteins and an ATPase complex that synthesize ATP at the expense of proton gradient, converts light energy into ATP. Nitrogenase, which is the responsible enzyme for hydrogen production, delivers electrons from ferrodoxin, reduces protons to molecular hydrogen by consuming two ATP molecules to pass one electron from the enzyme (Kars and Gündüz, 2010; Koku et al., 2002). Hydrogen production by PNS bacteria is demonstrated in Figure 1.9. The hypothesized electron path and the reaction are shown in Equations 1.9 and 1.10, respectively.

$$\text{Substrate} \rightarrow \text{TCA cycle} \rightarrow \text{NAD/NADH} \rightarrow (Fd)_{ox}/\ (Fd)_{red} \rightarrow \text{Nitrogenase} \qquad (1.9)$$

$$2H^+ + 2e^- + 4\ ATP \rightarrow H_2 + 4\ ADP + 4P_i \qquad (1.10)$$

Efficiency of hydrogen production by PNS bacteria can be reduced by uptake hydrogenase which converts molecular hydrogen to protons and electrons.

In PNS bacteria, hydrogen production is not the only process to dispose excess reducing equivalents in the cell. They can also produce poly-β- hydroxybutyric acid (PHB), which is an intracellular storage compound, when there is high carbon to nitrogen ratio. PHB and hydrogen production are two processes that compete with each other for reducing equivalents in the cell. Mainly, nature of carbon source and acetate assimilation pathways of bacteria determine the partition of metabolism between hydrogen and PHB production (Kars and Gündüz, 2010; Koku et al., 2002).

PHB production and its relationship with hydrogen production will be explained in next sections.

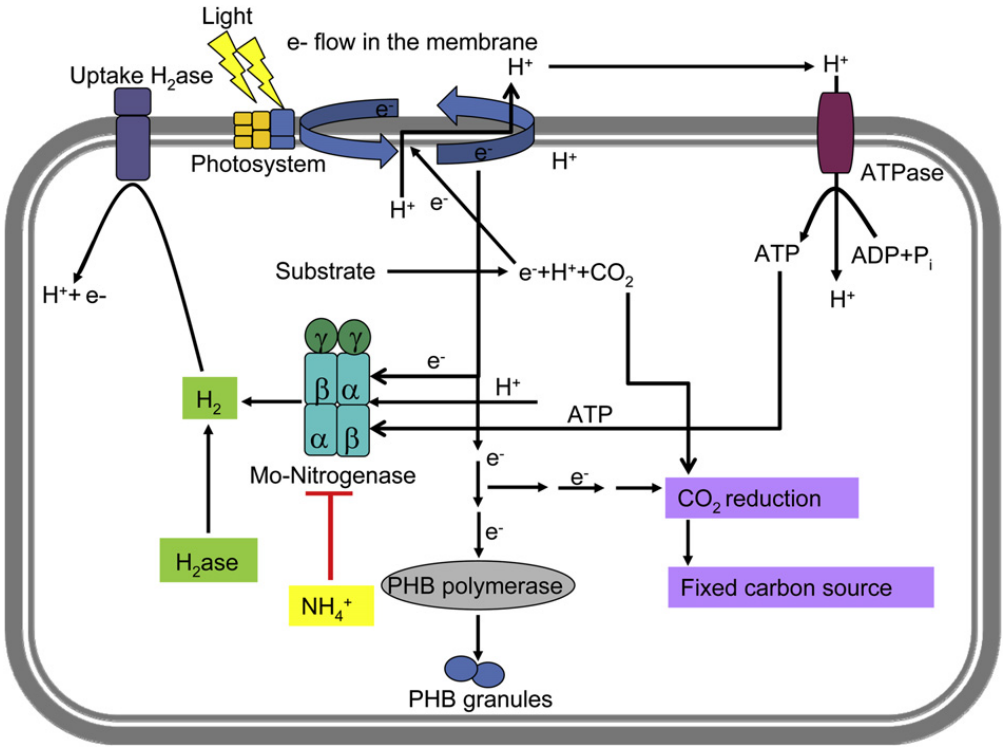

Figure 1.9 The general view of hydrogen production in a PNS bacterium (Kars and Gündüz, 2010).

1.7 Enzymes in Hydrogen Production

There are two main enzymes that function in hydrogen metabolism of H_2 producing bacteria.

1.7.1 Hydrogenase

Hydrogenase is the name of group of metalloproteins that catalyze the reversible oxidation of hydrogen into two protons (H^+) and two electrons (Das et al., 2006). The reaction catalyzed by hydrogenases is shown in Equation 1.11.

$$H_2 \leftrightarrow 2H^+ + 2e^- \quad (1.11)$$

Hydrogenases are classified according to the metal atoms at their active sites. [FeFe]-hydrogenases and [NiFe]- hydrogenases are the most well known types (Kars and Gündüz, 2010).

[FeFe]-hydrogenases which contain two iron atoms at their active sites, are found in green microalgae. They are responsible for reversible reduction of protons to H_2 under anoxic conditions. Oxygen irreversibly inactivates these enzymes therefore H_2 production is arrested under oxygenic photosynthesis (Eroğlu and Melis,2011).

[NiFe]-hydrogenases contain one nickel and one iron atom at their active sites. Some of the subgroups of [NiFe]-hydrogenases are membrane bound uptake hydrogenases, hydrogen sensors and membrane associated H_2 evolving hydrogenases (Kars and Gündüz, 2010). Uptake [NiFe]-hydrogenases are present in cyanobacteria and nitrogen fixing bacteria. They are composed of two subunits which are small and large subunits and encoded by *hupL* and *hupS* genes, respectively. These enzymes function in seperating hydrogen, which is generated as side product of nitrogenase, into protons and electrons. Cyanobacteria also contain a bidirectional hydrogenase which can either produce or consume hydrogen depending on the redox condition of the cell (Eroğlu and Melis,2011).

In PNS bacteria, uptake hydrogenases decrease efficiency of hydrogen production by converting molecular hydrogen to protons and electrons. Therefore, inactivation of uptake hydrogenases increase hydrogen yield. For instance, Kars et al. (2008) reported that *hupSL* mutants of *R.sphaeroides* O.U.001 evolved 20 % more hydrogen gas than the wild type evolved. Similarly, Öztürk et al. (2006) stated that hydrogen production rate and substrate conversion efficieny of *R.capsulatus* (YO3), which is the *hup*$^-$ mutant strain of *R.capsulatus* MT1131, were higher than those of the wild type.

1.7.2 Nitrogenase

Nitrogenases, which are complex metalloproteins, catalyze reduction of dinitrogen (N_2) to ammonia (NH_3). In this way, these enzymes contrubute to nitrogen cycle on earth by converting molecular nitrogen to a chemical form that can be used by other organisms (Kars and Gündüz, 2010; Dixon and Kahn, 2004). During nitrogen fixation, nitrogenase catalyzes reduction of protons to H_2 which is produced as an obligatory side product. In the absence of dinitrogen catalyzes only hydrogen production (Ghirardi et al., 2009).

Nitrogenases are divided into three groups according to the metal atom in the catalytic sites of the enzymes. Hydrogen production by cyanobacteria and PNS bacteria is catalyzed by nitrogenases that contain molybdenum at the catalytic site (Eroğlu and Melis, 2011; Ghirardi et al., 2009). The reactions catalyzed by Mo-nitrogenase both in the presence and absence of dinitrogen are shown below:

$$N_2 + 8H^+ + 8e^- + 16ATP \rightarrow 2NH_3 + H_2 + 16\ ADP + 16\ P_i \quad (1.12)$$

$$2H^+ + 2e^- + 4ATP \rightarrow H_2 + 4ADP + 4\ P_i \quad (1.13)$$

Nitrogenase has two components that are named according to their metal composition. The small component, which functions in the transfer of electrons from the electron donor to the dinitrogenase complex, is called Fe-protein (or dinitrogenase reductase). Fe protein is a homodimer possessing a single [4Fe4S] cluster where either ferrodoxin or flavodoxin bind to reduce the protein. Fe protein also contains a Mg-ATP binding site. Large subunit, which is a $\alpha_2\beta_2$ heterotetramer, is called molydenum-iron (Mo-Fe) protein (or dinitrogenase). It is the subunit that catalyzes reduction of the N_2 to NH_3. It contains two types of metallocluster. The first one is iron-sulfur cluster in which substrate binding and reduction takes place, and the second one, which is termed as P cluster, is [8Fe7S] cluster that mediates electron transfer between the Fe-protein and iron sulfur cluster of the dinitrogenase (Dixon and Kahn, 2004; Ghirardi et al., 2009).

For the enzyme mechanism, reduction of Fe protein by electron donors such as ferrodoxin or flavodoxin is necessary. After the Fe protein, which is bound with 2 ATP molecules, is reduced, it forms a complex with MoFe protein. Subsequently, electrons are transferred between the two proteins in an ATP dependent manner. The cycle of association and dissociation of Fe protein with Mo-Fe protein is required to transfer each electron and it is repetated until the adequate numbers of electrons are accumulated. The schematic representation of the enzyme mechanism is shown in Figure 1.10. Nitrogenase is a slow enzyme due to the rate limiting dissocation step (Dixon and Kahn, 2004; Rees and Howard, 2000). In addition to that, large amount of ATP is required for enzyme activity. Moreover, both of the subunits are extremenly sensitive to oxygen which irreversibly destroys the enzyme (Dixon and Kahn, 2004).

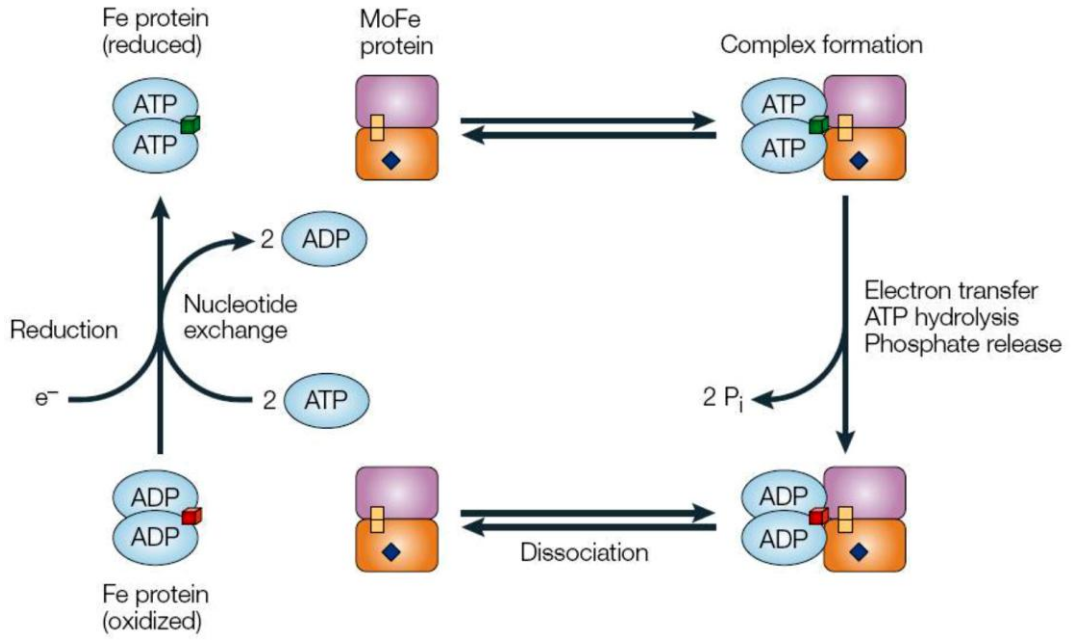

Figure 1.10 The schematic representation of nitrogenase mechanism. The Fe protein dimer is in light blue color and the small cube inside representing the [4Fe–4S] cluster The small yellow cubes inside MoFe protein represent P clusters and the blue diamond inside represents FeMo cofactor (Dixon and Kahn, 2004).

The genes that encode nitrogenase are *nifH, nifD and nifK. NifH* encodes dinitrogenase reductase, *nifD* and *nifK* encode the dinitrogenase complex (Eroğlu and Melis, 2011).

There are nitrogenases that contain iron or vanadium at their catalytic sites. Under Mo depleted conditions some organisms such as *Azotobacter vinelandii* and *R.capsulatus,* induce synthesis of these nitrogenases. Reactions catalyzed by alternative nitrogenases are shown below:

Fe-nitrogenase: $N_2 + 21H^+ + 21e^- \rightarrow 2NH_3 + 7.5H_2$ (1.14)

V-nitrogenase: $N_2 + 12H^+ + 12e^- \rightarrow 2NH_3 + 3H_2$ (1.15)

1.7.2.1 Regulation of Nitrogenase

Nitrogenase consumes large amounts of ATP and reducing power. Therefore, synthesis and activity of nitrogenase is controlled by strict regulatory mechanisms. In addition to oxygen, which irreversibly inactivates the enzyme, avaliability of light and molybdenum affects it. For instance, light stimulates synthesis of nitrogenases. Moreover, ammonium, which is the product of nitrogen fixation has inhibitory effect on nitrogenase (Koku et al., 2002). Ammonium affects not only activity of the enzyme but also expression of it via the help of ammoinum regulatory mechanisms (Masepohl et al., 2004). Expression of nitrogen fixation genes, as well as synthesis and activity of nitrogenases is regulated at three levels (Masepohl et al., 2002). The schmatic scheme of nitrogen regulation is given in Figure 1.11.

First level of control is a two component NtrB-NtrC regulatory system which serves global control in response to the nitrogen. At this level of control, transcriptional activators of nitrogenase genes, which are *nifA1, nifA2* and *anfA*, are regulated. In the absence of NH_4, NtrB, the key regulator, activates NtrC by phosphorylating. NtrC then goes and activates transcription of *nifA1, nifA2, anfA* that encode transcriptional activators of nitrogenase genes. In the presence of NH_4, NtrB is inactivated by a PII signal transduction protein, GlnB protein. GlnB goes and binds to NtrB which cannot activate NtrC. Consequently, NifA activators are not transcribed and as a result *nif* genes are not transcribed when there is NH_4 (Dixon and Kahn, 2004; Masepohl et al., 2002).

The second level of control is independent of Ntr system and it controls NifA transcriptional activators. It was observed that in the presence of NH_4, NifA mediated *nifH* transcription is still inhibited although *nifA* gene is overexpressed from constituve promoters. PII regulatory proteins, GlnB and GlnK, inhibit the

activity of NifA1 and NifA2 when NH_4 is present (Masepohl et al., 2002). In many diazotrophic bacteria including *R.rubrum* and *R.capsulatus*, GlnB and GlnK was demostrated to be regulators of NifA activity (Zhang et al., 2000; Drepper et al., 2003).

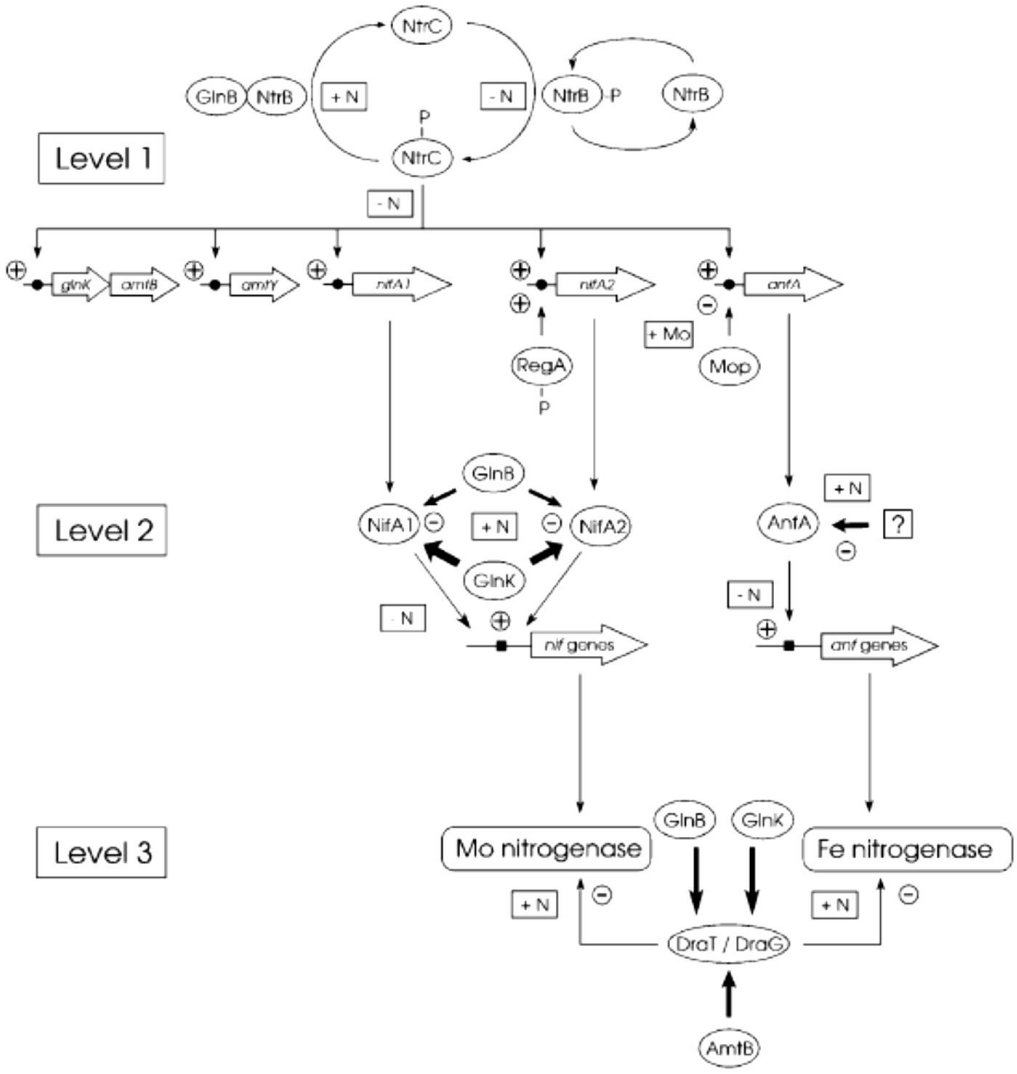

Figure 1.11 The levels of ammonium regulation on nitrogenase enzyme complex in *R.capsulatus.* Availability of NH_4 is represented by [+N] and [-N], respectively meaning presence and absence of NH_4 (Masepohl et al., 2002).

Post-translational regulation of nitrogenase is the third level of control. The activity of nitrogenase is controlled by reversible ADP-ribosylation of NifH in response to NH4. ADP-ribosylation is catalyzed by the draT gene product (dinitrogenase reductase ADP-ribosyltransferase), which inactivates Fe protein of nitrogenase. Reactivation of nitrogenase is performed by draG gene product (dinitrogenase reductase activating glycohydrolase) (Masepohl et al., 2002).

1.8 Poly-β-hydroxy butyric acid (PHB)

1.8.1 Polyhydroxyalkonates (PHAs)

PHAs are polyesters of various hydroxyalkanoates that are produced as storage materials or as a sink for reducing equivalents by many gram-positive and gram-negative bacteria. Bacteria synthesize and accumulate PHAs when there is limited amount of nutrients such as nitrogen, phosphorus and excess amount of carbon source. Once the limiting nutrients become avaliable, intracellular depolymerases can degrade PHAs to utilize them as carbon and energy source (Lee,1996).

The first PHA, poly-3-hydroxybutyrate (PHB), was discovered in 1926 in *Bacillus megaterium* by the French scientist Lemoigne. He stated that this bacterium accumulated an intracellular homopolymer that consisted of 3-hydroxybutyric acids that were linked with ester bonds to the 3-hydroxyl group and the carboxylic acid of the next monomer (Zinn et al., 2001). In 1958, first investigations about the effect of growth conditions on PHA metabolism were done by Macrae and Wilkinson who found out that PHA accumulation increased as the carbon to nitrogen ratio increased (Sudesh et al., 2000). In addition, their results showed that similar to polyphosphate and carbohydrate reserves, PHA accumulation happens in response to imbalance in growth caused by deficiency of nutrients. Then it was understood that bacteria

synthesize and store PHA when they have insufficient amount of nutrients that are needed for cell division, and have excess amount of carbon sources.

Later, it was shown that PHA synthesis when there is deficieny of magnesium, sulfate, nitrogen, phosphate and/or oxygen (Sudesh et al., 2000).

Presently, it is known that many species of gram positive and negative bacteria including cyanobacteria, purple sulfur and nonsulfur bacteria are capable of producing PHAs (Sudesh et al., 2000). More than 90 genera of archae and eubacteria which can produce PHA are found in aerobic and anaerobic habitats (Zinn et al., 2001). However, some of the species such as *Ralstonia eutropha* (or *Alcaligenes eutrophus*), *Alcaligenes latus, Azotobacter vinelandii, Pseudomonas oleovorans, Paracoccus denitrificans, Protomonas extorquens* are able to produce adequate amount of PHA for large scale (Chanprateep, 2010). Bacteria are able to produce PHA from various carbon sources such as simple carbohydrates, sucrose, cellulose, alkanes. In addition, waste effluents like molasses can be used to produce PHA. (Sudesh et al., 2000; Reddy et al., 2003). Production of PHA by various bacteria with their carbon sources is given in Table 1.4.

Table 1.4 PHA production by various bacteria (Reddy et al., 2003).

Microorganism	Carbon source	PHA	PHA content (%w/v)
Alcaligenes eutrophus	Gluconate	PHB	46–85
	Propionate	PHB	26–36
	Octanoate	PHB	38–45
Bacillus megaterium QMB1551	Glucose	PHB	20
Klebsiella aerogenes recombinants	Molasses	PHB	65
Methylobacterium rhodesianum MB 1267	Fructose/methanol	PHB	30
M. extorquens (ATCC55366)	Methanol	PHB	40–46
Pseudomonas aeruginosa	Euphorbia and castor oil	PHA	20–30
P. denitrificans	Methanol	P(3HV)	0.02
	Pentanol	P(3HV)	55
P. oleovorans	Glucanoate	PHB	1.1–5.0
	Octanoate	PHB	50–68
P. putida GPp104	Octanoate	PHB	14–22
P. putida	Palm kernel oil	PHA	37
	Lauric acid	PHA	25
	Myristic acid	PHA	28
	Oleic acid	PHA	19
P. putida BM01	11-Phenoxyun-decanoic acid	5POHV	15–35
Sphaerotilus natans	Glucose	PHB	40

PHB—polyhydroxybutyric acid), P(3HV)—polyhydroxvaleric acid, 5POHV—poly(3 hydroxy-5-phenylvalerate).

The general structure of PHAs is composed of 3-hydroxy fatty acid monomers which are arranged in head to tail manner that is the carboxylic group of one mononer forms an ester bond with the hydroxyl group of the adjacent monomer. PHA is generally produced as a polymer of 103 to 104 monomers (Naik et al., 2008; Suriyamongkol et al., 2007). The molecular mass of PHA, which varies according to the PHA producer, is in the range of 50 –1000 kDa. This molecular mass is high enough to have polymer characteristics that are similar to converntional plastics such as polypropylene (Sudesh et al., 2000).

PHAs are divided into three classes according to the carbon numbers of the monomers (Zinn et al., 2001; Suriyamongkol et al., 2007):

- Short Chain Length (scl) PHA: They contain monomers with carbon numbers ranging from C3 to C5.
- Medium Chain Length (mcl) PHA: They contain monomers with carbon numbers ranging from C6 to C14.
- Long Chain Length (lcl) PHA: They contain monomers with carbon numbers higher than C14.

Most of the microbes produce either scl PHA that mostly contain 3HB units (3-hydroxybutyrate) or mcl PHAs that have 3-hydroxyoctanoate (3HO) and 3-hydroxydecanoate (3HD) as the major monomers (Reddy et al., 2003). PHB (poly-β-hydroxybutyric acid) is the most common type of PHA and it has been studied most extensively. It is a homopolymer of 3-hydroxybtyric acid. The R group of its monomer is methyl (CH_3) (Zinn et al., 2001; Suriyamongkol et al., 2007). Poly (3-hydroxybutyrate-co-3-hydroxyvalerate) [P(3HB-3HV)] is one of the PHAs whicg is a co-polymer of PHB that is formed as a result of incorporation of 3-hydroxyvalerate (3-HV) into PHB (Reddy et al., 2003). The general structure of PHAs and PHB is shown in Figure 1.12.

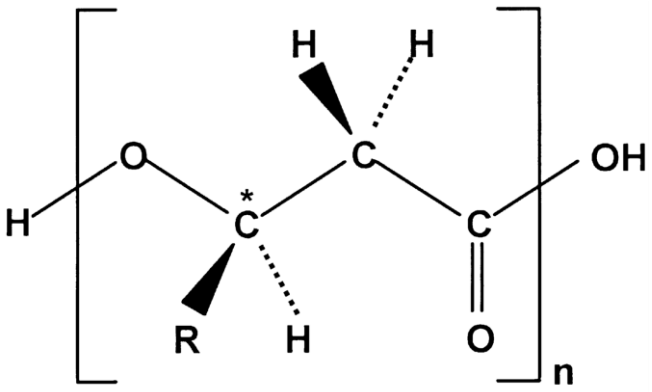

Figure 1.12 Chemical structure of PHAs. All monomers have one chiral center (*) in the R position. The chain length of R groups vary from C1 to C14. n=100-30000 monomers. For PHB the R group is methyl (CH_3) (Zinn et al.,2001)

1.8.2 PHA Granules

Bacteria produce PHA as an intracellular storage compound when there is deficiency of nutrients such as nitrogen, phosphorus, oxygen and when there is overabundance of carbon sources. It acts as carbon and energy source during starvation. They are even accumulated to levels as high as 90 % of the cell dry weight (Reddy et al., 2003, Naik et al., 2008, Sudesh et al., 2000; Zinn et al., 2001; Suriyamongkol et al., 2007). Additionally, depending on the physiological conditions, a PHA granule acts as a pool for reducing equivalents therefore it is proposed to be a redox regulator in the cell (Philippis et al., 1992, Mukhopadhyay et al., 2005, Sudesh et al., 2000).

PHA is accumulated in the cell cytoplasm, as seperate inclusions that are 0.2 – 0.5 μm in diameter (Sudesh et al., 2000; Zinn et al., 2001; Suriyamongkol et al., 2007). It is highly refractive so it can be visualized clearly under a phase contrast light

microscopy. When thin sections of PHA producing bacteria are examined by transmission electron microscopy, PHA inclusions are seen as electron-dense bodies (Sudesh et al., 2000).

PHA is accumulated in the form of mobile, amorphous, liquid granules. The number and size of PHA granules depend on the bacterial species, culture and enviromental conditions (Luengo et al., 2003). Microscopic pictures of PHB granules in PNS bacteria is shown in Figure 1.13.

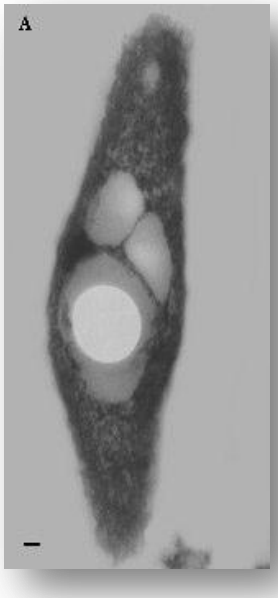

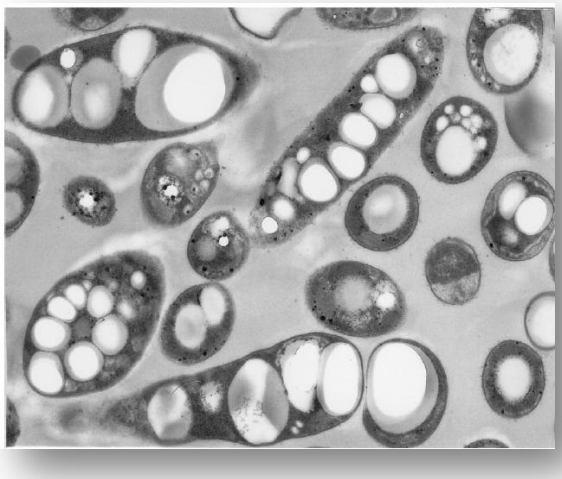

a) b)

Figure 1.13 a) A transmission electron micrograph of PHB granules in *R. sphaeroides* at 12 hours of the growth (Çetin et al., 2006). b) Electron micrograph of PHB granules in *R.capsulatus* (Kranz et al., 1997).

Within the cell, amorphous PHB polymers are enclosed in a lipid monolayer. Proteins, which are involved in the metabolism of PHB, are attached to the surface of the layer.In addition to PHB polmerase and PHB depolymerase, phasins, which function in formation and stabilization of the PHB granules, are located on the surface of the lipid layer (Sudesh et al., 2000; Zinn et al., 2001). The structure of a PHB granule is shown in Figure 1.14.

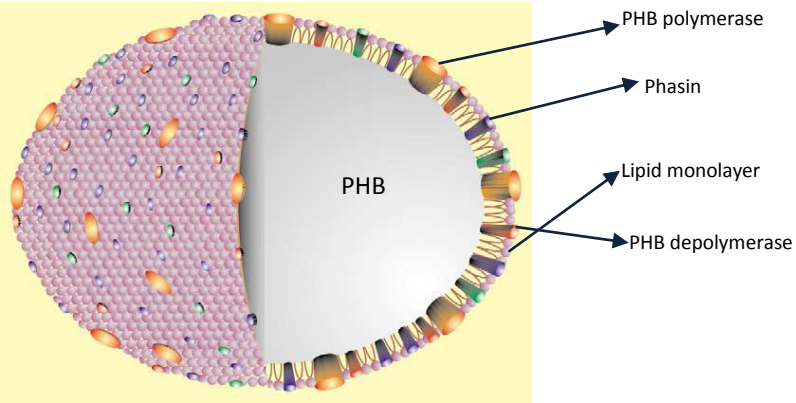

Figure 1.14 The structure of a PHB granule (Adapted from Luengo et al. (2003)).

Since PHB polymers are storage compounds bacteria are naturally capable of degrading the polymers in order to recover the stored carbon. They can decompose it into CO_2 and water by using their own PHB depolymerases. (Sudesh et al., 2000; Suriyamongkol et al., 2007). In studies done with *Ralstonia eutropha*, it was shown that the intracellular degradation of PHB inclusion occurs very slowly. The rate of the degradation was calculated to be about 10 times slower than the rate of its synthesis (Sudesh et al., 2000).

1.8.3 PHA Synthesis Pathways in Bacteria

There are two major PHA synthesis pathways that is classified according to the monomer composition of the produced PHA (Sudesh et al., 2000). One of the pathways, which leads to synthesis of scl PHA, mainly PHB, is represented by *Ralstonia eutropha* (formerly known as *Alcaligenes eutrophus*). Another type of synthesis pathway, which leads to production of mcl PHA is represented by *Pseudomonas* species (Sudesh et al., 2000; Zinn et al., 2001).

It was reported that purple non-sulfur bacteria produce high amounts of PHB under stress conditions (Brandl et al.,1991; Philippis et al., 1992; Hustede et al., 1993). Therefore, in the current study, first pathway which is represented by *R.eutropha,* is explained in detail.

1.8.3.1 PHB Biosynthesis

The biosynthetic pathway of PHB includes three enzymatic reactions, which are catalyzed by three different enzymes. PHB synthesis pathway is demonstrated in Figure 1.15.

The first reaction is the condensation of two acetyl-CoA molecules that are derived from TCA cycle, to acetoacetyl-CoA. β-ketothiolase, which is encoded by *phaA* gene, is the enzyme that catalyzes the first reaction. The second reaction is the reduction of acetoacetyl-CoA to (R)-3-hydroxybutyryl-CoA. NADPH-dependent acetoacetyl-CoA reductase, which is encoded by *phaB* gene, catalyzes the reaction by reducing acetoacetyl-CoA at position 3 and all resulting 3-hydroxybutyryl-CoA

are in the *R*-configuration. The final reaction is the polymerization of (R)-3-hydroxybutyryl-CoA monomers into PHB by PHB synthase, which is encoded by *phaC* gene (Reddy et al., 2003; Suriyamongkol et al., 2007; Zinn et al., 2001).

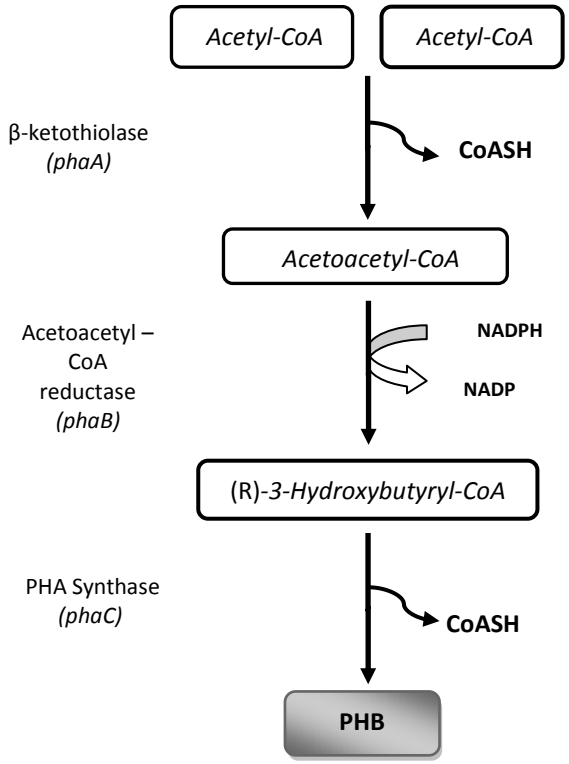

Figure 1.15 PHB synthesis pathway repesented by *Ralstonia eutropha*.

PHB synthase is the key enzyme of PHB biosynthesis (Steinbüchel and Füchtenbusch,1999; Rehm and Steinbüchel, 1999). It was stated by Kranz et al. (1997) that *phaA* single and *phaAB* double mutants were able to synthesize PHA when it was grown on acetone whereas *phaC* single mutants were unable. This result shows that PHB synthase is the necessary enzyme for PHB synthesis.

In *Ralstonia eutropha*, which is the model organism and studied in most detail, genes of the enzymes that function in PHB biosynthesis, *phaA, phaB, phaC*, are clustered in one operon. In contrast, in *R.capsulatus* and *R.sphaeroides, phaC* encoding the key enzyme is not linked to *phaA* and *phaB* genes (Rehm and Steinbüchel, 1999; Franchi et al., 2004; Kranz et al., 1997).

1.8.4 PHB Synthases

PHA synthases, which are the key enzymes of biosynthesis of PHAs, catalyze the polymerization of hydroxyalkanoates into PHA by using coenzyme A thioesters of hydroxyalkanoic acids as substrates (Rehm and Steinbüchel, 1999). They are divided into four major classes according to substrate specificities and subunit composition. The substrate specificity of the PHA synthases determines the composition of synthesized PHA (Rehm, 2006).

The type of PHA synhase that is involved in PHB synthesis is class I PHA synthases which are found in *Ralstonia eutropha* and in many other prokaryotes. Therefore, in this section, only Class I PHA synthases will be explained.

Substrates of class I PHA synthases are coenzyme A thioesters of various (*R*)- 3-hydroxy fatty acids that are made up of 3 to 5 carbon atoms (Rehm and Steinbüchel, 1999; Rehm, 2003). Class I PHA synthases possess only one type of subunit with molecular weights between 61 kDa and 73 kDa (Rehm, 2003). It was seen that *in vitro* PHA synthases occur as an equilibrium of monomeric and dimeric forms whereas presence of substrates and trimeric CoA analogs induce dimerization (Rehm,2003). In all PHA synthases, there are conserved residues which are cysteine-319, aspartate-480 and histidine-508. These residues were shown to be essential for

covalent catalysis (Rehm, 2006). The current model of active PHA synthases comprises two subunits that form homodimer in Class I PHA synthases. Accordingly, class I synthases have two thiol groups provided by the conserved cysteine residue of the PhaC subunit with at least two subunits of PhaC in the active PHA synthase. In this model, it is proposed that two thiol groups have key roles in covalent catalysis. One thiol group act as the loading site for 3-hydroxy-butyryl-CoA and the second one serves as the priming and elongation site. The highly conserved cysteine residues have been demonstrated to be involved in covalent catalysis (Rehm, 2003).

PHA synthases are classified as mixed class of proteins with respect to secondary structure prediction based on the multiple alignment since they are mainly composed of variable loop (49.7 %), α-helical (39.9 %) and β- sheet (10.4 %) (Rehm and Steinbüchel, 1999).

1.8.5 Regulation of PHB Biosynthesis

1.8.5.1 Regulation of PHB Production at the Enzymatic Level

It is well known that regulation of PHB synthesis takes place at the enzymatic level. Intracellular concentrations of acetyl-CoA and free coenzyme are the major factors in the regulation of PHB synthesis. It has been demonstrated that high intracellular NAD(P)H concentration and high ratios of NAD(P)H/NAD(P) stimulates PHB biosynthesis (Kessler and Witholt, 2001). Additionally, rate of PHB synthesis is controlled by either β-ketothiolase or acetoacetyl-CoA reductase enzymes. It was also shown that the final concentration and content of PHB is mostly related to the activity of PHB synthase (Jung et al., 2000).

Moreover, citrate synthase,which controls the avaliability of CoA, is an important regulator of the PHB biosynthesis pathway since presence of CoA regulates the activity of 3-ketothiolase, which is the first enzyme of the pathway. This is supported by a study done with *Ralstonia eutropha*. In the study, it was shown that isocitrate dehydrogenase-leaky mutant of *Ralstonia eutropha*, which possess low TCA cycle activity, produced PHB at a faster rate than the wild type. Studies done with recombinant strains showed that rate of PHB synthesis is controlled by 3-ketothiolase and acetoacetyl-CoA while the content of PHB is controlled by PHB synthase (Kessler and Witholt, 2001).

1.8.5.2 Regulation of PHB Production at the Transcriptional Level

In a variety of microorganisms, promoters have been experimentally identified and proposed based on the sequence upstream of the *pha* and *phb* synthetic genes. Phosphate starvation inducible promoter,which was identified in *Acinetobacter sp.* and appeared to be under *pho* regulon control, was one of those promoters. However, there is not much information about specific regulatory proteins involved in *pha* gene expression (Kessler and Witholt, 2001).

It was shown that LuxR regulatory protein controls not only bioluminescence system but also PHB synthesis in *Vibrio harvey*. This was proven by the mutants of *V.harvey* which cannot produce LuxR protein, was shown to be defective in PHB synthesis (Miyamoto et al., 1998). In addition to that, in *Azospirillum brasilense* SP7, it has been shown that *ntrB* and *ntrC* genes that are involved in nitrogen regulation also function in the regulation of PHB synthesis by ammonia (Sun et al., 2000). In contrast, Kranz et al. (1997) indicated that nitrogen regulatory cascade is not involved in PHA biosynthesis by *R.capsulatus.* In their study, it is stated that mutant

R.capsulatus cells, which are defective in the general nitrogen regulatory system were able to produce PHB polymers comprising over 50 % of cell volume.

Regulatory mechanisms at the transciptional level have been found in *Pseudomonas* species. A transcriptional regulator, called $PhbR_{PS}$ was found in a *Pseudomonas* species which can produce a PHB polymer. This regulatory protein was reported to be involved in the transcription of the gene that are required for synthesis of PHB (Matsusaki et al., 1998). Furthermore, a gene coding a putative regulatory protein, which is called PhaS, was identified in *P.putida* KT 2442. The primary structure of this protein shows homology to the sensor component of the two component regulatory systems that consist of a histidine protein kinase and response regulator domain. According to these data, in *Acetobacter vinelandii* a GacS trasmembrane sensor kinase homologue, which regulates the PHB polymer production, has been described (Castaneda et al., 2000).

In addition, an open reading frame whose putative translational product has similarity to the primary structure of a member of the prokaryotic histone H1-like family of regulators, was identified adjacent to the *pha* gene cluster in *P.aeruginosa* PAO1 (Timm and Steinbüchel, 1992).

It was demonstrated that the gene product of a homologue open reading frame of *P.oleovorans* called PhaF, is involved in transcriptional regulation of *pha* gene expression. It is presented that in the absence of substrates for PHA production, PhaF inhibits transcription of the *pha* genes by binding to DNA. When PHA granules are formed, DNA binding is reduced and *pha* genes are expressed (Kessler and Witholt, 2001). Moreover, a specific *pha* regulatory protein which is encoded by $phaR_{Pd}$ that

is located downstream of the genes coding for the PHB synthase and a granule associated proteini has been proposed for *Paracoccus denitrificans* (Maehara et al., 1999).

1.8.6 Properties and Applications of PHAs

PHAs are non-toxic, biocompatible, biodegradable thermoplastics that can be produced from renewable sources. In addition to those, they have a high degree of polymerization,are highly cristalline, optically active and isotactic which means repeating units are stereochemically regular. They are insoluble in water. Those properties make them highly competitive with petrochemical-derived plastics (Reddy et al., 2003). Therefore, they have a wide range of applications. They are initially were used in packaging films mostly in bags, containers and paper coatings. They can be used as biodegradable carriers for long term dosage of drugs, medicines and hormones. However, because of slow biodegradation their medical and pharmaceutical useage is limited (Reddy et al., 2003). PHAs are also used as raw materials for the synthesis of chiral compounds and for the production of paints (Rehm and Steinbüchel, 1999).

1.8.7 Biodegradability of PHA

One of the most important of features of PHA is that they are biodegradable. PHAs are degraded when they are exposed to soil, compost or marine sediment. Microorganisms secrete extracellular PHB depolymerases so that they can break down the polymer into hydroxy acids that can be utilized as carbon source for growth (Reddy et al., 2003). In addition to microbial activity biodegradation depends on the exposed surface area, moisture, temperature, pH, molecular weight and composition

of the polymer (Lee, 1996). Under aerobic conditions, products of biodegration of PHAs are CO_2 and water. Under anaerobic conditions, the biodegration results in formation of CO_2 and methane (Reddy et al., 2003). It is reported that PHAs can degraded at a high rate (3-9 months) by microorganisms (Jendrossek, 2001).

1.8.8 Competition Between Hydrogen and PHB Production

Hydrogen and PHB production have similar physiological roles which is disposing excess energy and reducing equivalents in the cell (Koku et al., 2002). In addition, both processes occur when there is high carbon to nitrogen ratio in the environment. Therefore, these two processes compete with each other for reducing equivalents in the cell (Hustede et al., 1993).

It was reported that PNS bacteria produce large amounts of PHB. For instance, it was indicated that *R.sphaeroides* cells could produce PHB between 60 and 80 % of their cell dry weight and *R. rubrum* could produce 45 % of its cell dry weight (Kemavongse et al., 2007). In addition, Brandl et al. (1991) reported that *R.sphaeroides* produced PHB 50.8 % of cellular dry weight when cells were grown on acetate.

Nature of the substrate appears to determine the partitioning of metabolism between hydrogen and PHB production. It is proposed that substrates, which are easily converted to acetyl units without forming pyruvate, yield mostly PHB (Koku et al., 2002). The competition between the processes and effect of substrate type on PHB production was demonstrated by Hustede et al. (1993). They made PHB synthase defective mutants and compared PHB and hydrogen production between the wild

type and mutant strain on various carbon sources. They observed that with acetate, mutant strain produced more hydrogen and less PHB than that of wild type and that on pyruvate the mutant formed nearly 20 % more hydrogen than the wild type. However, with lactate, fumarate, succinate or malate, the wild type and the mutant reported to have produced almost the same amount of hydrogen. In addition to this study, there are many studies which report increase in hydrogen production by *phb* mutated *R.sphaeroides* and *R.palustris* strains (Franchi et al., 2004, Kim et al., 2006, Yang and Lee, 2011). For example, Kim et al. (2011) reported that PHB synthase mutant *R.sphaeroides* cells produced approximately two folds higher hydrogen than that of the wild type when they were grown in acetate containing media. Moreover, PHB synthase mutant *R.palustris* was reported to be producing more hydrogen than the wild type (Yang and Lee, 2011).

1.9 Aim of The Study

In integrated systems, which are combinations of dark fermantation and photofermentation, the effluent of dark fermentation is used in photofermentation. The effluent of dark fermentation contains high concentrations of acetate, which is a factor that may influence efficiency of hydrogen production by PNS bacteria. Due to the fact that acetate is a suitable carbon source for PHB production and the effluents contain high concentrations of acetate, it is important to determine optimum acetate concentration for efficient hydrogen production.

Aim of this study is to investigate the effects of acetate concentrations on hydrogen and PHB production by *R.capsulatus.* In this way, optimum acetate concentration for effective photofermentative hydrogen production with low amount of PHB can be determined.

Additionally, it is aimed to examine the effects of acetate concentration at genetic level by doing gene expression analysis of the key enzymes of hydrogen production and PHB synthesis pathways, which are *nifD* and *phaC* encoding dinitrogenase and PHB synthase, respectively.

CHAPTER 2

MATERIALS AND METHODS

2.1 Bacterial Strain

Rhodobacter capsulatus (DSM1710) was obtained from Deutsche Sammlung von Mikroorganismen und Zellkulturen GmbH, Germany.

2.2 Storage and Activation of Bacteria

Bacteria were stored in 30 % glycerol at -80°C. For activation, bacteria were taken from stock cultures by using a sterile loop and inoculated on solid MPYE or modified Biebl and Pfenning defined media which were solidified by adding agar (1.5 %). The compositions of MPYE and BP medium are given in Appendix A. After bacteria grew on solid media, a colony was chosen and inoculated to liquid growth media.

2.3 Growth Media

R.capsulatus were grown in modified Biebl and Pfenning (BP) defined media which contained acetate (20 mM) and glutamate (2 mM) as carbon and nitrogen sources, respectively. The media also contained vitamin (thiamin, niacin, biotin), trace

element solutions and ferric citrate which were added after the sterilization of media by autoclaving. Trace element and ferric citrate solutions were sterilized by autoclaving and vitamin solutions were sterilized by using 2 μm sterile filters. Before sterilization, pH of growth media was adjusted to 6.3-6.4 by using NaOH. The compositions of media and the solutions are given in Appendix A.

2.4 Experimental set-up

2.4.1 Media

For hydrogen and PHB production experiments, bacteria were firstly grown in modified BP media which contained different concentrations of acetate and 2 mM glutamate as nitrogen source. Like growth media, initially pH of the media was adjusted to 6.3-6.4.

Table 2.1 Concentrations of acetate in media containing 2 mM glutamate as nitrogen source.

Medium number	Acetate concentration
1	10 mM
2	25 mM
3	50 mM
4	65 mM

2.4.2 Conditions

Bacteria were grown in 120 mL glass bottles. 10 % inoculation was done from actively grown cultures to the media containing different concentrations of acetate. Inoculums were taken from the cultures grown in the growth media. After inoculations, bottles were flushed with pure argon gas in order to acquire anaerobic atmosphere. All cultures were incubated at 30-32°C under illumination provided by tungsten lamps. Light intensity of the bioreactors was adjusted to 2500-2600 lux.

2.4.3 Hydrogen production set-up

Hydrogen production was evaluated by water-displacement method at which glass bottles were connected to water-filled graduated glass cylinders by using capillary tubes in order to measure evolved gas. The evolved gas in the bioreactors passes through the capillary tubes and replaces with the water. In this way, hydrogen production is measured volumetrically.

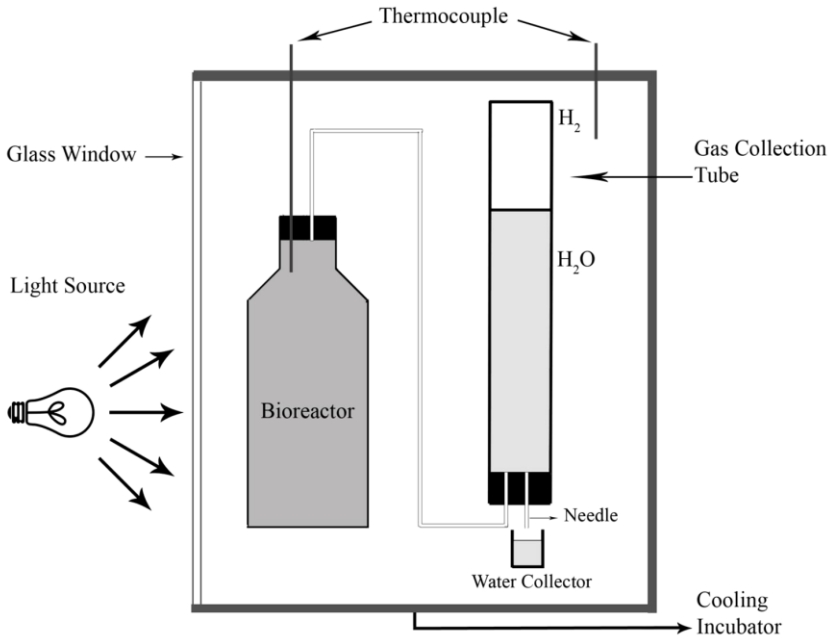

Figure 2.1 The schematic diagram of hydrogen production set-up (Sevinç, 2010).

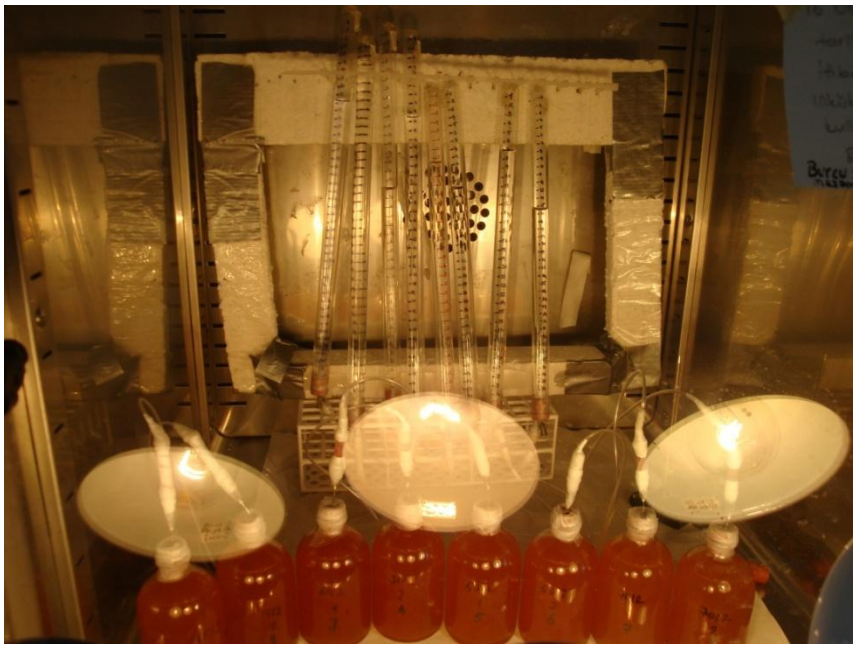

Figure 2.2 The experimental set-up for hydrogen production.

2.4.4 Analysis

For the cell growth and pH measurements, samples were taken periodically at time intervals (approximately in 24 hours). As soon as the sample was taken, equal volume of sterile BP medium without carbon and nitrogen source was injected into the culture in order to prevent negative pressure that might occur.

Organic acid composition was also monitored periodically. Unlikely, total PHB amount produced was evaluated at the end of the experiments.

2.4.4.1 Measurement of Cell Growth

Cell growth was measured spectrophotometrically at 660 nm and converted to dry weight per liter of culture. $OD_{660\ nm}$:1 corresponds to a cell density of 0.5427 g cell dry weight/L (Uyar 2008). Calibration curve that is used for dry cell weight calculation is given in Appendix B.

2.4.4.2 Measurement of pH

pH change was monitored periodically by measuring the pH of the samples taken from the cultures by using a pH meter (Mettler Toledo 3311).

2.4.4.3 Measurement of Hydrogen Production

Hydrogen production was monitored volumetrically (in mililitres) at time intervals. The purity of gas collected in glass cylinders was determined by a gas chromatography (Agilent Technologies 6890N) using a Supelco carboxen 1010

column. The carrier gas was argon with a flow rate of 26 ml/min and the temperature sets for oven, injector and detector were 140 ºC, 160 ºC and 170 ºC, respectively. A sample gas analysis chromatogram is given in Appendix C.

H_2 gas in the collected gas was evaluated after the composition of the total gas was determined by GC. For instance, GC result of a collected gas is as:

- 98.21 % H_2,
- 0.76 % air
- 1.01 % CO_2

H_2 gas in this tube, which has 162 mL collected gas, equals to:
0.98 x 162 = 158.4 mL

Later, mmoles of produced H_2 was determined by:

- Firstly mass of produced H_2 is calculated.

  Mass of H_2 (g) = Volume of H_2 produced (L) x the density of H_2 (0.089 g/L). (2.1)

- Secondly, mmoles of H_2 is calculated.

  Mmoles of H_2 = (Mass of H_2 (g) / 2) x 1000 (2.2)

2.4.4.4 Measurement of Organic Acid Consumption and Production

Samples taken at time intervals firstly centrifuged at 13000 rpm for 10 minutes (Eppendorf AG 22331 Hamburg Microcentrifuge) in order to precipitate bacteria and obtain clean supernatant which contain organic acids. The supernatant was filtered through nylon filters (45µm,13 mm Millipore) in order to make it pure. Filtered supernatants were analysed by High Performance Liquid Chromatography (HPLC) (Shimadzu LC 20A- Prominence Series) using Altech IOA-1000 column. A sample HPLC chromatogram and samples of calibration curves of the organic acids are given in Appendix D.

2.4.4.5 Measurement of Polyhydroxy butyric acid (PHB) Production

Total PHB production was measured by a gas chromatography (GC) method which involves lyophilization and methanolysis of bacterial pellet. As a result of methanolysis, intracellular PHB was converted to methyl 3-hydroxybutyric acid which was quantified by the GC. A sample chromatogram for PHB analysis is given in Appendix E.

At the end of the experiments, cell cultures were centrifuged (Sigma 3K30 High Speed Refrigerated Centrifuge) at 13000 rpm for 20 minutes to precipitate bacteria. After centrifugation, supernatant was removed and bacterial pellet was taken into an eppendorf and kept at -80°C. Then the samples were lyophilizated for 24 hours (Christ alpha 1-4 LD plus) in order to remove water from the pellets.

For calculation of cellular dry weight, weights of the eppendorfs were recorded before putting the pellet into it. Before starting methanolysis step, weights of the eppendorfs containing lyophilizated samples were recorded again. Then cellular dry weight of each sample was calculated by extracting the eppendorf weight from the total eppendorf weight with lyophilizated samples.

Methanolysis was performed by treating the lyophilizated biomass with acidic methanol (containing 15 % of H_2SO_4). Firstly, lyophilizated samples were taken into screw capped tubes. Then 2 ml of MeOH/ H_2SO_4 and 2 ml of chloroform was added to the samples. The caps of tubes were closed tightly and sealed with parafilm to prevent evaporation of chloroform.

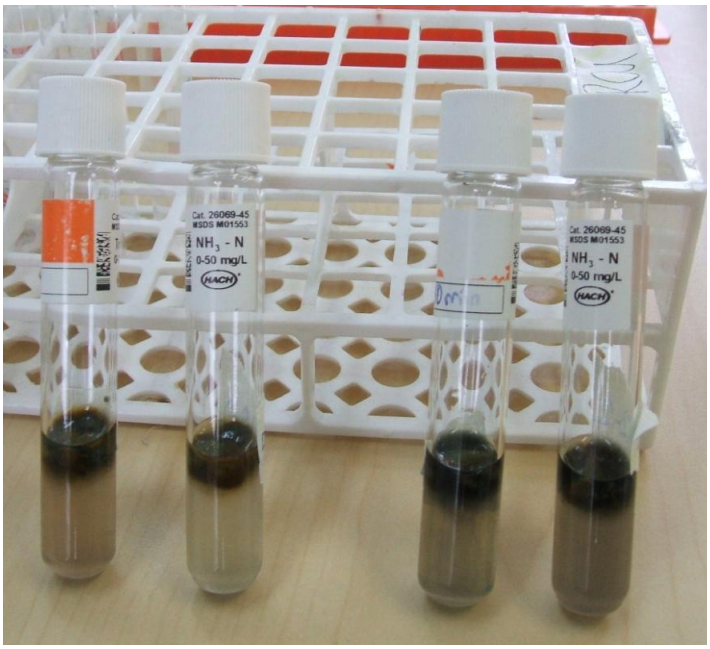

Figure 2.3 The lyophilizated samples in acidic methanol and chloroform.

Next, samples were incubated at 100°C for 3.5 hours. During incubation, at every 1 hour the samples were vortexed.

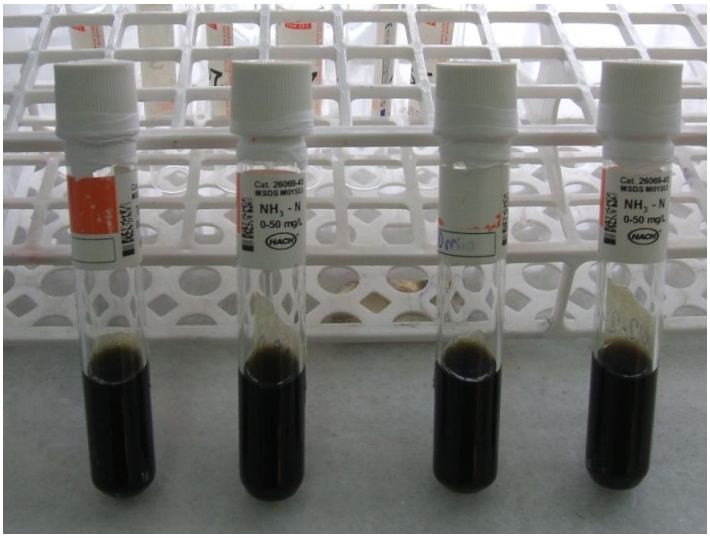

Figure 2.4 The vortexed samples during incubation at 100°C.

After the incubation is completed, samples were cooled to room temperature. Then 1 ml of distilled water was added and vortexed to achieve phase separation. Two phases were formed: upper water phase and lower chloroform phase. Upper phase was removed by taking with a serological pipette without disturbing the lower chloroform phase containing methyl 3-hydroxybutyric acid that was formed from PHB as a result of methanolysis. Prior to GC measurement, lower phase was filtered through a nylon filter (45μm,13 mm Millipore). 1 μL filtered chloroform phase was injected to the gas chromatography (Agilent Technologies 6890N).

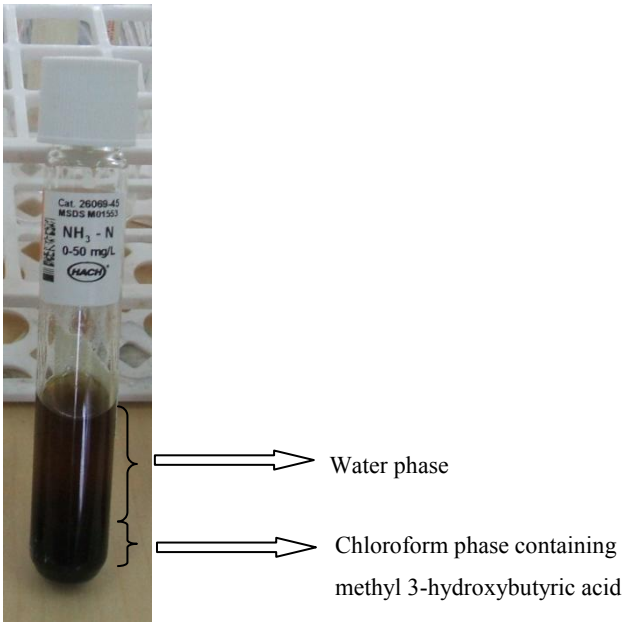

Figure 2.5 Formation of two phases after distilled water addition.

For the measurement by using GC, HP-FFAP column (30 m x 0.320 mm x 0.25 µm) and FID detector was used. Column pressure was constant (6.67 psi) and the carrier gas was argon with a flow rate 1 ml/min. The detector temperature was 250°C. Initial oven temperature was 70°C with a 1 min hold. Oven temperature had a 8°C/min ramp until the maximum temperature reached 160°C (1 min hold at 160°C). Back inlet temperature was 230°C, the split ratio was 20:1. Total run time was 13.25 min.

2.4.4.5.1 Calibration Curve

Prior to PHB measurements of samples calibration curve was drawn by preparing standard PHB solutions. Firstly, stock solution was prepared by dissolving 10 mg standard PHB in 2 ml chloroform. In order to dissolve PHB in chloroform, the solution was incubated at 60°C overnight. After the stock solution was made up, standard PHB solutions (0.5-5 mg/ml) were prepared. 2 ml of PHB solution were

subjected to acidic methanolysis which was explained in detail above. As a result of acidic methanolysis, methyl 3-hydroxybutyric acid is quantified by GC and calibration curve was drawn. A sample calibration curve for PHB measurement is shown in Appendix E.

2.5 Total RNA Isolation

2.5.1 Diethyl Pyrocarbonate (DEPC) Treatment

All pipette tips and eppendorfs used for RNA isolation were treated with % 0.1 DEPC solution overnight in order to inactivate RNases. DEPC treated materials were autoclaved and dried in oven. In addition to that, some of the solutions used during the procedure was prepared with DEPC treated water.

2.5.2 Isolation of Total RNA from *R.capsulatus* Cultures

Total RNA isolation was carried out by using TRI REAGENT. The procedure of the reagent provided by the manufacturer was followed for RNA isolation. RNA isolation was carried out under laminar flow to prevent contamination. Firstly, 2.5 ml of *R.capsulatus* cultures were centrifuged for 3 min at 13000 rpm at 4°C. The centrifugation was repeated several times until 100 mg bacterial pellet was obtained. Then the precipitated bacterial cells were treated with 100 µL of 5mg/mL lysozyme, mixed by pipetting and using vortex and then incubated at 37°C for 10 minutes. After incubation, 1 mL of TRI REAGENT was added and mixed well by pipetting several times to homogenize bacterial cells. Afterwards, the sample was incubated at room temperature for 5 min. Then 200 µL of cold chloroform per ml of TRI REAGENT was added and shaken by inversion for about 15 seconds. Then samples were incubated at room temperature for 15 min. After incubation, the samples were

centrifuged at 13000 rpm for 15 minutes at 4°C. The centrifugation forms 3 phases: red bottom phase was organic phase containing proteins, the white middle phase was containing DNA and the upper colorless aqueous phase was RNA containing phase. The upper phase was transferred into a new eppendorf. Before RNA precipitation, an additional step, which was acidic phenol-chloroform extraction, was performed to prevent DNA contamination. Equal volume of acidic phenol- chloroform was added to the RNA containing phase and then centrifuged at 13000 rpm for 2 min at 4°C. After the extraction repeated two times, 500 µL cold isopropanol per ml of TRI REAGENT was added, mixed by pipetting and incubated at RT for 10 min to precipitate RNA. Afterwards, the sample was centrifuged at 13000 rpm for 12 min at 4°C. At the end of the centrifugation, white RNA pellet was formed on the side and bottom of the eppendorf. Then supernatant was discarded and for washing RNA 1 ml of cold 70 % EtOH was added onto the pellet. In order to obtain clean RNA sample, 70 % EtOH added RNA sample was kept at -20°C overnight. Later the sample was centrifuged at 13000 rpm for 5 min at 4°C. After pouring the supernatant, the pellet was dried near flame. Then 30 µL of nuclease free water was added and the sample incubated at 55°C for 10 minutes to dissolve RNA. Isolated RNA samples were stored at -80°C.

2.5.3 Analysis of Isolated RNA

2.5.3.1 Analysis by Using Nanodrop

Purity and concentration of isolated RNA was determined by using Nanodrop (Thermo). 1.5 µL of isolated RNA was analyzed using 1.5 µL nuclease free water as a blank.

The purity of RNA samples was determined by the ratio of A_{260} to A_{280} ratio, which should be between 1.8-2.0 for a pure RNA sample.

2.5.3.2 Agarose Gel Electrophoresis of RNA Samples

Isolated RNA samples were run on 1 % agarose gels. Firstly, 0.6 g agarose was added into 60 mL TAE and dissolved by boiling at a micowave oven. After the homogenous molten agarose was cooled under tap water, 5 µL EtBr was added to the cooled gel for staining, and then the molten gel was poured onto tray. After the prepared gel cooled completely, RNA samples were loaded by mixing them with loading dye. Then the gel was run at 70 V for one hour. RNA bands were visualized on a software UV transilluminator and photographed by Vilber Lourmat Gel Imaging System.

2.6 Reverse Transcriptase – Polymerase Chain Reaction (RT-PCR)

2.6.1 Complementary DNA (cDNA) Synthesis

1 µg total RNA template and 20 pmole/µL of sequence-specific primer was added into a sterile tube. Then by adding nuclease free water the volume of the mixture was completed to 11 µL. Then the sample was incubated at 72°C for 5 min. After the incubation is completed, the samples were chilled on ice. Then 4µL of 5X reaction buffer, 2 µL of 10 mM 4 dNTP mix and nuclease free water was added. The final concentration of dNTP mix became 1.0 mM. Afterwards, the sample was incubated at 37°C for 5 min. 0.3 µL of RevertAid M-MuLV Reverse transcriptase was added and the mixture was incubated at 42°C for 60 min. The final concentration of the

enzyme was 60 units in the reaction mixture. Finally, the mixture was incubated at 70°C for 10 min to stop the reaction. Then chilled on ice and stored at -20°C.

Two negative controls were set up for cDNA synthesis. In the first control, RNA template was not added to the mixture to assure that there was no contamination in the components of the reaction mixture.

Prokaryotic genomes do not posses introns thus their mRNA sequences are same with their DNA sequences.Moreover, it may be difficult to remove all contaminating genomic DNA from prokaryotic RNA samples. Therefore, it is necessary to include a control during synthesis to make certain that the PCR product is not due to contaminating genomic DNA. Thus, the second control, which includes all the components except reverse transcriptase, was set up for cDNA synthesis.

2.6.2 Polymerase Chain Reaction (PCR)

2.6.2.1 Primer Design

Gene spesific primers were preferred for expression analysis of *nifD* and *phaC* genes. Gene specific primers were designed by using Primer 3 software program. Sequences of the genes were taken from NCBI Genome Database. Self dimer and heterodimer formations were tested for the reverse and forward primers by using Integrated DNA Technologies. The designed primers were checked on NCBI Blast program to assure that they are specific for *R.capsulatus*. Then, primers were synthesized by Alpha DNA and Gensutek (Ankara).

16S rRNA was used as internal control. 16S rRNA primers were designed by Sevilay Akköse (Akköse, 2008).

In RT-PCR on prokaryotic RNA, contamination of RNA with chromosomal DNA is generally observed and DNA contamination in RNA forms false-positive reaction products (Sybesma et al.,2001). Primers which generate 5'- tagged cDNA during reverse transcription were used. cDNA which posses tag sequnce on 5' is used as a specific template during PCR. In this way, reliability of reverse transcription is improved since this 5' tag sequence is not present on genomic DNA. cDNA with GC rich tag sequence on its 5' end provides a means for PCR amplification at relatively high annealing temperature (Cobley et. al., 2002). The schematic diagram of RT-PCR is shown in Figure 2.6.

Sequence of the primers that are used are shown in Table 2.2.

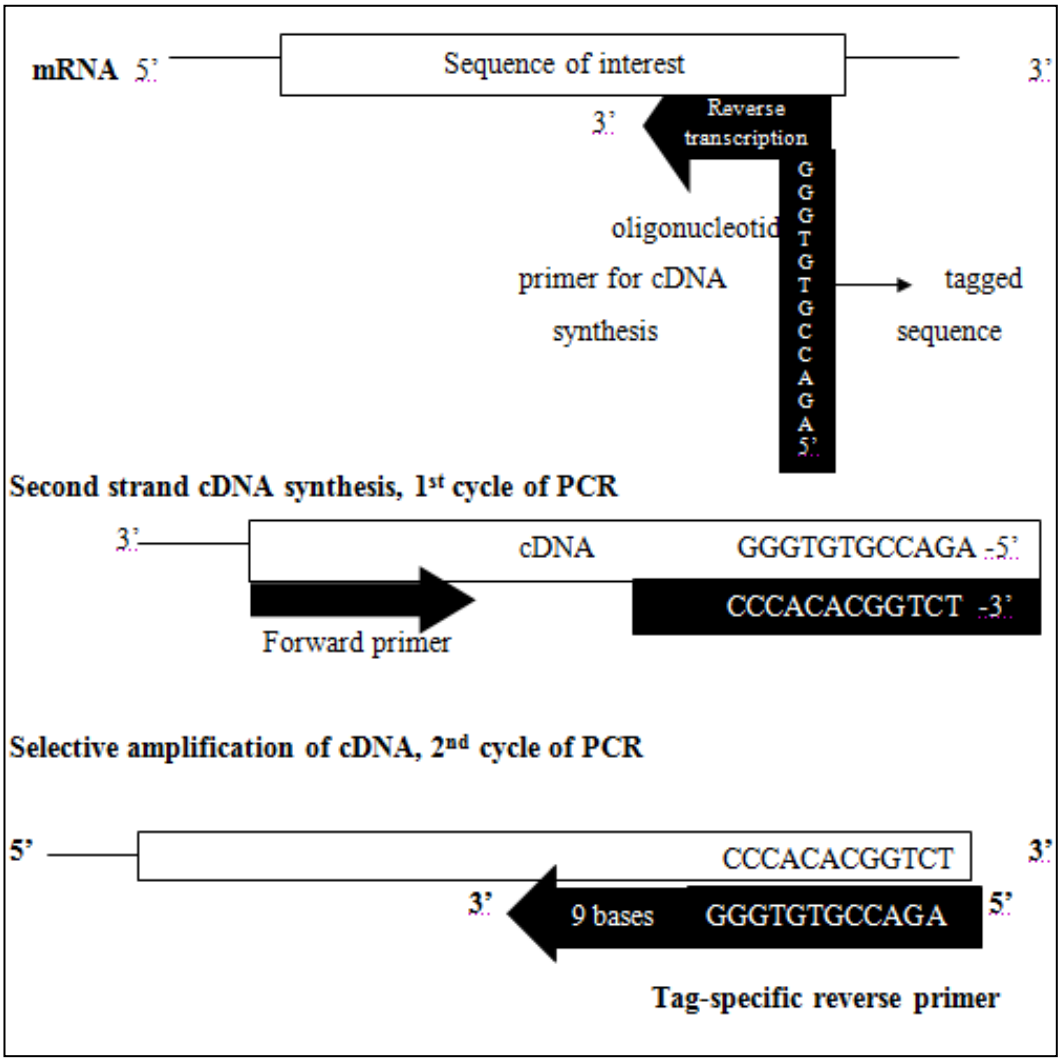

Figure 2.6 Principle of RT-PCR with tagged primer for cDNA synthesis and tag-specific primer for amplification of cDNA (Akköse, 2008).

Table 2. 2 Sequence of the primers that are used in RT-PCR.

phaC	cDNA primer	5'-AGA CCG TGT GGG GGT CAG CGT GGT GAA AAA G-3'
	Reverse primer	5'-AGA CCG TGT GGG GGT CAG CGT-3'
	Forward primer	5'-TCA CCG GCG AGA AAC AGG TG-3'
nifD	cDNA primer	5'-AGA CCG TGT GGG GCG GAT CTT CTC GAT GAA CT-3'
	Reverse primer	5'-AGA CCG TGT GGG GCG GAT CTT C-3'
	Forward primer	5'-CTA TGA CGA TCT GGG CAT GGT G-3'
16S rRNA	cDNA primer	5'-AGA CCG TGT GGG CCG CGT TGG ATT AGG TA-3'
	Reverse primer	5'-AGA CCG TGT GGG CCG CGT TG-3'
	Forward primer	5'-CGC CAC TGG TGT TCC TCC GAA-3'

2.6.2.2 PCR Conditions and Compositions

PCR reactions were made in 50 µL aliquots and reaction was performed by thermal cycler (Apollo^{TM} ATC 401 Thermal Cycler and Thermo Thermal Cycler). Hot start start sprotocol was applied to *nifD* and *phbC*. PCR conditions and compositions were given in the Tables 2.3 and 2.4.

Table 2.3 Final concentrations of PCR ingredient.

PCR Ingredients	Final Concentrations
Reaction buffer	1X
$MgCl_2$	1.5 mM
dNTP mix	0.2 mM of each
Forward Primer	0.2 µM
Reverse Primer	0.2 µM
cDNA	0.1-0.3 µg/50 µL
Tag DNA polymerase	1.25 units/50 µL

Table 2.4 PCR amplification programs for *nifD, phbC* and *16S rRNA.*

	nifD	***phbC***	***16S rRNA***
Initial Denaturation	at 94°C for 6 minutes	at 94°C for 6 minutes	at 94°C for 10 minutes
	Hold at 95°C		No hold
Denaturation	at 94°C for 30 seconds	at 94°C for 30 seconds	at 94°C for 30 seconds
Annealing	at 63.4°C for 30 seconds	at 63.6°C for 30 seconds	at 63.2°C for 30 seconds
Extension	at 72°C for 30 seconds	at 72°C for 30 seconds	at 72°C for 30 seconds
Cycle #	30	35	30
Final extension	at 72°C for 10 minutes	at 72°C for 10 minutes	at 72°C for 10 minutes
Final hold at 4°C			

2.6.2.3 Agarose Gel Electrophoresis of PCR Products

PCR products were run on 2 % agarose gels. Firstly, 2 g agarose was added into 100 mL TAE and dissolved by boiling at a micowave oven. After the homogenous molten agarose was cooled under tap water, 5 µL EtBr was added to the cooled gel for staining, and then the molten gel was poured onto tray. After the prepared gel cooled completely, RNA samples were loaded by mixing them with loading dye. Then the gel was run at 120 V for one hour. DNA bands were visualized on a software UV transilluminator and photographed by Vilber Lourmat Gel Imaging System.

2.6.2.4 Densitometric Analysis

The gel photographs were processed with Image J software to determine band intensities. Densitometric measurement ratio was calculated by:

$$\frac{DBI\ of\ gene\ of\ interest}{DBI\ of\ the\ internal\ control} \tag{2.3}$$

DBI stands for the "density of band intensity" and the internal control is the *16S rRNA* gene.

2.7. Statistical Analysis

Each experimantal data is the mean of 4 times replications with ±standard deviation.

Densitometric measurement data was subjected to statistical test by using the program Graphpad Prism 5 (Graphpad Software Inc, USA). Tukey's Multiple Comparison Analysis was applied to compare different groups. The mean differences were significant at the 0.05 level.

CHAPTER 3

RESULTS AND DISCUSSION

During the photofermentation step of two stage hydrogen production systems effluents of dark fermentation contain high amount of acetate. Acetate is one of the main organic acids for both hydrogen and PHB production by *R.capsulatus.* It is a suitable carbon source for PHB production rather than hydrogen production . Acetate concentration influences hydrogen production and it is important to determine optimum acetate concentration for efficient hydrogen production with low PHB production when the desired product is hydrogen.

The aim of this study was to investigate the effects of acetate concentration on hydrogen and PHB production by *R. capsulatus. R. capsulatus* cells were grown in media containing different concentrations of acetate. The experimental set up was as described in Section 2.4., Samples were taken at time intervals to evaluate cell growth, hydrogen production and pH. Acetate consumption and production of other organic acids were also examined by HPLC analysis. Total PHB production was determined by doing measurements at the end of each run.

3.1 Effect of Initial Acetate Concentration on Cell Growth

Cell growth at different acetate concentrations (10-65 mM) was evaluated by measuring absorbance at 660 nm. Absorbance values were multiplied by 0.5427, which corresponds to OD_{660}: 1 in order to convert the values to dry cell weight (dcw).

Growth curve of a microbial population in batch cultures includes several phases. First phase is the lag phase, which is the duration between the inoculation and the initiation of growth. Length of lag phase changes depending on the age of inocula, medium composition and growth conditions. The second phase is the exponential phase at which cell division occurs and number of cells increases exponentially. As the essential nutrients in the media are consumed and waste products accumulate, exponential growth stops and the population enter to stationary phase. In this phase, cell number does not increase or decrease whereas many cell functions such as energy metabolism may be carried on. The final phase is the death phase whereby cell number decreases. Death phase is also exponential but rate of cell death is much slower than that of cell growth (Madigan and Martinko, 2006).

Growth curve and bar graph showing initial and maximum dry cell weight of *R.capsulatus* cells at initial acetate concentrations is given at Figure 3.1.

Cell growth was detected at all initial acetate concentrations. From the growth curve, it is seen that growth pattern at all acetate concentrations nearly followed the basic growth curve of a microbial population. Lag phases at all acetate concentrations almost did not exit since inoculum was taken from a culture that was in the exponential phase. In addition to inoculum age, composition of the medium affected

the lag phase. As previously indicated at Section 2.4, composition of the media that the inocula were grown was exactly the same.

At low acetate concentrations (10 mM and 25 mM), bacteria entered the death phase earlier than those of high acetate concentrations (50 mM and 65 mM). The reason for this may be the early depletion of acetate in media. Additionally, it seems that exponential growth at 65 mM was slower than that of 50 mM. The biomass concentration at 65 mM is lower than that at 50 mM up to the 120^{th} hour.

It has been noted that, cell growth at all acetate concentrations showed similar pattern with a growth curve of a microbial population. Apart from the growth pattern, it is also important to mention about the biomass concentration. To begin with, by looking at the growth curve (Figure 3.1a) the highest and the lowest growth, were observed at 65 mM and 10 mM acetate, respectively.

From the bar graph, (Figure 3.1b) it is seen that initial biomass concentrations were approximately 0.1 gdw/Lc and the same in all runs while maximum dry cell weight (Xmax) increased with increasing acetate concentration. To illustrate, the highest maximum biomass concentration was at 65 mM and 50 mM acetate, which were 0.85 gdw/Lc and 0.77 gdw/Lc, respectively. The lowest biomass concentration was at 10 mM acetate, which was 0.57 gdw/Lc (Table 3.1). This result is consistent with previous studies which showed that biomass concentration increased with the acetate concentration. For instance, Shi and Yu (2006), who also worked with *R.capsulatus*, demonstrated that there was higher growth when the acetate concentration was increased from 20 mM to 40 mM. Additionally, effects of acetate concentration on bacterial growth were reported by Barbosa et al. (2001) who studied with *Rhodoseudomonas* species. They observed elevated growth when acetate

concentrations were increased to 22 and 11 mM from 6 mM. Moreover, Sangkharak and Prasertsan (2007) stated in their study done with *R.sphaeroides* N20 that biomass concentration increased with the increase of acetate concentration from 3.0 g l^{-1} to 4.5 g l^{-1}.

From these results, it seems that acetate is a good carbon source for *R.capsulatus* growth. Nevertheless, high biomass concentration is not desirable for efficient hydrogen production since light penetration in the culture is reduced. In other words, shading caused by high biomass decreases light intensity in the culture and affects hydrogen production negatively (Barbosa et al., 2001; Özgür et al., 2010).

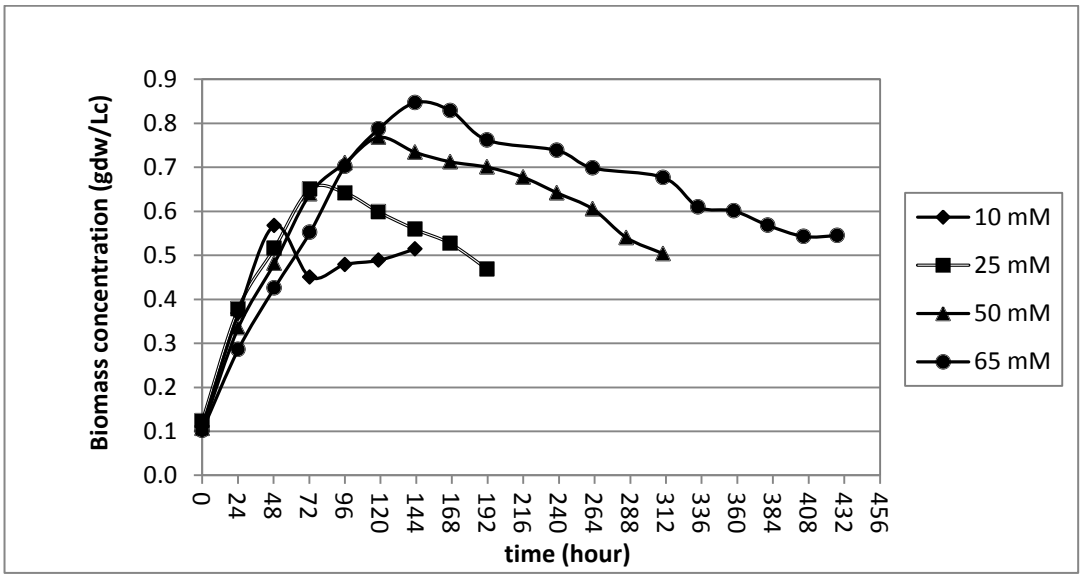

(a)

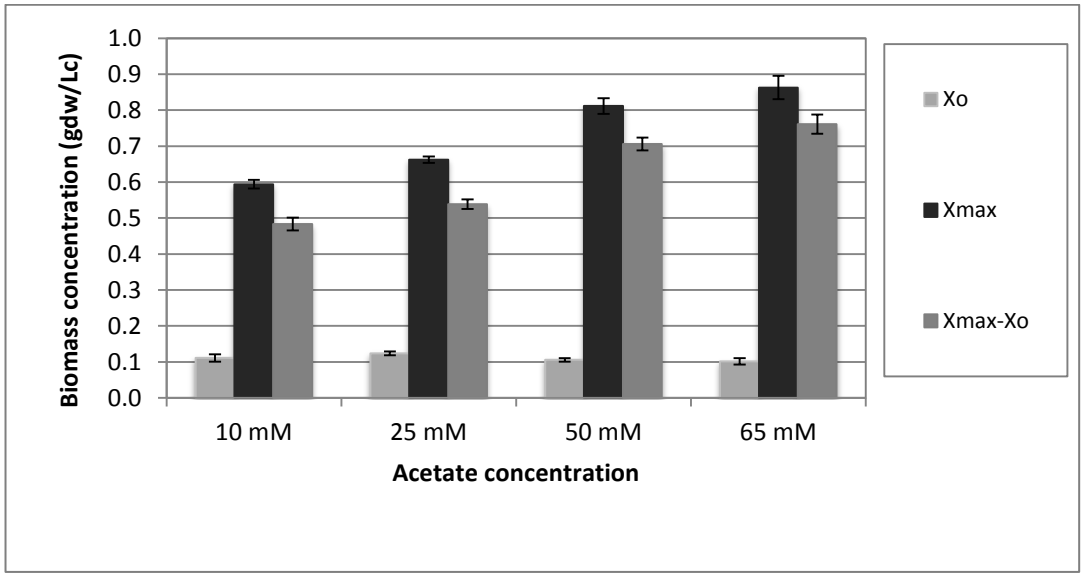

(b)

Figure 3.1 a) Growth curve of *R.capsulatus* in media containing different concentrations of acetate. b)The bar graph of initial and maximum dry cell weight of *R.capsulatus* in media containing different concentrations of acetate. Xo: Initial biomass concentration, Xmax: Maximum biomass concentration.

3.1.1 Modelling of Bacterial Cell Growth

Rate of *R.capsulatus* growth at exponential phase is fast. After cell growth slows down, it reaches to an asymptotic value before entering death phase. By exclusion of death phase the shape of the growth curve becomes "S" shaped so it may be called sigmoidal curves. "Logistic Model" is one of the models that is widely used to analyze these kind of cell growth curves. Logistic model was developed by Verhulst (1838) and is commonly used for bacterial cell growth in growth media (Nath et al., 2008; Sevinç 2010; Uyar 2008, Koku et al., 2003). In previous studies done both with *R.capsulatus* and *R.sphaeroides*, cell growth was reported to fit the logistic model (Androga 2009; Sevinç 2010; Özkan 2011, Uyar 2008).

The logistic model equation is:

$$dX/dt = k_c X(1-X/X_{max}) \quad (3.1)$$

where k_c is the specific growth rate (h^{-1}), X is the biomass concentration (gdw/Lc) and X_{max} is maximum biomass concentration (gdw/Lc). Integration of this equation gives:

$$X = \frac{X_{max}}{[1+\exp(-kc.t)\left(\frac{X_{max}}{X_0-1}\right)]} \quad (3.2)$$

where X_o is the initial biomass concentration at the lag time (gdw/Lc).

For kinetic analysis of the growth, the experimental data from the start of cell growth of the death phase were fitted to logistic model by using Curve Expert 1.3. The logistic growth model at 50 mM acetate concentration is given as an example in Figure 3.2. The other curves fitted to logistic model for *R.capsulatus* cells are given in Appendix G.

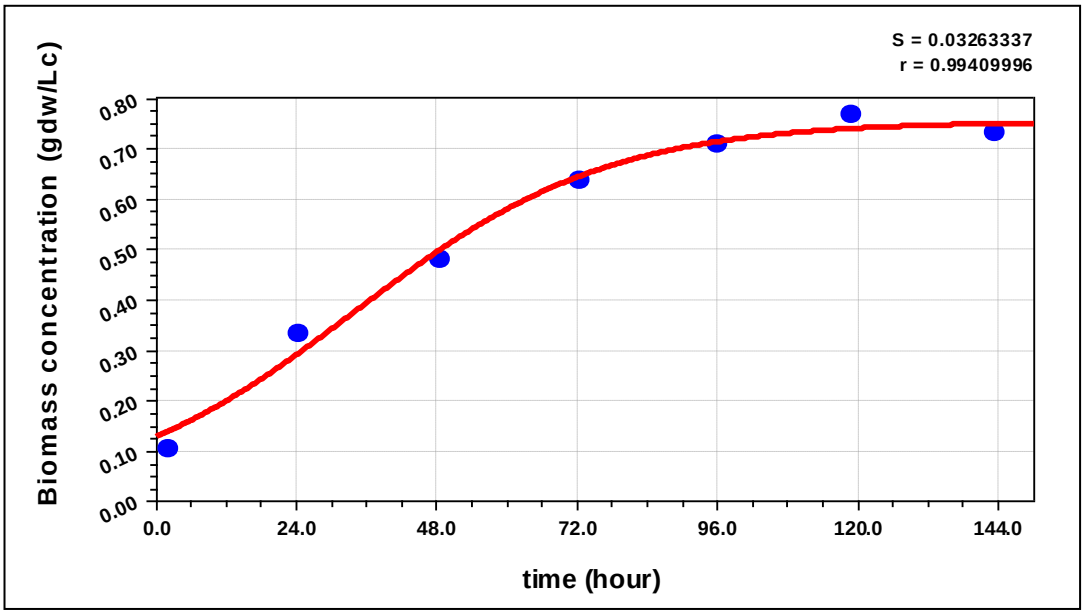

Figure 3.2 The logistic growth model of *R.capsulatus* cells for the growth in 50 mM acetate.

From experimental data specific growth rate was also determined by using the equation:

$$\mu = \frac{\ln \frac{X_2}{X_1}}{t_2 - t_1} \tag{3.3}$$

where X is the bacterial cell concentration; t is the time in hours and μ is the specific growth rate. By using this equation, specific growth rate at exponential phase is determined.

From the model, initial and maximum biomass concentrations ($X_{0,m}$, $X_{max,m}$), specific growth rate constant (k_c) and the extent of the fit was obtained. Along with those parameters, experimantal specific growth rate (μ), initial and maximum biomass concentrations ($X_{0,e}$, $X_{max,e}$) are given in Table 3.1.

Table 3.1 Comparison of experimental and logistic model constants for *R.capsulatus* cells grown at different initial acetate concentrations. (subscript "e" represents experimental values; subscrip "m" represents model values).

	10 mM	**25 mM**	**50 mM**	**65 mM**
R	0.975	0.977	0.994	0.987
$X_{0,e}$ (gdw/Lc)	0.111	0.124	0.106	0.102
$X_{0,m}$ (gdw/Lc)	0.051	0.065	0.130	0.119
$X_{max,e}$ (gdw/Lc)	0.567	0.650	0.768	0.847
$X_{max,m}$ (gdw/Lc)	0.500	0.587	0.754	0.802
μ_{max} (L/h)	0.034	0.023	0.017	0.015
k_c (L/h)	0.136	0.107	0.046	0.039

It is seen from the table that r values at all acetate concentrations are close to 1 which indicates that the experimantal data fitted well to the logistic model. The maximum biomass concentration increases with increasing acetate concentration. μ_{max} and k_c values decrease as the acetate concentration increases. This shows that growth was slower at high acetate concentrations. Mostly, experimental values are close to model values.

3.2 Effect of Initial Acetate Concentration on Hydrogen and PHB Production

PHB is produced as an intracellular storage compound when there is high carbon to nitrogen ratio in the media which is also a favorable condition for hydrogen production (Kars and Gündüz, 2010; Koku et al., 2002) Hydrogen and PHB production are two processes that compete for reducing equivalent in the cell (Hustede et al. , 1992; Khatipov et al. 1998). In many studies, acetate was reported to be a suitable carbon source for PHB production. To illustrate, Hustede et al. (1992) showed in their study with *R.sphaeroides*, that acetate is a good carbon source for PHB production while a poor one for hydrogen production. Moreover, Khatipov et al. (1998) demonstrated in their study with a strain of *R.sphaeroides*, that acetate is the most advantageous substrate for PHB production. Lorrungruang et al. (2006) also reported that it was a convenient substrate for PHB production because it is precursor of acetyl-coA in PHB synthesis.

The competition between those pathways was proven by mutation studies performed with some other PNS bacteria. For instance, Kim et al. (2011) mutated the key enzyme of PHB synthesis pathway, *phbC,* in *R.sphaeroides* KD131. They presented in the study that hydrogen yield increased around two fold when the acetate was the sole carbon source. In addition, Yang and Lee (2011) who mutated *phbC* of *R.palustris* WP3-5, demonstrated that the total collected biogas volume produced by the mutant strain was 1.7 times higher than that of the wild type. Therefore, high concentrations of acetate may decrease efficiency of hydrogen production by *R.capsulatus.* In this study, *R.capsulatus* cells were grown in media containing different acetate concentrations so as to determine optimum acetate concentration for efficient hydrogen production. Experimental set-up is as given in Section 2.4.3.

Hydrogen production was evaluated daily and total PHB production was measured at the end of the run.

3.2.1 Hydrogen Production at Different Initial Acetate Concentrations

Hydrogen production at different initial acetate concentrations is given in Figure 3.3. Hydrogen production was observed at all initial acetate concentrations. Yet, initiation of hydrogen production was not the same at different initial acetate concentrations. To illustrate, at 10 mM and 25 mM acetate, hydrogen production started earlier; between 24^{th} hour and 48^{th} hour, hydrogen production at these concentrations were about 1-2 mmole. However, this amount of hydrogen gas evolved after the 48th hour at 50 mM and 65 mM.

When the cumulative hydrogen amount is examined, it is seen that, total hydrogen gas increased in parallel with acetate concentration.The lowest cumulative hydrogen production, which was 2.5 mmole, was observed at 10 mM acetate. The highest cumulative hydrogen production was observed at 50 mM and 65 mM acetate, which were 11.7 and 11.4 mmoles, respectively (Table 3.2). In addition, hydrogen production at low acetate concentrations (10 and 25 mM) ceased earlier than those of high concentrations (50 and 65 mM) probably due to early depletion of acetate in the media. On the other hand, hydrogen production at 50 mM and 65 mM lasted for longer periods. The reason for this is the injection of BP medium to the culture. As it has been mentioned in Section 2.4.4, samples were taken periodically form the culture for analysis. As soon as the samples were taken, equal volumes of BP medium, which does not contain acetate and nitrogen, were injected to the culture. Yet, it contained solutions of vitamin, trace elements and ferric citrate. BP medium injection was necessary in order to prevent negative pressure that may occur in the

culture. In this way, necessary elements, which are needed for nitrogenase enzyme to work, are kept at a certain level. Kars et. al. (2006) showed in their study, in which they investigated the effects of iron concentration on hydrogen production, that at iron salt concentrations lower than 0.1 mM low amount of cumulative hydrogen was produced. It was also indicated that hydrogen production was not observed in the absence of iron. Moreover, Uyar (2008), also showed that at lower iron concentrations (2.04 and 20.4 μM in the form of Ferric (III) citrate) cumulative hydrogen production was low. From these results, in the current study, it is obvious that iron concentraton did not decrease in media during the runs as ferric citrate was added continuously and therefore hydrogen production at 50 mM and 65 mM persisted until the acetate was consumed.

Vitamin solution addition is another factor that caused hydrogen production to last. It is known that vitamins are required for the long term preservation of the bacteria. It is stated that when there is absence or lack of vitamins, bacteria weaken and lose their colonial characteristics (Koku et al.,2003). So by continuously adding vitamins to the culture, bacteria were preserved and hydrogen production lasted longer.

Although cumulative hydrogen production at 50 and 65 mM acetate concentrations was almost equal, the hydrogen amount throughout the experiment was higher at 50 mM acetate (Figure 3.3). This might be because of the inhibitory effect of higher acetate concentration. In a previous study by Asada et al. (2008) it was reported that 84 mM and 168 mM acetate concentrations were inibitory to hydrogen production by immobilized *R.sphaeroides* strains.

From these results, it can be concluded that hydrogen production was limited at low acetate concentrations. Similar results were shown in studies done with *R.capsulatus*

and other purple non sulfur bacteria. Özgür et al. (2010) who studied with *R.capsulatus* demonstrated that there was higher hydrogen production at 40 mM acetate than those at 10 and 20 mM acetate concentrations. Likewise, Barbosa et al. (2001) who studied with a *R.palustris* strain and *Rhodopseudomonas* species, showed that evolved hydrogen gas decreased when acetate concentration was decreased from 22 mM to 6 mM.

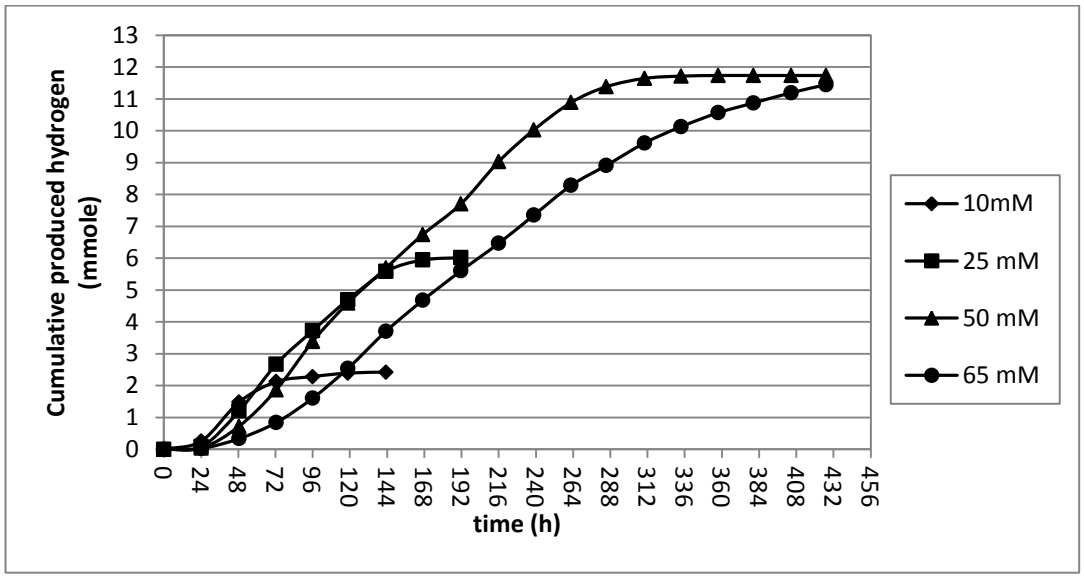

Figure 3.3 Hydrogen production by *R.capsulatus* in media containing different concentrations of acetate and 2 mM glutamate.

Table 3.2 Cumulative hydrogen amount and maximum biomass of *R.capsulatus* in media containing different concentrations of acetate and 2 mM glutamate.

Acetate concentration (mM)	Cumulative hydrogen amount (mmole)	Maximum biomass (gdw/Lc)
10 mM	2.4	0.58
25 mM	6.0	0.65
50 mM	11.7	0.77
65 mM	11.4	0.85

3.2.1.1 Modelling of Hydrogen Production at Different Initial Acetate Concentrations

In Figure 3.3, hydrogen production curve is given. As it is seen from the figure, hydrogen production increases slowly from start of the experiment up to a certain point. Then hydrogen production increases rapidly with a constant rate and finally approaches to an asymptotic value without further increase.

Modified Gompertz Model is a commonly used kinetic model which can be applied to hydrogen production data (Mu et al., 2007; Nath et al., 2008; Wang and Wan, 2009).

The equation for the Modified Gompertz Model is:

$$H = H_{max} \exp\left\{- \exp\left[\frac{Rmax^e}{Hmax}(\lambda - t)+1\right]\right\} \quad (3.4)$$

H and H_{max} are the instantaneous and the maximum cumulative hydrogen amounts in millimoles, respectively. R_{max} is the maximum hydrogen production rate (slope of the straight line cutting the time axis at λ, which is the lag time in hours) in millimole per hour. In the current study, Curve Expert 1.3 was used to fit the experimental data to the model. The curves fitted to this model for *R.capsulatus* cells at different initial acetate concentrations are obtained. One of the curves is given in Figure 3.4 for 50 mM acetate. Other model curves are given in Appendix E.

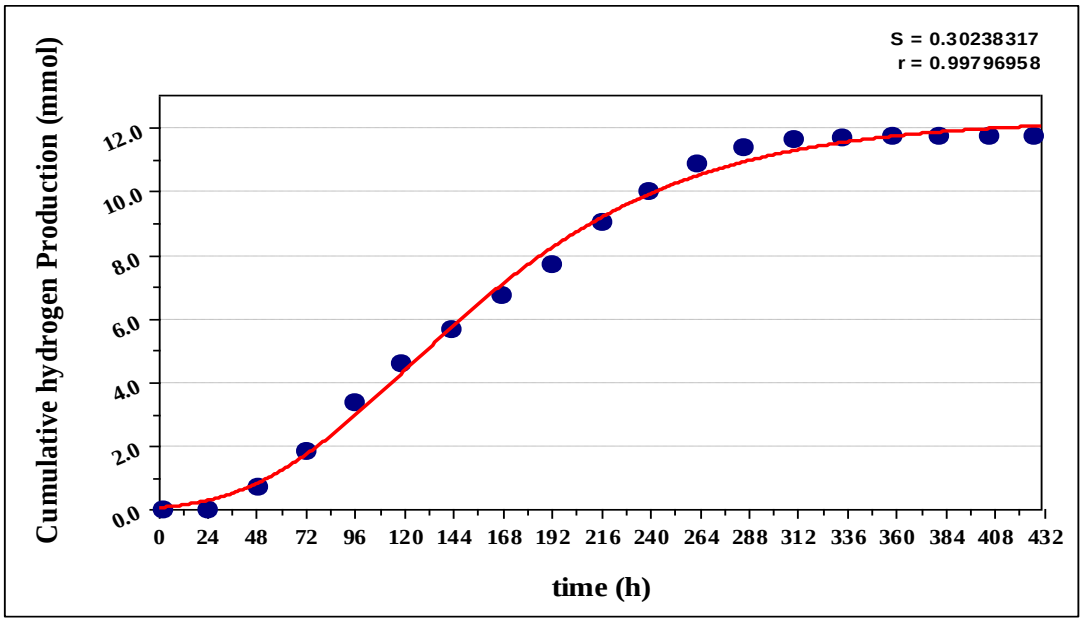

Figure 3.4 The Modified Gompertz Model of *R.capsulatus* for 50 mM acetate concentration

From the experimental data, maximum cumulative hydrogen production ($H_{max,e}$), maximum rate of hydrogen production ($R_{max,e}$) and the lag time ($\lambda_{,e}$) were calculated. From the model, maximum cumulative hydrogen production ($H_{max,m}$), maximum rate of hydrogen production ($R_{max,m}$) and the lag time ($\lambda_{,m}$) were evaluated. In addition to these values, r value which is the extent of fit, is calculated. R value shows the similarity between experimental results and the model The results are shown in Table 3.3

Table 3.3 Comparison of the Modified Gombert Model paremeters with the experimental values obtained at different initial acetate concentrations.

	10 mM	**25 mM**	**50 mM**	**65 mM**
r	0.999	0.999	0.998	0.999
$\mathbf{H_{max,e}}$	2.4	6.0	11.7	11.5
$\mathbf{H_{max,m}}$	2.4	6.3	12.3	12.3
$\mathbf{R_{max,e}}$	0.04	0.05	0.05	0.04
$\mathbf{R_{max,m}}$	0.05	0.06	0.06	0.04
$\boldsymbol{\lambda_{,e}}$	15	23	33	53
$\boldsymbol{\lambda_{,m}}$	21	31	46	65

From the table it is seen that r values at all acetate concentrations are close to 1 which indicates that the experimental data at all concentrations fit well to the model. In addition, experimental maximum cumulative hydrogen production (H_{max}), maximum rate of hydrogen production (R_{max}) and the lag time (λ) values are quite close to the model values.

Maximum cumulative hydrogen production increases as the acetate concentration increases. Similarly, lag time increases in parallel with acetate concentration.

3.2.2 Effect of Initial Acetate Concentration on PHB Production

PHB production at each acetate concentration was determined when the hydrogen production ceased. Therefore, when the hydrogen production stopped, cell pellets were collected by centrifugation. So those total PHB amount values give total PHB production after the cease of hydrogen production.

Total PHB amount at the end of the each run and percent of cellular dry weight values are given in Table 3.4 and Figure 3.5. was observed that the PHB amount increased with increasing acetate concentration. The lowest total PHB amount and the highest total PHB amount was seen at 10 mM and 65 mM acetate, respectively.

Total PHB amount produced at 10 mM was 0.12 mg/ml and it was lower than 1% of cellular dry weight. As it is seen from the growth curve (Figure 3.1), there was a slight increase in growth after 72^{th} hour although cells entered death phase. It is known that PHB can be used as a carbon and energy source and can be degraded (Sudesh et al., 2000). Consequently, it might be asserted that this increase in growth may be due to utilization of PHB by the cells.

PHB production was about 3.85 % and 11.92 % of cellular dry weight at 25 mM acetate and 50 mM acetate, respectively. At 65 mM acetate PHB amount was nearly 40 % of the cellular dry weight. This amount was 10.4 folds and 3.4 folds were higher than that at 50 mM and 25 mM, respectively. There was also huge difference between the total PHB amount at 25 mM and 50 mM acetate concentrations. To demonstrate, the PHB amount at 50 mM was 3.1 folds higher than that at 25 mM acetate concentration. Cumulative hydrogen amount with total PHB amount values

show that higher concentrations of acetate is required for both of these processes. These results are in good agreement with the previous studies carried out with other PNS bacteria. To illustrate, in a study done with *R.palustris* 42 OL, it was shown that *R.palustris* produced PHB up to 8.8 % of CDW while growing in a media containing 60 mM sodium acetate and approximately 4.5 mM NH_4Cl as carbon and nitrogen source, respectively (Philippis et al. 1992). In addition, Sangkharak and Prasertsan (2007) presented in their study done with *R.sphaeroides* N20 that PHB increased with the increase of acetate concentration from 3.0 g l-1 to 5.0 g l-1. Hustede et al. (1993) also examined PHB production by growing *R.sphaeroides* cells at 10 and 30 mM acetate concentrations. They reported that the total PHB produced at 30 mM was 2 folds higher than that at 10 mM acetate. However, total PHB amount produced by *R.sphaeroides* is much higher than that of *R.capsulatus*. In the study, the PHB amount was found to be 30 % and 70 % of cellular dry weight at 10 mM and 30 mM acetate, respectively. The dissimilar acetate assimilation pathways of *R.sphaeroides* and *R.capsulatus* account for the huge difference between the PHB amounts. In the pathway that *R.sphaeroides* uses for acetate assimilation, which is ethylmalonyl-CoA pathway, initial steps are the same with the pathway of PHB synthesis. In other words, initial steps of both pathways include formation 3-hydroxybutyryl-coA from two acetyl-coA molecules. They separate at PHB polymerazaiton/Crotonyl-coA formation steps. Thus, simultaneous PHB synthesis can take place during acetate assimilation in *R.sphaeroides* cells which explains more PHB formation compared to *R.capsulatus.* The pathway that *R.capsulatus* cells use is the citramalate cycle which does not possess shared steps with PHB synthesis pathway (Kars and Gündüz, 2010). Another PNS bacterium which was reported to be high PHB producer is *Rhodospirillum rubrum* Ha. Hustede et al (1993) showed that *R.rubrum* Ha accumulated PHB up to 44 % of CDW when it was grown in a 10 mM acetate medium. As it is seen, total PHB amount produced by *R.capsulatus* is much lesser when compared to *R.rubrum* Ha. Acetate assimilation pathway, which *R. rubrum* uses, may have caused it to produce high amounts of PHB. It was stated that *R.rubrum* has an unknown acetate assimilation pathway (Kars and Gündüz, 2010).

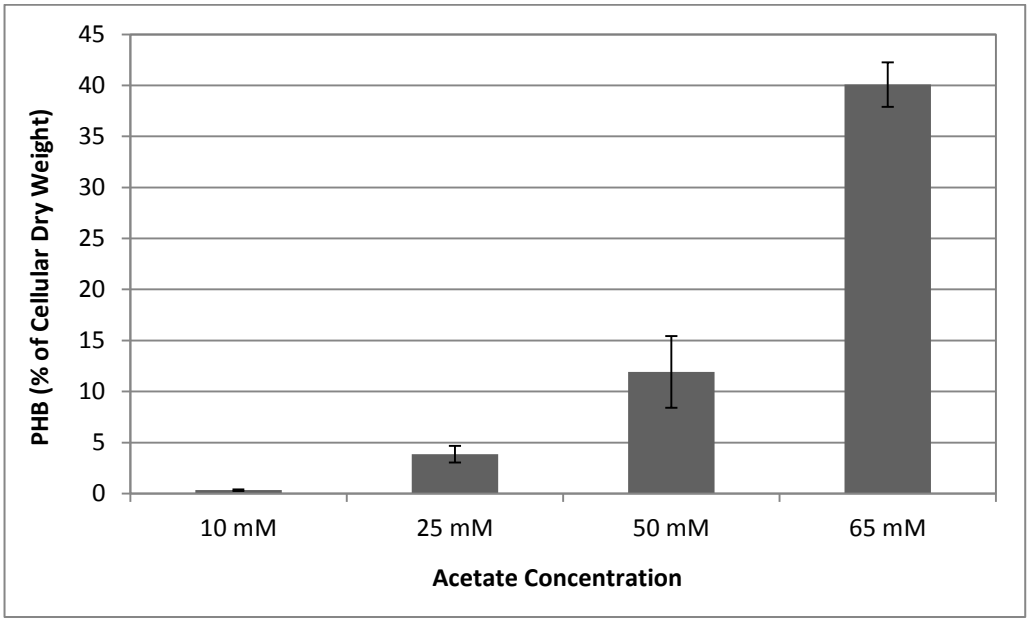

Figure 3.5 PHB production by *R.capsulatus* in media containing different concentrations of acetate and 2 mM glutamate.

A parameter which is called product yield factor for PHB is also evaluated. It is defined as the ratio of total PHB amount (grams) to the cellular dry weight (grams). Product yield factors at different acetate concentrations is given in table 3.4. Similarly, the highest value was observed at 65 mM acetate concentration.

Table 3.4 PHB production by *R.capsulatus* in media containing different concentrations of acetate and 2 mM glutamate.

Acetate concentration (mM)	**Total PHB amount (mg/ml)**	**PHB amount (% of cellular dry weight)**	**Product Yield Factor (g PHB/g cdw)**
10 mM	0.12	0.33	0.003
25 mM	1.43	3.85	0.038
50 mM	4.40	11.92	0.119
65 mM	12.91	40.08	0.401

3.2.3 Molar Productivity, Molar Yield, Product Yield Factor and Light Conversion Efficiency

Cumulative amount of hydrogen produced at the end and total PHB amount is not sufficient to give information about the effects of different acetate concentrations on both hydrogen and PHB production. Therefore, the parameters which are significant for analysis of hydrogen production should be evaluated. The parameters used in this study are molar productivity, molar yield, product yield factor and light conversion efficiency.

3.2.3.1 Molar Productivity

Molar productivity is calculated by:

$$\frac{Produced\ total\ H_2\ gas\ (mmole)}{culture\ volume\ \ L\ \ x\ t\ (hour)} \tag{3.5}$$

In this equation, t represents the duration of hydrogen production time from the end of the lag phase to the end of the hydrogen production. Culture volume in the current study is 0.11 L. Molar productivty can also be considered as molar rate of hydrogen production. Molar productivity at different acetate concentrations is shown at Figure 3.6 and Table 3.5. It is seen that the highest and the lowest molar productivity values were obtained at 25 mM and 65 mM acetate concentrations, respectively (Table 3.5 and Figure 3.6).

When productivity values at 50 mM and 65 mM are compared, it is clear that although cumulative hydrogen production was almost equal at 50 mM and 65 mM,

the productivity was higher at 50 mM (Table 3.1). This result shows that hydrogen production at 50 mM was more efficient compared to 65 mM. Total PHB amount, which was 3.4 folds higher at 65 mM than that of 50 mM, also confirms this result (Table 3.4).

Low amount of hydrogen was produced at 25 mM compared to 50 mM (Table 3.2). However, productivity was higher at 25 mM than that of 50 mM. The reason for the lower productivity might be due to the total PHB production which was higher at 50 mM than that of 25 mM (Table 3.4).

Similar results were reported by Özgür et al. (2010) who demonstrated that hydrogen productivity (in mg/Lc.h) decreased as the acetate concentration increased from 30 mM to 50 mM. Likewise, lower molar productivity values at high acetate concentrations (at 60 mM and 80 mM) were illustrated by Androga et al. (2011) who studied in large scale with uptake hydrogenase mutant *(hup$^-$) R.capsulatus* strain. These results strongly indicate that at high acetate concentrations hydrogen productivity is reduced.

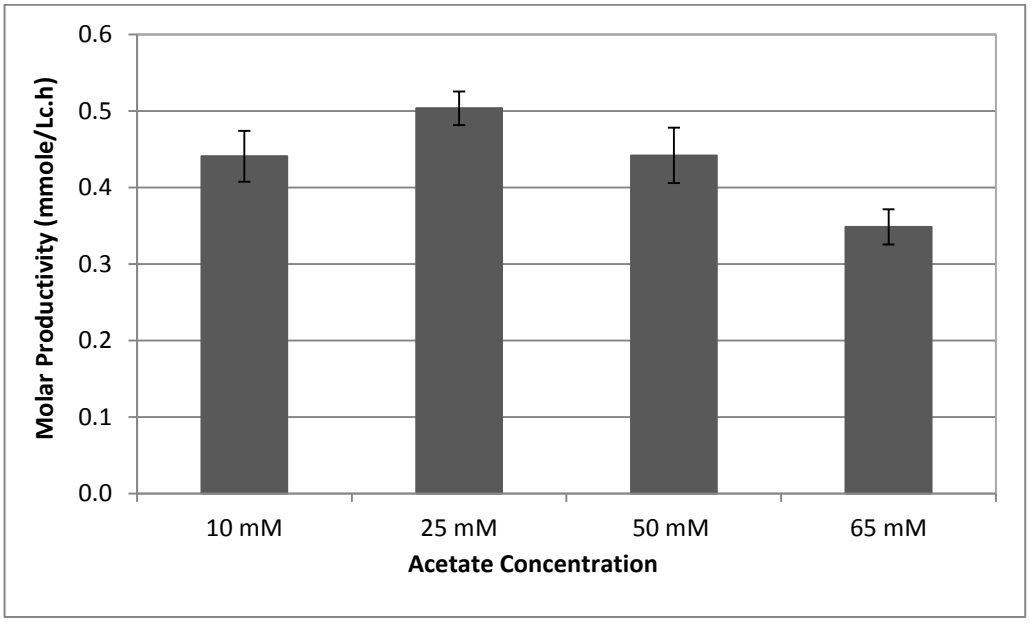

Figure 3.6 Molar productivity at different initial acetate concentrations.

3.2.3.2 Molar Yield

Molar yield is defined as the percentage of the ratio of moles of evolved hydrogen gas to the theoretical moles of hydrogen gas that could be produced from consumed substrate. Molar yield can also be referred as substrate conversion efficiency as it gives the percentage of substrate that was used for hydrogen production.

According to equation 3.7, 4 moles of hydrogen gas is expected to be produced per mole of consumed acetate. Molar yield values at different initial acetate concentrations are shown at Figure 3.7 and Table 3.5.

Molar yield is calculated by:

$$\frac{Produced\ total\ H_2\ gas\ \ mmole}{Theoretical\ millimoles\ of\ H_2\ gas\ that\ would\ be\ produced\ from\ utilized\ organic\ acids}\ x\ 100 \quad (3.6)$$

$$C_2H_4O_2 + 2H_2O \rightarrow 4H_2 + 2CO_2 \quad (3.7)$$

The highest and the lowest molar yield values were obtained at 50 mM and 65 mM, respectively. On the other hand, molar yield values at 25 mM and 50 mM were virtually equal. In other words, more than 50 % of the consumed substrate was converted to hydrogen at all concentrations except at 65 mM. The reason for the lower molar yield at 65 mM is definitely the total PHB amount which was 10 % of cellular dry weight. Androga et al. (2011) showed that molar yield values decreased with increasing acetate concentration. In addition, Özgür et al. (2010) indicated that the highest substrate conversion efficieny was observed at 30 mM acetate rather than at higher acetate concentrations.

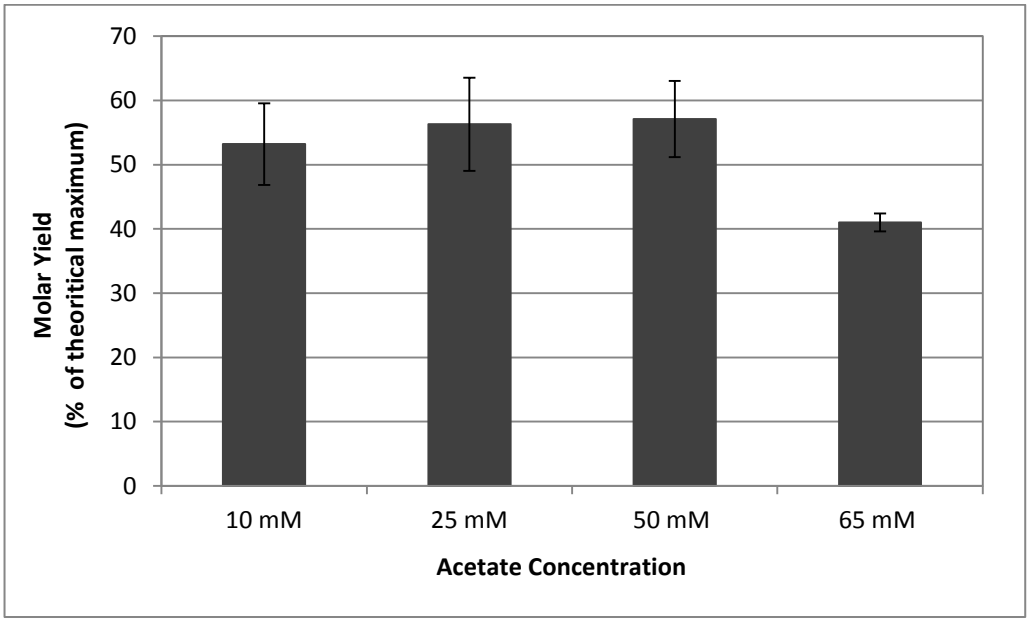

Figure 3.7 Molar yield at different initial acetate concentrations.

3.2.3.3 Product Yield Factor

Product yield factor is defined as the ratio of cumulative hydrogen amount to the maximum dry cell weight.

Product yield factor is calculated by:

$$\frac{Produced\ total\ H_2\ gas\ (mmole)}{Maximum\ dry\ cell\ weight\ (g)} \tag{3.8}$$

Product yield factor values at different acetate concentrations are given at Figure 3.8 and Table 3.5.

The lowest product yield factor was seen at 10 mM acetate; the highest product yield factor was observed at 50 mM acetate. In contrast to molar productivity and molar yield values, product yield factor at 25 mM was lower than that at 65 mM and 50 mM.

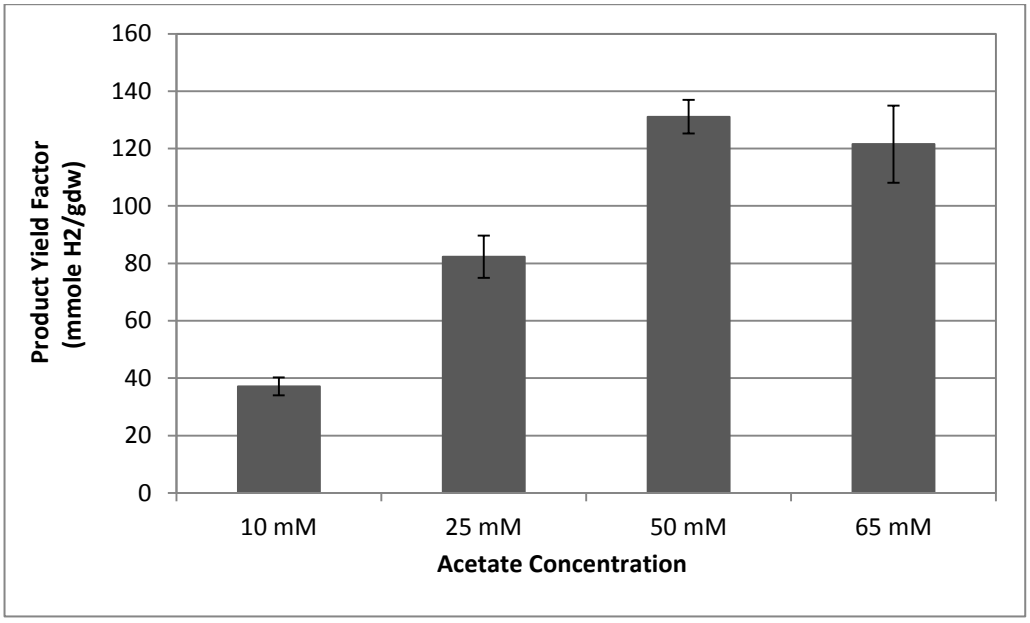

Figure 3.8 Product yield factor at different initial acetate concentrations.

3.2.3.4 Light Conversion Efficiency

b

Light conversion efficiency is calculated by:

$$\eta \ \% \ = \frac{33.6 \ x \ \rho H_2 \ x \ \mathrm{VH}}{I \ x \ A \ x \ t} \ x \ 100 \qquad (3.9)$$

In the equation, VH_2 is the volume of produced hydrogen in liters; ρH_2 is the density of the produced hydrogen gas in g/L; I is the light intensity (W/m^2); A is the irreadiated area (m^2) and t is the duration of hydrogen production from the end of the lag phase to the end of the experiment. Light converison efficiency at different acetate concentrations is given at Figure 3.9 and Table 3.5. Similar to molar yield and molar productivity, light conversion efficiency at 65 mM acetate is low compared to 25 mM and 50 mM acetate concentrations.

As has been indicated in Section 3.1, biomass concentraton was higher at 65 mM acetate than that at 25 and 50 mM. So the low light conversion efficiency at 65 mM may be owing to increased biomass which decreases light intensity because of shading (Barbosa et al., 2001; Özgür et al., 2010).

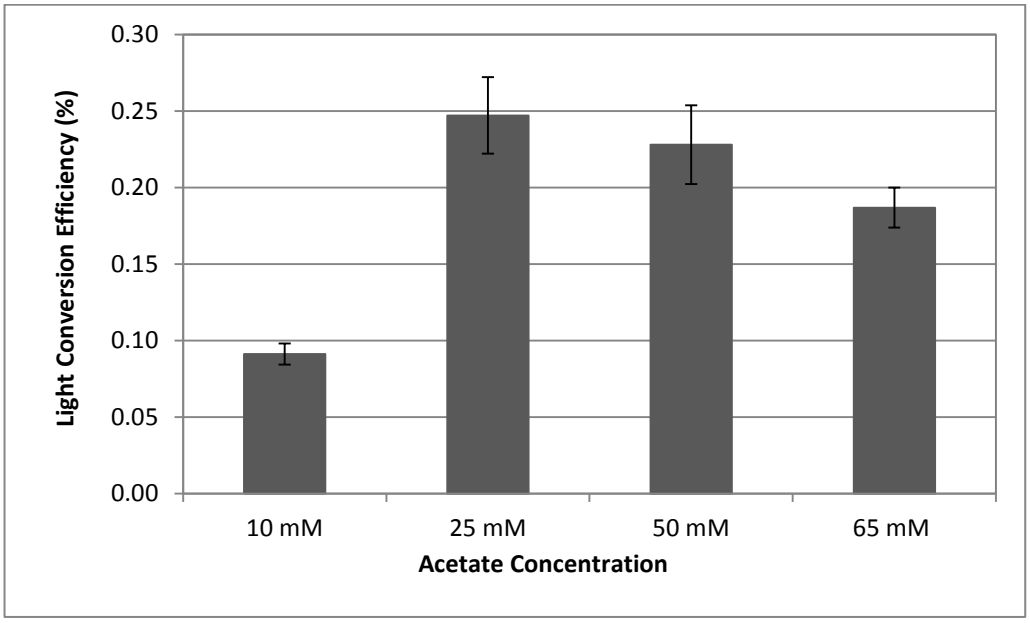

Figure 3.9 Light conversion efficiency at different initial acetate concentrations.

Table 3.5 Cumulative hydrogen amount, productivity, molar yield, product yield factor by *R.capsulatus* in media containing different concentrations of acetate and 2 mM glutamate.

Acetate Concentration (mM)	Molar Productiviy (mmole/Lc.h)	Molar Yield (% of theoretical max)	Product Yield Factor ($mmoleH_2/dw$)	Light Conversion Efficiency (%)
10 mM	0.44	53.2	37.2	0.09
25 mM	0.50	56.3	82.3	0.25
50 mM	0.44	57.1	131.1	0.23
65 mM	0.35	41.0	121.5	0.19

To sum up, the lowest molar productivity and molar yield was observed at 65 mM although the highest cumulative hydrogen amount was also seen at 65 mM acetate concentration (Table 3.5). As mentioned previously, total PHB amount was much more higher at 65 mM than that at 25 mM and 50 mM acetate concentrations (Table 3.4 and Figure 3.5). From these results, it might be concluded that high acetate concentration above a certain level promotes PHB production rather than hydrogen production.

3.3 Effect of Initial Acetate Concentration on pH

Initial pH of the cultures containing different concentrations of acetate (10-65 mM) was adjusted to around 6.4 by adding 5 M NaOH during the preparation of the media. KH_2PO_4 buffer was also added into media in order to keep pH of the cultures in the desirable range. Culture samples were taken to examine pH change during the runs. pH change at different initial acetate concentrations are demonstrated at Figure 3.10.

At all acetate concentrations, there is a parallel increase in biomass concentration with the pH (Figure 3.1a and 3.10). It was previously reported by Pekgöz (2010) and Akköse (2008) that pH change and growth was correlated.

At the beginning of the runs, the initial pH of the cultures was around 6.6 while during the runs pH was within the range 6.6-7.6 which was optimum for hydrogen production (Sasikala et al., 1991). As previously mentioned, pH of the cultures were maintained in the optimum range since KH_2PO_4 buffer was added in to the media. In spite of the fact that pH was in the optimum range at all concentrations, pH at 50 mM and 65 mM acetate (generally over 7.2) was higher when compared to 10 mM and 25 mM (Figure 3.10). Therefore, elevated acetate concentration seems to cause increase of pH in the culture. This was also indicated by Kim et al. (2006) who studied with *R.sphaeroides.* They showed that pH increased from 6.8-7.0 to 9.2-9.4 when acetate was the carbon source. Additionally, when compared to some other carbon sources acetate was shown to cause increase in pH. For instance, Kars et al. (2006) and Uyar et al. (2009) demonstrated that pH was higher in acetate containing media than in those that contain malate or lactate as carbon sources.

Most importantly, it was stated that there is a correlation between elevated pH levels and PHB production (Hustede et al., 1993; Khatipov et al, 1998; Brandl et al., 1991). Hustede et al. (1993) demonstrated that wild type *R. sphaeroides* cultures produced more hydrogen and less PHB when they were grown in buffered acetate containing media. The correlation between pH and PHB was investigated by Khatipov et al. (1998) as well. They showed high PHB production and low hydrogen production by *R.sphaeroides* when the initial pH of the lactate medium was changed from 6.8 to 7.5. It was stated that the final pH of the medium reached almost to 10 and hydrogen production became ten folds lower than before. In this study, as has been stated, pH

at 50 mM and 65 mM acetate was higher than that at 10 mM and 25 mM which may have caused more PHB production at those concentrations.

From previous and current results, it can be concluded that elevated acetate concentration may cause pH increase in culture, which will eventually lead to more PHB production. Therefore, for efficient hydrogen production, it is important to use buffered systems in order to maintain pH level in desired range.

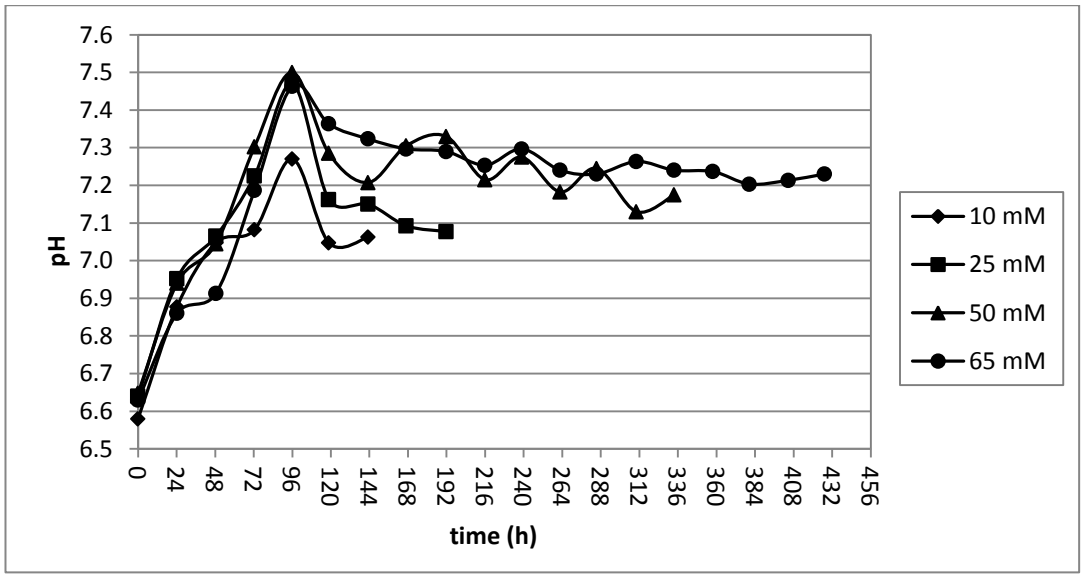

Figure 3.10 pH change in media containing different concentrations of acetate.

3.4 Consumption of Acetate and Formation of Lactic, Propionic and Formic Acids

3.4.1 Consumption of Acetate

Acetate utilization by *R.capsulatus* cells with respect to time is given in Figure 3.11. In 10, 25 and 50 mM acetate containing media, acetate was consumed completely whereas in 65 mM acetate containing cultures it was not totally used up. Nearly 3 mM acetate was unused in 65 mM acetate containing media.

In 10 mM and 25 mM acetate containing cultures, acetate was consumed on the third and seventh day of the experiment, respectively. This accounts for the early cease in hydrogen production at those concentrations.

Interestingly, although acetate was finished completely on the third day, there was a slight increase in cell growth in 10 mM acetate containing cultures (Figure 3.1a). It is known that PHB can be used as carbon and energy source when degraded (Sudesh et al. 2000). Therefore, the reason for the increase in cell growth may be due to the use of accumulated.

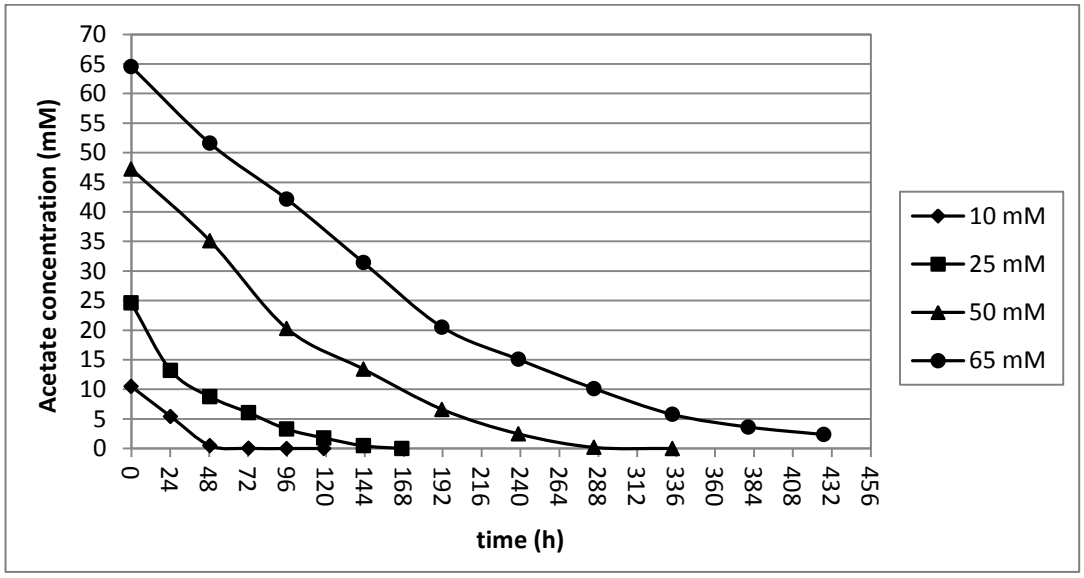

Figure 3.11 Acetate consumption by *R.capsulatus* in media containing different concentrations of acetate.

3.4.1.1 Modelling of Acetate Consumption

Integration method is commonly used in the kinetic analysis of several chemical processes (Sevinç, 2010). In this study, integration method is applied to the data of acetate consumption. The equation for the integration method is:

$$-\frac{dC}{dt} = k.C^n \tag{3.10}$$

where k is the rate constant and n is the order of reaction. A function of concentration, f(C) is obtained by integration of equation 3.6. The rate equations and the corresponding functions of concentrations for zeroth, first and second order processes are:

Zeroth order: $C\text{-}C_0 = -k\ (t\text{-}t_0)$ (3.11)

First order: $\ln \frac{C}{C_0} = -k\ (t\text{-}t_0)$ (3.12)

Second order: $\frac{1}{C} - \frac{1}{C_0} = k\ (t\text{-}t_0)$ (3.13)

For analysis, every rate equation is tried for each concentration by using concentration versus time graph presented in Figure 3.9 and equations of best fitting curves were determined. The rate constants (k), and the coefficient of determination values (R^2) of experimental data are shown in Table 3.6. In addition, the curve for 25 mM is given in Figure 3.12 as an example. Curves for other acetate concentrations are given in Appendix H.

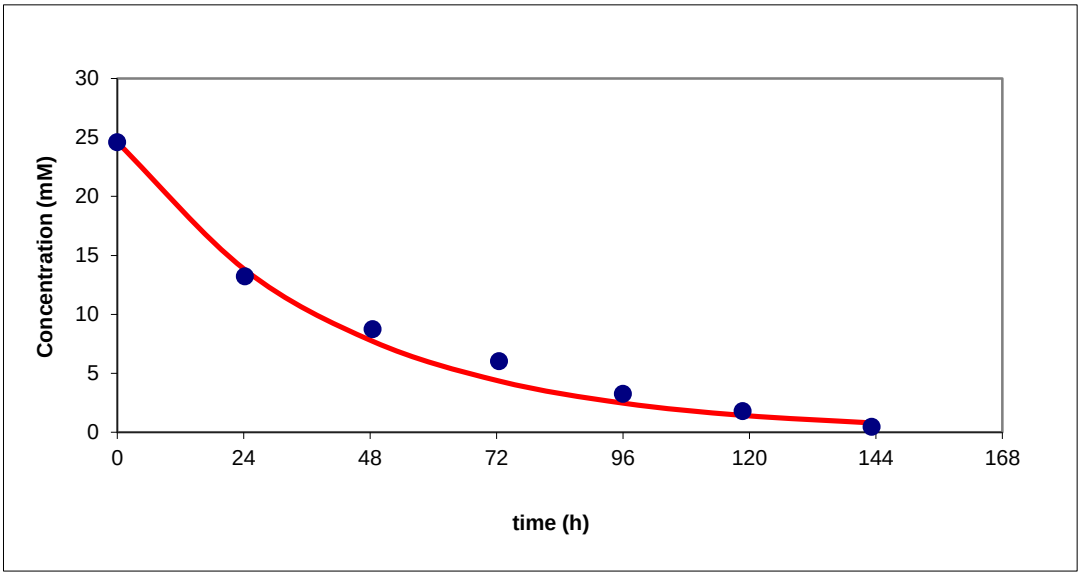

Figure 3.12 First order kinetics for acetate consumption at 25 mM initial concentration.

Table 3.6 Extent of the fits and rate constants for acetate consumption at different initial acetate concentrations.

	Zeroth Order (n=0)		**First Order (n=1)**		**Second Order (n=2)**	
Acetate Concentration	**k_0**	**R^2**	**k_1**	**R^2**	**k_2**	**R^2**
10 mM	0.1664	0.8989	**0.0755**	**0.9021**	0.4572	0.5542
25 mM	0.2038	0.7124	**0.0239**	**0.9479**	0.0079	0.5005
50 mM	0.2106	0.9377	**0.0108**	**0.9469**	0.0162	0.3437
65 mM	0.1974	0.9533	**0.0065**	**0.9654**	0.0006	0.7224

It is seen from the table that at all initial acetate concentrations, acetate was consumed through first order kinetics. It is also seen that rate constant (k_1) decreases with increasing acetate concentration.

Apart from these parameters, half life values at different initial acetate concentrations were also evaluated. Half life is the time in which one half of the initial concentration of a substance is consumed. Half life for a first order process is calculated according to the equation:

$$t_{1/2} = \ln 2/k \qquad (3.14)$$

Half life values at different initial acetate concentrations are given in Table 3.7. It is seen that half life values increase with increasing acetate concentration.

Table 3.7 Half life values at different initial acetate concentration.

Acetate Concentration	$t_{1/2}$ (hours)
10 mM	9.2
25 mM	29.0
50 mM	64.2
65 mM	106.6

Özgür et al., (2010) reported in their study with *R.capsulatus*, that acetate was consumed through first order kinetics at 30 mM or lower initial acetate concentrations which is inconsistent with the current work. However, they showed that acetate was consumed through second order kinetics when the initial acetate concentration was 40 mM or higher. The possible reason for this difference is the dissimilarity in carbon sources of the growth media used in these two studies. The growth media used by Özgür et al. contained 7.5 mM malate whereas growth media used in the present study consisted of 20 mM acetate as only carbon source. In other words, *R.capsulatus* cells in the current study were adapted to utilize acetate since they were grown in acetate containing growth media before inoculation to hydrogen production media. Therefore, they consumed it through first order kinetics. This was also presented in previous studies done by using *R.sphaeroides* cells (Koku et al., 2003; Eroğlu et al., 1999). In these studies, it was indicated that malate was consumed through first order kinetics by the *R.sphaeroides* cells which were grown in malate containing growth media before inoculation to hydrogen production media. For instance, Eroğlu et al. (1999) examined substrate consumption kinetics at different initial malate concentrations which were 7.5 mM, 15 mM and 30 mM and it was stated that *R.sphaeroides* cells were grown in malate containing media. As has been mentioned, they showed that malate was consumed through first order kinetics.

On the other hand, Uyar et al. (2009) who used *R.sphaeroides,* reported that when acetate was the only carbon source, consumption of it did not fit to either first or second order. Similar to studies mentioned above, *R.sphaeroides* were grown in malate containing growth media. On the contrary, in the same study, it was shown that when cells were grown in media, which contained butyrate and propionate as minor and acetate as the main substrates, it was observed that acetate was consumed with first order after the minor substrates in the media were depleted.

From the results obtained, it can be concluded that switch of carbon source from one to another may cause changes in the order of substrate consumption rate by purple non- sulfur bacteria. Özgür et al. (2010) suggested that shift in kinetics of substrate consumption from first order to second order at 40 mM or higher initial acetate concentrations, may imply alteration in metabolism of acetate. From this comment, it may be noted that this alteration is caused by PHB synthesis that occurred when the carbon source was changed. Thus, it might be asserted that it is important not to change carbon source in the growth media in order not to promote PHB synthesis which is a process reducing efficiency of hydrogen production.

3.4.2 Formation of Lactic Acid, Propionic Acid and Formic Acid

Along with consumption of acetic acid, formation of lactic acid, propionic acid and formic acid was also evaluated. Change in concentrations of them with respect to time is given in Figures 3.13-3.15.

Changes in lactic acid and propionic acid concentrations with respect to time is shown in Figures 3.13-3.14. Lactic acid and propionic acid concentrations were

lower than 1 mM at all initial acetate concentrations. It is seen from the graphs that more lactic acid and propionic acid formation was observed at high acetate concentrations (50 mM and 65 mM) compared to low acetate concentrations (10 mM and 25 mM). In addition, it is seen that there is fluctuation in concentrations of those acids during the experiment. From this, it may be concluded that they were formed and then consumed by *R.capsulatus* cells.

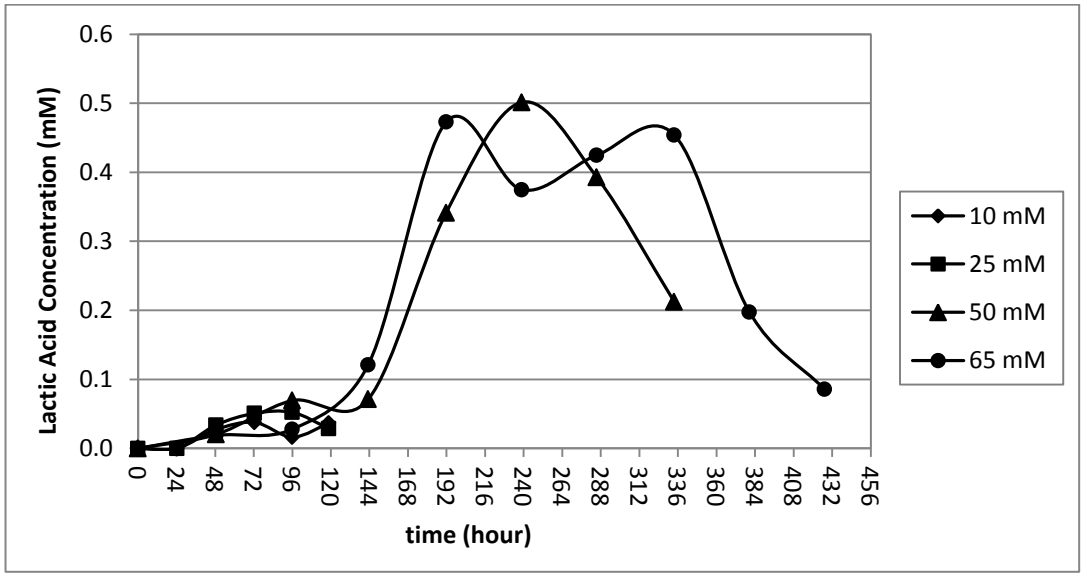

Figure 3.13 Formation of lactic acid by *R.capsulatus* in media containing different concentrations of acetate.

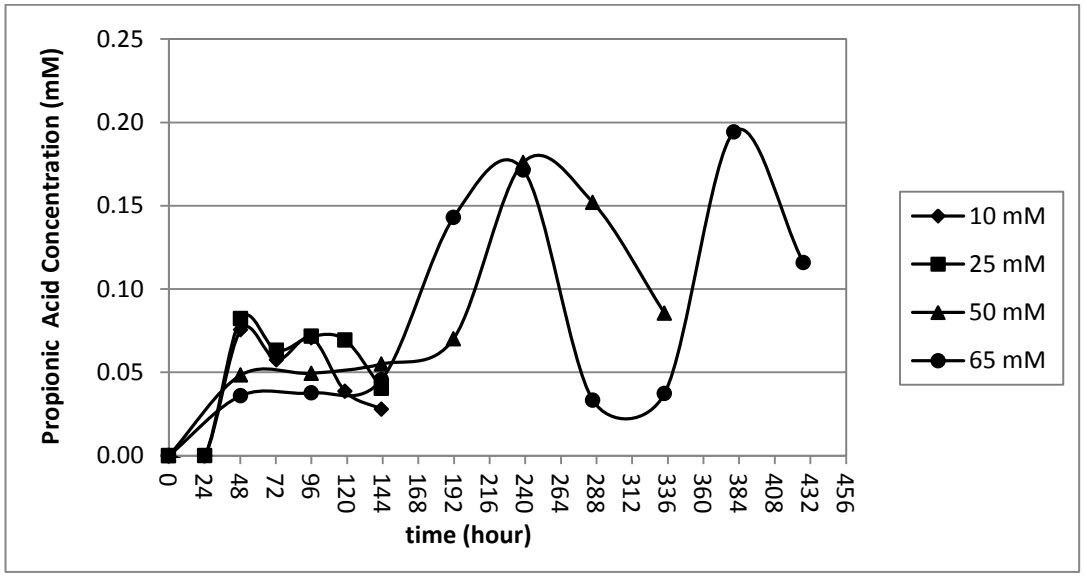

Figure 3.14 Formation of propionic acid by *R.capsulatus* in media containing different concentrations of acetate.

Changes in formic acid concentration with respect to time is given in Figure 3.15. Conversely, large amounts of formic acid was formed compared to lactic acid and propionic acid. Furthermore, in contrast to lactic acid and propionic acid, there was a gradual increase in formic acid concentration which means that formic acid was accumulated in the media instead of being consumed. Formic acid formation during hydrogen production was also observed in previous studies done by Özkan (2011), Pekgöz (2010), Sevinç (2010) and Androga (2009). It was outlined by Laurinavichene et al. (2008) in their study that formate did not support neither growth nor H_2 production by *R.capsulatus* B10. This explains formic acid accumulation in the media. High amount of formic acid production may have been owing to the NAD-dependent formate dehydrogenase, which catalyzes reversible conversion of CO_2 and $NADH,H^+$ to formic acid or by the action of pyruvate formate lyase , which forms formate from pyruvate (Androga, 2011).

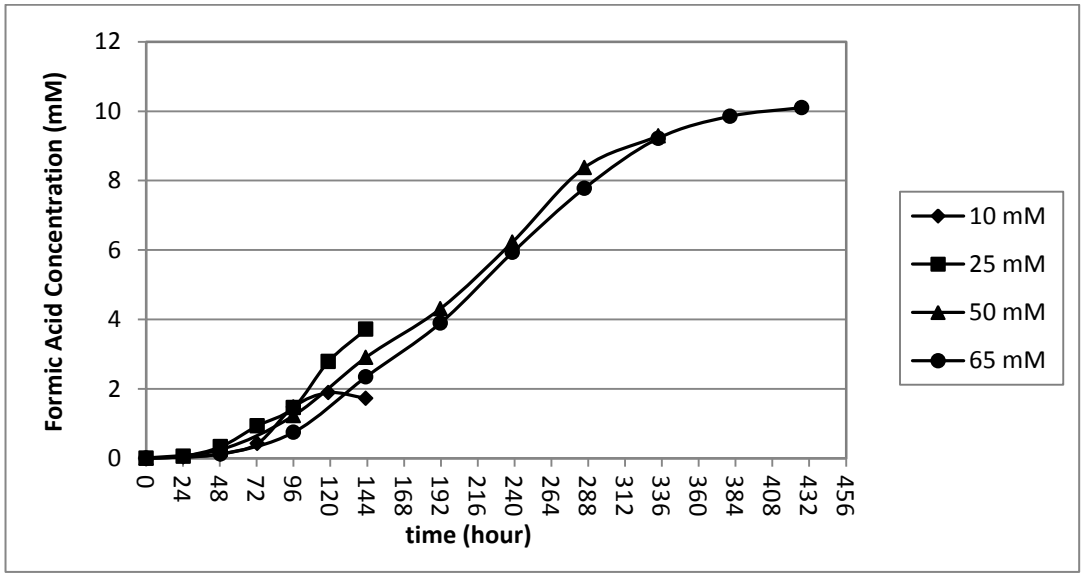

Figure 3.15 Formation of formic acid by *R.capsulatus* in media containing different concentrations of acetate.

3.5 Expression Analysis of the Key Genes of Hydrogen Production and PHB Synthesis

Acetate is one of the main carbon sources used for hydrogen production by PNS bacteria. In addition, dark fermentor effluents which contain high concentrations of acetate may decrease efficiency of hydrogen production by stimulating cell growth and PHB production. Therefore, determination of optimum acetate concentration for hydrogen production by PNS bacteria is necessary. Hydrogen production and PHB synthesis are two competing grown in acetate as carbon source. Therefore, it is important to examine the effects of acetate on the expression levels of the genes encoding key enzymes of these two processes. It was previously shown that expression of nitrogenase genes change with respect to different ammonium, iron and molybdenum concentrations (Akköse,2008; Akköse et al., 2009; Kars et al., 2006). Therefore, it is important to examine the effects of acetate on hydrogen and

PHB production at transcritional level. In this section, changes in expression levels of *nifD* (encodes α subunit of dinitrogenase) and *phaC* (encodes PHB synthase) at different initial acetate concentrations was studied.

R.capsulatus cells were grown at media containing different concentrations of acetate for gene expression analysis (Table 2.1). The cultures were grown in 50 mL sterile bottles which are connected to the glass cyclindirical tubes as explained in Section 2.4.3. Each run was terminated at the 68^{th} hour and total RNA isolation was performed. A sample gel photograph of isolated RNA is given in Appendix I. Quantification was done as explained in Section 2.6.2.4. Densitometric measurement ratio was calculated by dividing band intensity of *nifD* or *phaC* PCR products by band intensity of *16S rRNA* (internal control) PCR products.

During cDNA synthesis, controls, which do not contain reverse transcriptase (RT) were included in order to assure that there was no DNA contamination in the RNA samples.

The results were subjected to statistical tests by using the program Graphpad Prism 5 to determine significant difference between means of groups ($\alpha = 0.05$).

3.5.1 Effect of Acetate Concentration on Expression Levels of *nifD*

PCR products of *nifD* on 2% agarose gel are given in Figure 3.16. It is seen that at all initial acetate concentrations *nifD* was expressed. Length of PCR products is 163 base pair (bp). Products of PCR performed with cDNA controls (without reverse

transcriptase) confirm that there was no DNA contamination in the RNA samples (Figure 3.16b).

The expression levels of *nifD* gene at different acetate concentrations is given in Figure 3.17. Densitometric measurement ratio at all concentrations were higher than 0.4. Statistical analysis (done with Graphpad Prism 5) shows that the changes in *nifD* expression levels with respect to acetate concentration are not statistically significant. From this, it may be concluded that at all acetate concentrations *nifD* is expressed properly.

Although the changes were not statistically significant, it is seen from the bar garph that there were differences in *nifD* expression levels between the acetate concentrations (Figure 3.17). To illustrate, the lowest *nifD* expression was observed at 10 mM acetate concentration. The highest *nifD* expression, which was approximately 1.5 folds higher than that at 10 mM, was seen at 65 mM acetate. The expression levels at 25 mM and 50 mM were almost equal. These results are in good agreement with hydrogen production results (Figure 3.3). As previously mentioned, the highest cumulative hydrogen amount was at 50 mM and 65 mM acetate concentrations (Table 3.2). Therefore, it is expected to observe high *nifD* expression in these concentrations. Although cumulative hydrogen amount was lower at 25 mM than those at higher concentrations, *nifD* expression is quite high and almost equal to expression level at 50 mM. The reason for this is that RNA isolation was performed when cells were at the phase at which they were actively producing hydrogen.

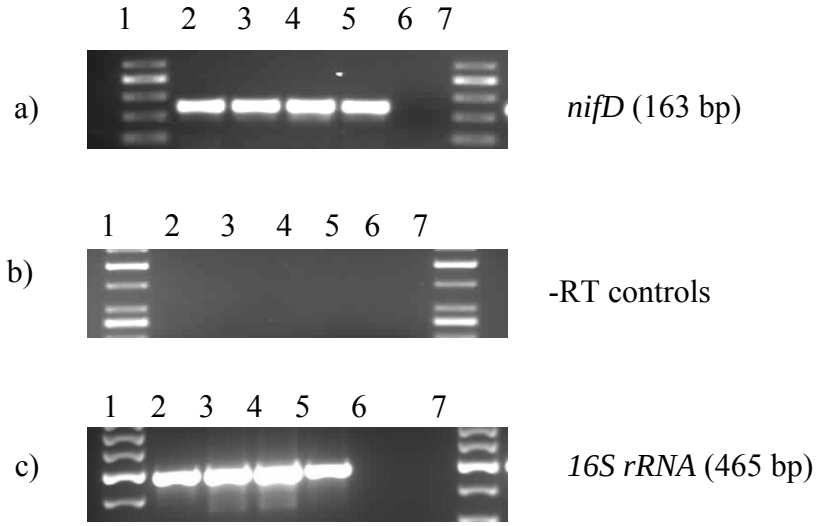

Figure 3.16 PCR products of a) *nifD* b) False positive control of *nifD* c) internal control: *16S rRNA* at different acetate concentrations. (2 % agarose gel) (Lanes 1,7: DNA Ladder (50 base pair); Lanes 2: 10 mM acetate containing medium; Lanes 3: 25 mM acetate containing medium; Lanes 4: 50 mM acetate containing medium; Lanes 5: 65 mM acetate containing medium; Lanes 6: No template control)

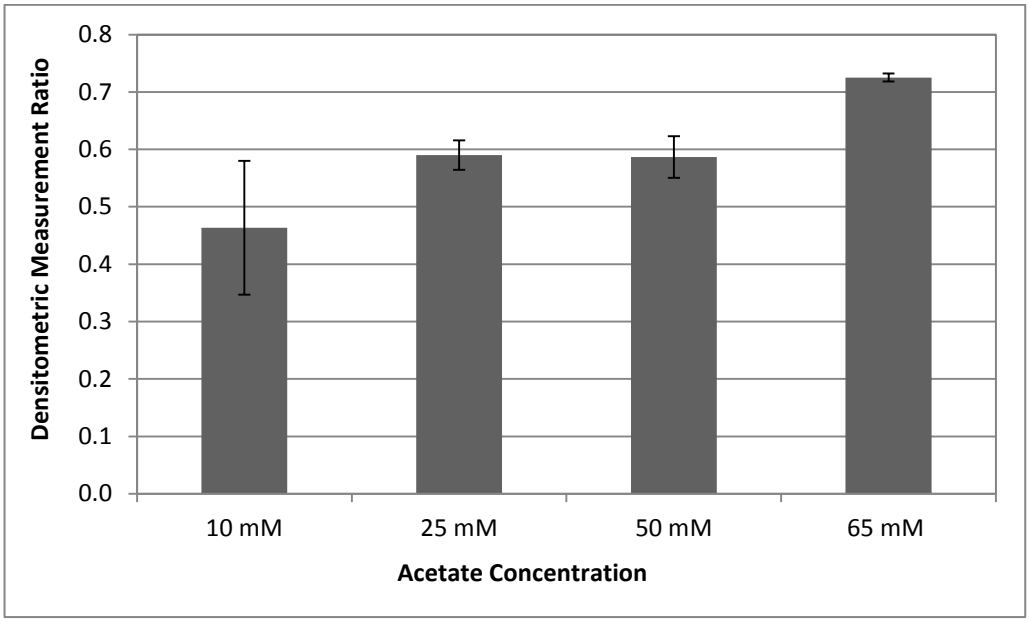

Figure 3.17 The expression levels of *nifD* gene at different acetate concentrations.

3.5.2 Effect of Acetate Concentration on Expression Levels of *phaC*

PCR products of *phaC* on 2% agarose gel are given in Figure 3.18. It is seen that at all initial acetate concentrations *phaC* was expressed. Length of PCR products is 145 bp. Products of PCR performed with cDNA controls (without reverse transcriptase) confirm that there was no DNA contamination in the RNA samples (Figure 3.18b).

The expression levels of *phaC* at different acetate concentrations are shown in Figure 3.19. Similar to *nifD*, at all initial acetate concentrations *phaC* was expressed. Densitometric measurement ratios were higher than 0.4 at all concentrations.

Statistical analysis (done with Graphpad Prism 5) shows that the changes in *phaC* expression levels with respect to acetate concentration are not significant. From this, it may be concluded that at all acetate concentrations *phaC* is expressed and its expression did not change depending on the acetate concentration.

Although the changes in the expression levels is statistically not significant, from the bar graph it is seen that *phaC* expression at 65 mM is higher compared to the other concentrations. Densitometric measurement ratio at 65 mM was approximately 1.3 folds higher than those at 10 mM, 25 mM and 50 mM. The significance of the difference may have been observed at acetate concentrations higher than 65 mM.

When the ratio values at lower concentrations (10 mM, 25 mM and 50 mM) are considered, it appears that there is no significant difference in the expression levels between the concentrations as shown statistically. Although total PHB amount at 10

mM and 25 mM were lower compared to 50 mM (Figure 3.5; Table 3.4), *phaC* expression levels are almost equal (Figure 3.18). It was previously reported by Kranz et al. (1997) that in *R.capsulatus* enzymes of PHB biosynthesis pathway are always present and the pathway is controlled post-translationally. These results may also indicate that there may be a post-translational control of PHB biosynthesis. However, the highest *phaC* expression was observed at 65 mM acetate which is the concentration that the highest total PHB amount was obtained (Figure 3.5; Table 3.4). Therefore, a transcriptional control of *phaC* in *R.capsulatus* is also possible. As previously explained in Section 1.8.5.2, some regulatory proteins, mechanisms which control *pha* synthetic genes were described in some other microorganisms (Kessler and Witholt, 2001). Hence, PHB synthesis seems to be regulated at both transcriptional and post-translational levels. Although no such regulatory control was described for *R.capsulatus* yet, it is possible that such systems exist. It is not clear whether such a system is related to acetate concentration.

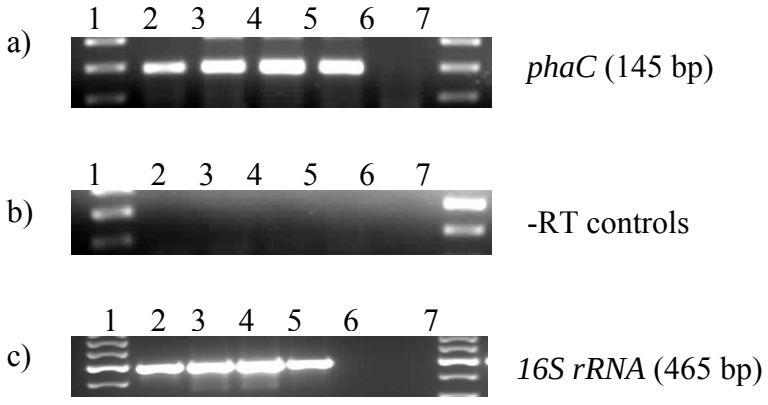

Figure 3.18 PCR products of a) *phaC* b) False positive control of *phbC* c) internal control: *16S rRNA* at different acetate concentrations. (2 % agarose gel) (Lanes 1,7: DNA Ladder (50 base pair); Lanes 2: 10 mM acetate containing medium; Lanes 3: 25 mM acetate containing medium; Lanes 4: 50 mM acetate containing medium; Lanes 5: 65 mM acetate containing medium; Lanes 6: No template control)

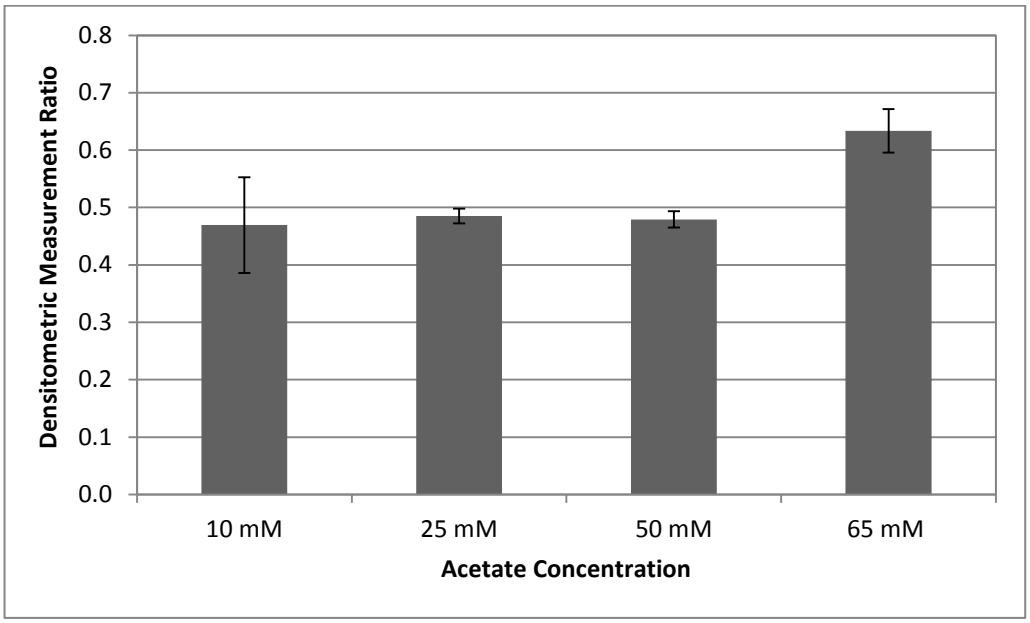

Figure 3.19 The expression levels of *phaC* at different acetate concentrations.

CHAPTER 4

CONCLUSION

The relationship between hydrogen and PHB production should be understood well in order to obtain a high yield in hydrogen production. In the present study, effects of acetate concentration on hydrogen and PHB production by *R.capsulatus* DSM 1710 were examined. Additionally, gene expression analyses of the genes that encode key enzymes of the pathways (*nifD* and *phaC*) were examined.

Based on the obtained results and discussion of these results, the followings are concluded:

i. Biomass concentration increased in parallel with the increased acetate concentration. However, this is not desirable for efficient hydrogen production since hydrogen production is affected negatively due to low light penetration in the culture. Cell growth at all acetate concentrations was found to fit the "Logistic Growth Model".

ii. Hydrogen production was limited at low acetate concentrations. The highest cumulative hydrogen amount was obtained at 50 mM and 65 mM acetate concentrations. In addition, hydrogen production at all concentrations was found to fit "Modified Gompertz Model".

iii. Total PHB amount increased in parallel with increasing acetate concentration.

iv. The highest total PHB amount was observed at 65 mM and the highest molar productivity, molar yield and light conversion efficiency were obtained at 25 mM and 50 mM acetate concentrations. Therefore, optimum acetate concentration for efficient hydrogen production with low PHB was found to be between 25 mM- 50 mM.

v. In integrated systems, dark fermentation effluents should be diluted before photofermentation step in order to acquire optimum acetate concentration.

vi. *R.capsulatus* DSM 1710 cells which are adapted to acetate by growing in acetate containing medium was found to consume acetate through first order kinetics.

vii. At all acetate concentrations *nifD* expression was observed and the results of expression level were found to be in correlation with hydrogen production results.

viii. At all acetate concentrations *phaC* expression was observed and the results of expression level were found to be in correlation with total PHB amount results.

REFERENCES

Akköse, S. 2008. Expression Analysis of Nitrogenase Genes in *Rhodobacter sphaeroides* O.U.001 Grown Under Different Physiological Conditions. Msc Thesis in Biology Department, Middle East Technical University, Ankara, Turkey.

Akköse, S., Gündüz, U., Yücel, M., Eroğlu, İ. 2009. Effects of ammonium ion, acetate, and aerobic conditions on hydrogen production and expression levels of nitrogenase genes in *Rhodobacter sphaeroides* O.U.001. International Journal of Hydrogen Energy 34, (21): 8818-8827.

Asada, Y., Ohsama M., Nagai, Y. et al. 2008. Re-evaluation of hydrogen productivity from acetate by some photosynthetic bacteria. International Journal of Hydrogen Energy, 33, (19): 5147-5150.

Asada, Y. and Miyake, J. 1999. Photobiological Hydrogen Production. Journal of Bioscience and Bioengineering, 88, (1): 1-6.

Androga, DD. 2009. Biological Hydrogen Production on Acetate in Continues Panel Photobioreactors Using *Rhodobacter capsulatus*. M.Sc.Thesis in Chemical Engineering Department, Middle East Technical University, Ankara, Turkey

Androga, DD., Özgür, E., Eroğlu, I., Gündüz, U., Yücel, M. 2011a. Significance of carbon to nitrogen ratio on the long-term stability of continuous photofermentative hydrogen production. International Journal of Hydrogen Energy, 36: 15583-15594.

Androga, DD., Özgür, E., Eroğlu, I., Gündüz, U., Yücel, M. 2011b. Factors affecting the long term stability of biomass and hydrogen productivity in outdoor photofermentation. International Journal of Hydrogen Energy, 36: 11369-11378.

Barbosa, J.M., Rocha M.S.J., Tramper J., Wijfels H.R. 2001. Acetate as a carbon source for hydrogen production by photosynthetic bacteria. Journal of Biotechnology, 85: 25-33.

Basak, N., Das, D. 2007. The prospect of purple non-sulfur (PNS) photosynthetic bacteria for hydrogen production: the present state of the art. Journal of Microbiology, 23: 31-42.

Benemann, J.R. 1997. Feasibility analysis of photobiological hydrogen production. International Journal of Hydrogen Energy, 22: 979-987.

Brandl, H., Gross, A.R.,Robert W.L., Lloyd, R., Fuller, C.R. 1991. The accumulation of poly (3-hydroxyalkonates) in *Rhodobacter sphaeroides.* Arch Microbiol, 155: 337-340.

Brentner, L.B., Peccia, J., Zimmerman J.B. 2010. Challenges in Developing Biohydrogen as a Sustainable Energy Source: Implications for a Research Agenda. Environmental Scienceand Technology, 44, (7): 2243-2254.

Burris, R. H. 1991. Nitrogenases. The Journal of Biological Chemistry, 266, (15): 9339-9342.

Castaneda, M., Guzman, J., Moreno, S., Espin, G. 2000. The GacS sensor kinase regulates alginate amd poly-beta-hydroxybutyrate production in *Azotobacter vinelandii.* Journal of Bacteriology, 182: 2624-2628.

Chanprateep, S. 2010. Current trends in biodegradable polyhydroxyalkanoates. Journal of Bioscience and Bioengineering, 110,(6): 621-632.

Claassen, P.A.M., De Vrije, T. 2006. Non-thermal production of pure hydrogen from biomass: HYVOLUTION. International Journal of Hydrogen Energy, 31: 1416-1423.

Cobley, J.G., Clark, A.C., Weerasurya, S., Queseda, F.A., Xiao, J.Y., Bandrapali, N, et al. 2002. CpeR is an activator required for expression of the phycoerythrin operon (cpeBA) in the cyanobacterium Fremyella diplosiphon and is encoded in the phycoerythrin linker-polypeptide operon (cpeCDESTR). Molecular Microbiology, 44 (6): 1517-1531.

Çetin, D., Gündüz, U., Eroğlu, İ., Yücel, M. and Türker, L. 2006. Poly-β-hydroxybutyrate accumulation and releasing by hydrogen producing bacteria, *Rhodobacter sphaeroides* O.U.001. A transmission electron microscopic study. African Journal of Biotechnology, 5, (22): 2069-2072.

Das, D., Veziroğlu, T.N. 2008. Advances in biological hydrogen production processes. International Journal of Hydrogen Energy, 33: 6046-6057.

Das, D., Veziroğlu, T.N. 2001. Hydrogen production by biological processes: a survey of literature. International Journal of Hydrogen Energy, 26: 13-28.

Das et al. 2006. Role of Fe-hydrogenase in biological hydrogen production. Current Science, 90, (12): 1627-1637.

Dasgupta et al. 2010. Recent trends on the development of photobiological processes and photobioreactors for the improvement of hydrogen production. International Journal of Hydrogen Energy, 35: 10218-10238.

Dixon, R., Kahn, D. 2004. Genetic regulation of biological nitrogen fixation. Nature Reviews Microbiology, 2, (8): 621-631.

Drepper, T., Groß, S., Yakunin, A.F., Hallenbeck, P.C., Masepohl, B., Klipp, W. 2003. Role of GlnB and GlnK in ammonium control of both nitrogenase systems in the phototrophic bacterium *Rhodobacter capsulatus.* Microbiology, 149: 2203-2212.

Eroglu, İ., Aslan, K., Gündüz, U., Yücel, M., Türker L. 1999. Substrate consumption rates for hydrogen production by *Rhodobacter sphaeroides* in a column photobioreactor. Journal of Biotechnology, 70: 103-113.

Eroğlu, E. and Melis, A. 2011. Photobiological hydrogen production: Recent advances and state of the art. Bioresource Technology, 102: 8403-8413.

Franchi, E., Tosi, C., Scolla, G., Penna, G.D., Rodriguez, F. and Pedroni, P.M. 2004. Metabolically Engineered *Rhodobacter sphaeroides* RV strains for Improved Biohydrogen Photoproduction Combined with Disposal Of Food Wastes. Marine Biotechnology, 6: 552-565.

Ghirardi, M.L., Dubini, A., Yu, J.and Maness, PC. 2009. Photobiological hydrogen-producing systems. Chemical Society Reviews, 38: 52-61.

Hallenbeck P.C., Benemann J.R. 2002. Biological hydrogen production; fundamentals and limiting processes. International Journal of Hydrogen Energy, 27: 1185-1193.

Hallenbeck, P.C. and Ghosh, D. 2009. Advances in fermentative biohydrogen production: the way forward? Trends in Biotechnology, 27, (5): 287-297.

Hallenbeck, P.C., Ghosh, D., Skonieczny M.T., Yargeau V. 2009. Microbiological and engineering aspects of biohydrogen production. Indian Journal of Microbiology, 49: 48-59.

Halbleib, C. M., Ludden, P. W. 2000. Regulation of Biological Nitrogen Fixation. Journal of Nutrition, 132,(12): 1081-1084.

Hallenbeck, P.C., Ghosh, D. 1987. Molecular aspects of nitrogen fixation by photosynthetic prokaryotes. Critical Reviews in Microbiology, 14, (1): 1-48.

Holladay, J.D., Hu, J., King, D.L., Wang, Y. 2009. Catalysis Today, 139: 244-260.

Hustede, E., Steinbüchel, A., Schlegel H.G. 1993. Relationship between the photoproduction of hydrogen and accumulation of PHB in non-sulfur bacteria. Appl Microbiol Biotechnology, 103: 187-194.

Igarashi, R. Y., Seefeldt, L. C. 2003. Nitrogen fixation: the mechanism of the mo-dependent nitrogenase. Critical Reviews in Biochemistry and Molecular Biology**,** 38: 351–384.

Imhoff, F.J. 1995. Taxonomy and physiology of phototropic purple bacteria and green sulfur bacteria. Anoxygenic Photosynthetic Bacteria, 2: 1-15.

Imhoff, J.F., Truper, H.G., Pfenning, N. 1984. Rearrangement of the species and genera of the phototrophic purple nonsulfur bacteria. International Journal of Systemetic Bacteriology, 34: 240-343.

Imhoff J.F. 2006. The Phototrophic Alpha-Proteobacteria. Prokaryotes, 5: 41-64.

Jendrossek, D. 2001. Microbial degradation of polyesters. Adv Biochem Eng Biotechnol, 71: 293-325.

Kapdan, I.K., Kargi, F. 2006. Bio-hydrogen production from waste materials. Enzyme and Microbial Technology, 38: 569-582.

Kars, G., Gündüz, U., Yücel, M., Rakhely, G., Kovacs, K.L., Eroğlu, İ. 2006. Evaluation of hydrogen production by *Rhodobacter sphaeroides* O.U.001 and its *hup*SL deficient mutant using acetate and malate as carbon sources. International Journal of Hydrogen Energy, 9, (34): 2184-2190.

Kars, G., Gündüz, U., Yücel, M., Türker, L., Eroğlu, İ. 2006. Hydrogen production and transcriptional analysis of *nif*D, *nif*K and *hup*S genes in *Rhodobacter sphaeroides* O.U.001 grown in media with different concentrations of molybdenum and iron. International Journal of Hydrogen Energy, 31: 1536-1544.

Kars, G., Gündüz U. 2010. Towards a super H_2 producer: Improvements in photofermentative biohydrogen production by genetic manipulations. International Journal of Hydrogen Energy, 35, (13): 6646-6656.

Kemavongse K., Prasertsan P., Upaichit A., Methacanon P. 2008. Poly-β-hydroxyalkanoate production by halotolerant *Rhodobacter sphaeroides* U7. World J Microbial Biotechnology, 24: 2073-2085.

Kemavongse, K., Prasertsan, P., Upaichit, A., Methacanon, P. 2007. Effect of cosubstrate on production of poly-beta-hydroxybutyrate (PHB) and copolymer PHBV from newly identified mutant *Rhodobacter sphaeroides* U7 cultivated under aerobic-dark condition. Songklanakarin Journal of Science and Technology, 29, (4): 1101-1113.

Kessler, B., Witholt, B. 2001. Factors involved in the regulatory network of polyhydroxyalkanoate metabolism. Journal of Biotechnology, 86: 97-104.

Khatipov, E., Miyake, M., Miyake, J.,Asada, Y. 1998. Accumulation of poly- β-hydroxybutyrate by *Rhodobacter sphaeroides* on various carbon and nitrogen sources. FEMS Microbiology Letters, 162: 39-45.

Kim, MS., Baek J.S., Lee J.K.. 2006. Comparison of H_2 accumulation by *Rhodobacter sphaeroides* KD131 and its uptake hydrogenase and PHB synthase deficient mutant. International Journal of Hydrogen Energy, 31, (1): 121-127.

Kim, MS., Kim, DH., Son HN., Ten L.H., Lee J.K. 2011. Enhancing photo-fermentative hydrogen production by *Rhodobacter sphaeroides* KD131 and its PHB synthase deleted-mutant from acetate and butyrate. International Journal of Hydrogen Energy, 36: 3964-13971.

Koku, H., Eroğlu, I., Gündüz, U., Yücel, M., Türker, L. 2002. Aspects of the metabolism of hydrogen production by Rhodobacter sphaeroides. International Journal of Hydrogen Energy, 27: 1315-1329.

Koku, H., Eroğlu, İ., Gündüz U., Yücel M., Türker L. 2003. Kinetics of biological hydrogen production by the photosynthetic bacterium *Rhodobacter sphaeroides* O.U. 001. International Journal of Hydrogen Energy, 28: 381-388.

Kothari, R., Buddhi, D., Sawhney R.L. 2008. Comparison of environmental and economic aspects of various hydrogen production methods. Renewableand Sustainable Energy Reviews, 12: 553-563.

Kovács, K.L., Marótia, G., Rákhelya, G. 2006. A novel approach for biohydrogen production. International Journal of Hydrogen Energy, 31: 1460-1468.

Kovacs, K.L., Bagyinka, C., Bodrossy, L., Csaki, R., Fodor, B., Györfi, K., Hanczar, T., Kalman, M., Osz, J., Perel, K., Polyak, B., Rakhely, G., Takacs, M., Toth, A., Tusz, J. 2000. Recent advances in biohydrogen research. European Journal of Physiology, 439: 81-83.

Kranz, R.G., Gabbert K.K., Locke, T.A. and Madigan, M.T. 1997. Polyhydroxyalkanoate Production in *Rhodobacter capsulatus*: Genes, Mutants, Expression, and Physiology. Applied and Environmental Microbiology, 63, (8): 3003-3009.

Lee, HS., Vermaas, F.J.W. and Ritmann, B.E. 2010. Biological hydrogen production: prospects and challenges. Trends in Biotechnology, 28, (5): 262-271.

Lee, SY. 1996. Bacterial Polyhydroxyalkanoates. Biotechnology and Bioengineering, 49: 1-14.

Levin, D.B, Pitt, L., Love, M. 2004. Biohydrogen production: prospects and limitations to practical application. International Journal of Hydrogen Energy, 29: 173 – 185.

Lorrungruang C., Martthong J., Sasaki K., Noparatnaraporn N. 2006. Selection of Photosynthetic Bacterium *Rhodobacter sphaeroides* 14F for Polyhydroxyalkanoate Production with Two-Stage Aerobic dark Cultivation. Journal of Bioscience and Bioengineering, 102, (2): 128-131.

Luengo, J.S., Garcia, B., Sandoval A., Naharro, G. and Olivera, E.R. 2003. Bioplastics from microorganisms. Current Opinion in Microbiology, 6: 251-260.

Madigan, Michael T., and John M. Martinko. 2006. Pearson Prentice Hall.

Maehara, A., Ueda, S., Nakano, H., Yamane, T. 1999. Analyses of polyhydroxyalkanoic acid granule-associated 16-kilodalton protein and its putative regulator in the *pha* locus of *Paracoccus denitrificans.* Journal of Bacteriology,181: 2914-2921.

Masepohl, B., Drepper, T., Klipp, W. 2004. Genetics and regulation of nitrogen fixation in free-living bacteria (Klipp W; Masepohl B; Gallon J R and Newton W E; editors.),141-173, Kluwer Academic Publishers, Netherlands.

Masepohl, B., Drepper, T., Paschen, A., Groß, S., Pawlowski, A., Raabe, K., Riedel, K., Klipp, W. (2002). Regulation of nitrogen fixation in the phototrophic purple bacterium *Rhodobacter capsulatus*. *Journal of Molecular Microbiology and Biotechnology* 4,3, 243-248.

Matsusaki, H., Manji, S., Taguchi, K., Kato, M., Fukui, T., Doi, Y. 1998. Cloning and molecular analysis of the poly(3-hydroxybutyrate) and poly(3-hydroxybutyrate-co-3-hydroxyalkanoate) biosynthesis genes in *Pseudomonas* sp. Strain 61-3. Journal of Bacteriology, 180: 6459-6467.

Meister, M., Saum, S., Alber, B.E., Fuchs, G. 2005. L-malyl-coenzyme A/beta-methylmalyl-coenzyme A lyase is involved in acetate assimilation of the isocitrate lyase-negative bacterium *Rhodobacter capsulatus*. Journal of Bacteriology, 187, (4): 1415-1425.

Meherkotay, S., Das, D. 2008. Biohydrogen as a renewable energy resource-Prospects and potentials. International Journal of Hydrogen Energy, 33: 258-263.

Melis, A. 2002. Green algae hydrogen production: progress, challenges and prospects. International Journal of Hydrogen Energy, 27: 1217-1228.

Melis, A. and Melnicki M.R. 2006. Integrated biological hydrogen production. International Journal of Hydrogen Energy, 3: 1563-1573.

Mu, Y., Yu, HQ., Wang G. 2007. A kinetic approach to anaerobic hydrogen-producing process. Water Research, 41: 1152-1160.

Mukhopadhyay, M., Patra, A. and Paul, A.K. 2005. Production of poly(3-hydroxybutyrate) and poly(3-hydroxybutyrate-co-3-hydroxy-valerate) by *Rhodopseudomonas palustris* SP5212. World Journal of Microbiology*and* Biotechnology, 21: 765-769.

Miyake, J. 1990. Application of photosynthetic systems for energy conversion". In: Veziroglu T N, Takashashi P K (editors). Hydrogen energy progress VIII. Proceedings 8th WHEC held in Hawaii. New York, Elsevier Science Pub Co 755–764.

Miyamoto, K. 1997. Renewable biological systems for alternative sustainable energy production. FAO Agricultural Services Bulletin (edited by Miyamoto K), Food and Agriculture Organization of the United Nation, 1-5

Miyamoto, C.M., Sun, W.Q., Meighen, E.A. 1998. The LuxR regulator protein controls synthesis of polyhydroxybutyrate in *Vibrio harveyi.* BBA Protein Struct. Mol. Enzym., 1384: 356-364.

Momirlan, M.,Veziroğlu, T.N. 2002. Current status of hydrogen energy. Renewable and Sustainable Energy Reviews, 6: 141-179.

Naik, S., Gopal, S.K.V., Somal P. 2008. Bioproduction of polyhdroxyalkoates from bacteria: a metabolic approach. World J Microbial Biotechnology, 24: 2307-2314.

Nath, K., Das, D. 2004. Improvement of fermentative hydrogen production: various Approaches. Appl. Microbiol. Biotechnol., 65: 520–529.

Nath, K., Muthukumar M., Kumar A., Das Debabrata D. 2008. Kinetics of two-stage fermantation process for the production of hydrogen. International Journal of Hydrogen Energy, 33: 1195-1203.

Ni, M., Leung, D.Y.C., Leung, M.K.H., Sumathy, K. 2006. An overview of hydrogen production from biomass. Fuel Processing Technology, 87: 461-472.

Özgür, E., Uyar, B., Öztürk, Y., Yücel, M., Gündüz, U., Eroğlu, İ. 2010. Biohydrogen production by *Rhodobacter capsulatus* on acetate at fluctuating temperatures. Resources, Conservation and Recycling, 54: 310-314.

Özgür, E., Afşar, N., Vrije, T., Yücel, M., Gündüz, U., Claassen A.M.P., Eroğlu İ. 2010. Potential use of thermophilic dark fermentation effluents in photofermentative hydrogen production. Journal of Cleaner Production, 18: 23-28.

Öztürk, Y., Yücel, M., Daldal, F., Mandacı, S., Gündüz, U., Türker, L., Eroğlu, I. 2006. Hydrogen production by using *Rhodobacter capsulatus* mutants with genetically modified electron transfer chains. International Journal of Hydrogen Energy, 31: 1545 –1552.

Pekgöz, G. 2010. Deletion Mutation of *glnB* and *glnK* Genes in *Rhodobacter capsulatus* to Enhance Biohydrogen Production. Msc Thesis in Biotechnology Department, Middle East Technical University, Ankara, Turkey.

Pellerin, N.B., and Gest, H. 1983. Diagnostic Features of the Photosynthetic Bacterium Rhodopseudomonas sphaeroides. Current Microbiology, 9: 339-344.

Philippis, RD., Ena, A., Guastini, M., Sili, G., Vincenzini, M. 1992. Factors affecting poly-β-hydroxybutyrate accumulation in cyanobacteria and in purple non-sulfur bacteria. FEMS Microbiology Reviews, 103: 187-194.

Reddy, C.S.K., Ghai, R., Kalia R.V.C. 2003. Polyhydroxyalkanoates: an overview. Bioresource Technology, 87: 137-146.

Rees, D.C. and Howard J.B. 2000. Nitrogenase: standing at the crossroads. Current Opinion in Chemical Biology, 4: 559-566.

Rehm, B.H.A. 2006. Genetics and biochemistry of polyhydroxyalkanoate granule self-assembly: The key role of polyester synthases. Biotechnology Letters, 28: 207-213.

Rehm, B.H.A. 2003. Polyester synthases: natural catalysts for plastics. Biochemical Journals, 376: 15-33.

Rehm, B.H.A., Steinbüchel, A. 1999. Biochemical and genetic analysis of PHA synthases and other proteins required for PHA synthesis. International Journal of Biological Macromolecules, 25: 3-19.

Ribbe, M., Gadkari, D., and Meyer, O. 1997. N_2 fixation by *Streptomyces thermoautotrophicus* involves a molybdenum-dinitrogenase and a manganese-superoxide oxidoreductase that couple N_2 reduction to the oxidation of superoxide produced from O_2 by a molybdenum-CO dehydrogenase. J Biol Chem, **272**, 26627-26633.

Rosen, M.A., Scott, D.S. 1992. Hydrogen energy progress IX, Proceedings of the Ninth World Hydrogen Energy Conference. Paris (France), 1992: 457.

Sangkharak K., Prasertsan P. 2007. Optimization of polyhydroxybutyrate production from a wild type adn two mutant strains of *Rhodobacter sphaeroides* using statictical method. Journal of Bacteriology, 132: 331-340.

Sasikala, K., Ramana, C.H., Rao, P.R. 1991. Environmental regulation for optimal biomass yield and photoproduction of hydrogen by *Rhodobacter sphaeroides* O.U.001. International Journal of Hydrogen Energy, 16: 597-601.

Sasikala, K., Ramana, C.V., Rao, P.R., Kovacs, K.L. 1993. Anoxygenic phototropic bacteria: physiology and advances in hydrogen technology. Advances in Applied Microbiology,10: 211–215.

Sevinç, P. (2010). Kinetic Analyses of the Effects of Temperature and Light Intensity on Growth, Hydrogen Production, and Organic Acid Utilization by *Rhodobacter capsulatus.* Msc Thesis in Biotechnology Department, Middle East Technical University, Ankara, Tu

Siemann, S., Schneider, K., Dröttboom**,** M., and Müller, A. 2002. The Fe-only nitrogenase and Mo nitrogenase from *Rhodobacter capsulatus*. A comparative study on the redox properties of the metal clusters present in the dinitrogenase components. Eur J. Biochem 269: 1650–1661.

Shi, X.Y.*and* Yu H.Q. 2006. Conversion of individual and mixed volatile fatty acids to hydrogen by *Rhodopseudomonas capsulata*. International Biodeterioration*and* Biodegradation, 58: 82-88.

Steinbüchel, A. and Füchtenbusch, B. 1998. Bacterial and other biological systems for polyester production. Trends Biotechnology, 16: 419-427.

Sudesh, K., Abe, H., Doi, Y. 2000. Synthesis, structure and properties of polyhydroxyalkonates: biological polyesters. Progress in Polymer Science, 25: 1503-1555.

Sun, J., Peng, X., van Impe, J., van der Leyden, J. 2000. The *ntr B* and *ntr C* genes are involved in the regulation of poly-3-hydroxybutyrate biosynthesis by ammonia in *Azospirillum brasilense* Sp7. Appl. Environ. Microbiol, 66: 113-117.

Suriyamongkol, P., Weselake, R., Narine, S., Moloney, M., Shah, S. 2007. Biotechological approaches for the production of polyhydroxyalkanoates in microorganisms and plants- A review. Biotechnological Advances, 25: 148-175.

Sybesma, W., Hugenholtz, J., Mierau, I., Kleerebezem M. 2001. Improved efficiency and reliability of RT-PCR using tag-extended RT primers and temperature gradient PCR. Biotechniques, 31: 466-472.

Trotsenka Y.A., Belova L.L. 2000. Biosysnthesis of Poly-(3-Hydroxybutyrate) and Poly(3-Hydroxybutyrate-*co*-3-Hydroxyvalerate) and its regulation in bacteria. Microbiology, 69, (6): 635-645.

Timm, A., Steinbüchel, A. 1992. Cloning and molecular analysis of the poly (3-hydroxyalkanoic acid) gene locus of *Pseudomonas aeruginosa* PAO1. Eur.J.Biochem., 209: 15-30.

Uyar, B., Eroğlu, İ., Yücel, M., Gündüz, U. 2009. Photofermentative hydrogen production from volatile fatty acids present in dark fermentation effluents. International Journal of Hydrogen Energy, 34: 4517-4523.

Uyar, B. 2008. Hydrogen Production by Microorganisms in Solar Bioreactor, Ph.D. Thesis in Biotechnology Engineering Department, Middle East Technical University, Ankara, Turkey.

Wang, J., Wan W. 2009. Kinetic models for fermentative hydrogen production: A review. International Journal of Hydrogen Energy, 34: 3313-3323.

Yang, CF., Lee, CM. 2011. Enhancement of photohydrogen production using *phbC* deficient mutant *Rhodopseudomonas palustris* strain M23. Bioresource Technology, 102: 5418-5424.

Jung, Y-M., Park, J-S., Lee, Y-H. 2000. Metabolic engineering of *Alcaligenes eutrophus* through the transformation of cloned *phb*CAB genes for the investigation of the regulatory mechanism of polyhydroxyalkanoate biosynthesis. Enzyme and Microbial Technology, 26: 201-208.

Zinn, M., Witholt, B., Egli, T. 2001. Occurrence, synthesis and medical application of bacterial polyhydroxyalkanoate. Advanced Drug Delivery Reviews, 53: 5-21.

Zhang, Y., Pohlmann, E.L., Ludden, P.W., Roberts, G.P. 2000. Mutagenesis and functional characterization of the *glnB, glnA,* and *nifA* genes from the photosynthetic bacterium *Rhodospirillum rubrum.* Journal of Bacteriology, 182, (4): 983-992.

APPENDIX A

COMPOSITION OF THE MEDIA AND THE SOLUTIONS

Table A.1 Composition of the growth medium (20 mM Acetate /10 mM Glutamate)

Component	Growth Medium
KH_2PO_4 (22 mM)	3g/L
$MgSO_4$. $7H_2O$	0.5 g/L
$CaCl_2$. $2H_2O$	0.05 g/L
Acetate (20 mM)	1.15 ml/L
Na-glutamate (10 mM)	1.85 g/L
Vitamin solution (10X)	0.1 ml/L
Fe- Citrate (50X)	0.5 ml/L
Trace elements (10X)	0.1 ml/L

Table A.2 Composition of the hydrogen production medium (30 mM Acetate /2 mM Glutamate)

Component	Growth Medium
KH_2PO_4 (22 mM)	3g/L
$MgSO_4$. $7H_2O$	0.5 g/L
$CaCl_2$. $2H_2O$	0.05 g/L
Acetate (30 mM)	1.72 ml/L
Na-glutamate (2 mM)	0.36 g/L
Vitamin solution (10X)	0.1 ml/L
Fe- Citrate (50X)	0.5 ml/L
Trace elements (10X)	0.1 ml/L

Table A.3 Composition of trace element solution (10X)

Component	Amount
$ZnCl_2$	700 mg/L
$MnCl_2.4H_2O$	1000 mg/L
H_3BO_3	600 mg/L
$CoCl_2.6H_2O$	2000 mg/L
$CuCl_2.2H_2O$	200 mg/L
$NiCl_2.6H_2O$	200 mg/L
Na_2MoO_4. $2H_2O$	400 mg/L
HCl (25 % v/v)	10 ml/L

Table A.4 Composition of vitamin solution (10X)

Component	Amount
Thiamin chloride hydrochloride	5 g/L
Niacin (Nicotinic acid)	5 g/L
D+ Biotin	0.15 g/L

Ferric Citrate Solution (50X) :

5 g ferric citrate is dissolved in 100 mL distilled water.

Trace element and ferric citrate solutions were sterilized by autoclaving whereas vitamin solution was sterilized by using sterile filters.

Table A.5 Composition of Liquid MPYE-Medium (Enriched Medium)

Component	Amount
Bacto-pepton	3 g/L
Yeast extract	3 g/L
$MgCl_2$ (1M)	1.6 ml
$CaCl_2$ (1M)	1 ml

pH is adjusted to 7. by adding 5 M NaOH.

For preparation of solid MPYE medium 15 g agar is added to 1 L liquid MPYE medium.

Solutions and Buffers

TAE

40 mM Tris base (Buffer grade)

1mM EDTA disodium dihydrate

Glacial acetic acid

Ethidium Bromide

10 mg EtBr is dissolved in 1 ml distilled water.

APPENDIX B

OPTICAL DENSITY-DRY CELL WEIGHT CALIBRATION CURVE

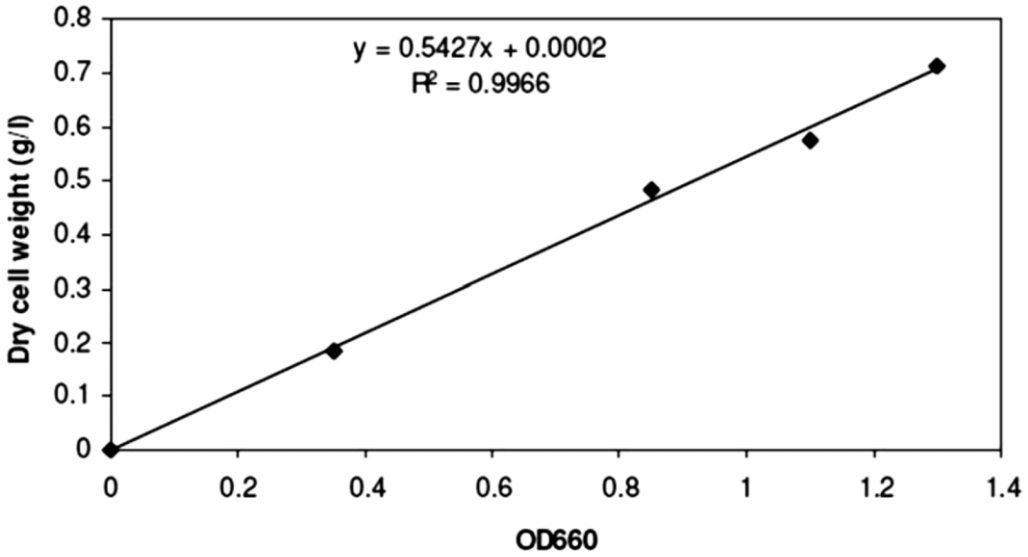

Figure B.1 Calibration curve and the regression trend line for *Rhodobacter capsulatus (*DSM 1710) dry weight versus OD660 (Uyar, 2008).

APPENDIX C

SAMPLE GAS CHROMATOGRAM

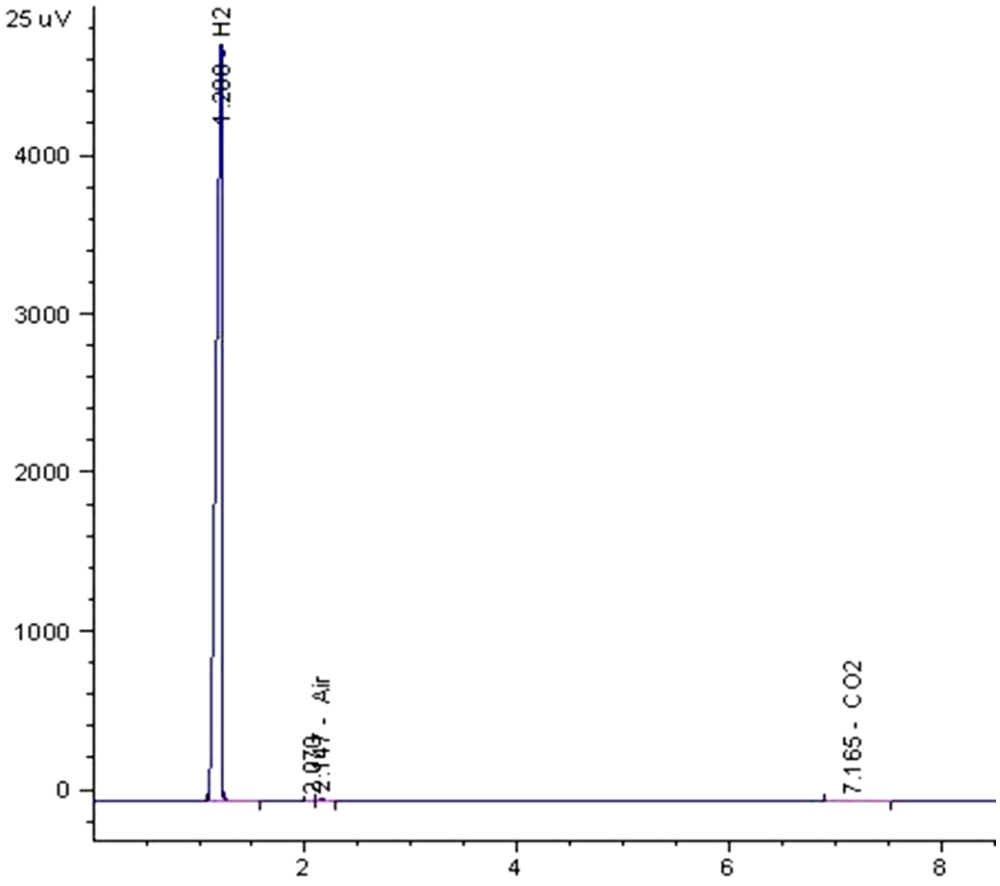

RetTime [min]	Type	Area [25 uV*s]	Amt/Area	Norm %	Grp	Name
1.208	BB	1.78157e4	5.36760e-3	92.790983		H2
2.147	VB	104.16668	4.30476e-2	4.351104		Air
7.165	BB	52.88443	5.56929e-2	2.857913		CO2
Totals :				100.000000		

Figure C.1 A sample chromatogram for GC analysis of the collected gas (Pekgöz, 2010).

APPENDIX D

ORGANIC ACID ANALYSIS

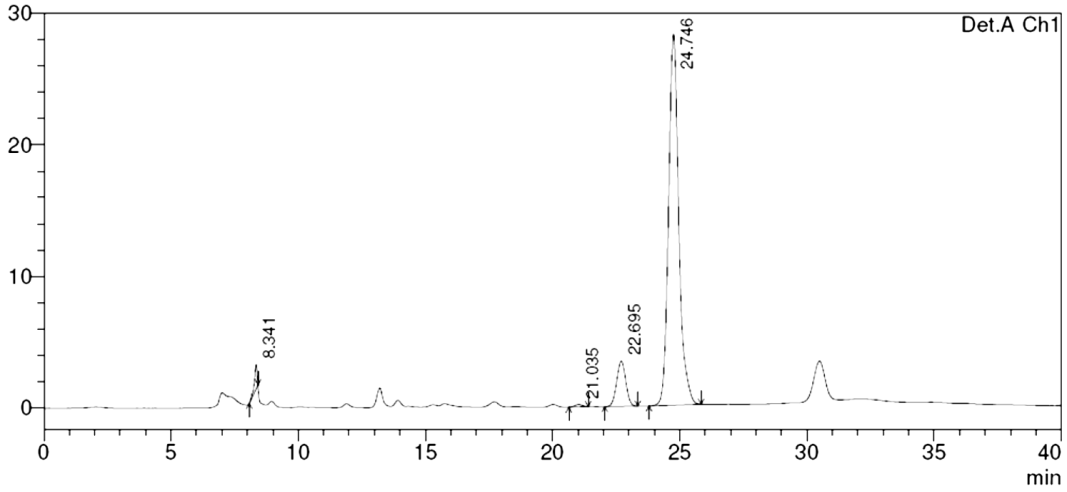

PeakTable

Detector A Ch1 210nm

Peak#	Ret. Time	Area	Height	Area %	Height %
1	8.341	14689	1859	1.654	5.516
2	21.035	3735	182	0.420	0.542
3	22.695	86422	3453	9.730	10.248
4	24.746	783359	28200	88.196	83.694
Total		888205	33695	100.000	100.000

Figure D.1 A Sample HPLC analysis chromatogram. Peak 1 (mobile phase- H2SO4), Peak 2 (lactic acid), Peak 3 (formic acid) and Peak 4 (acetic acid) (Pekgöz, 2010).

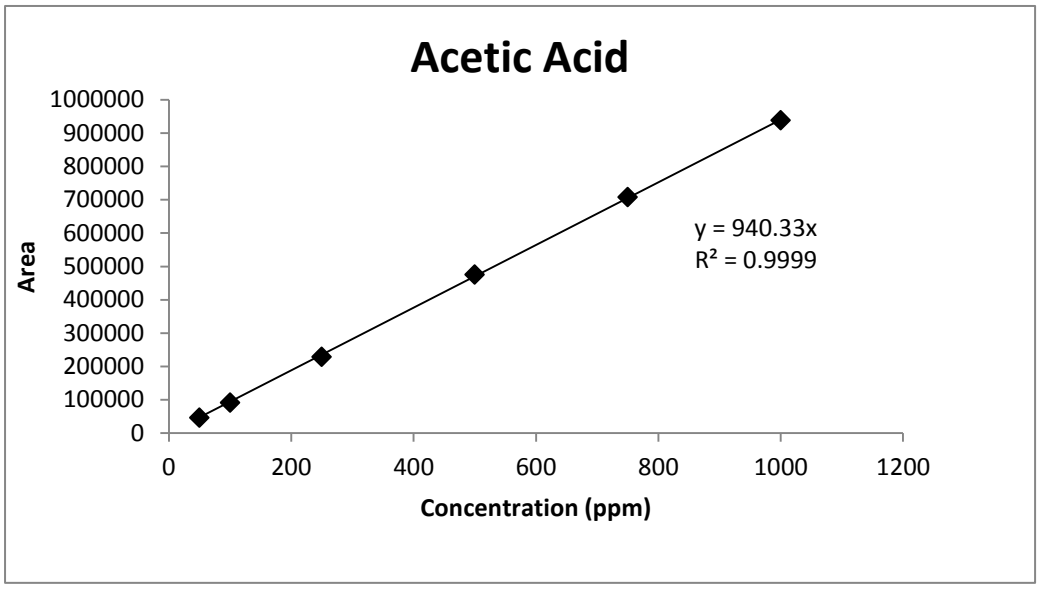

Figure D.2 Sample acetic acid calibration curve

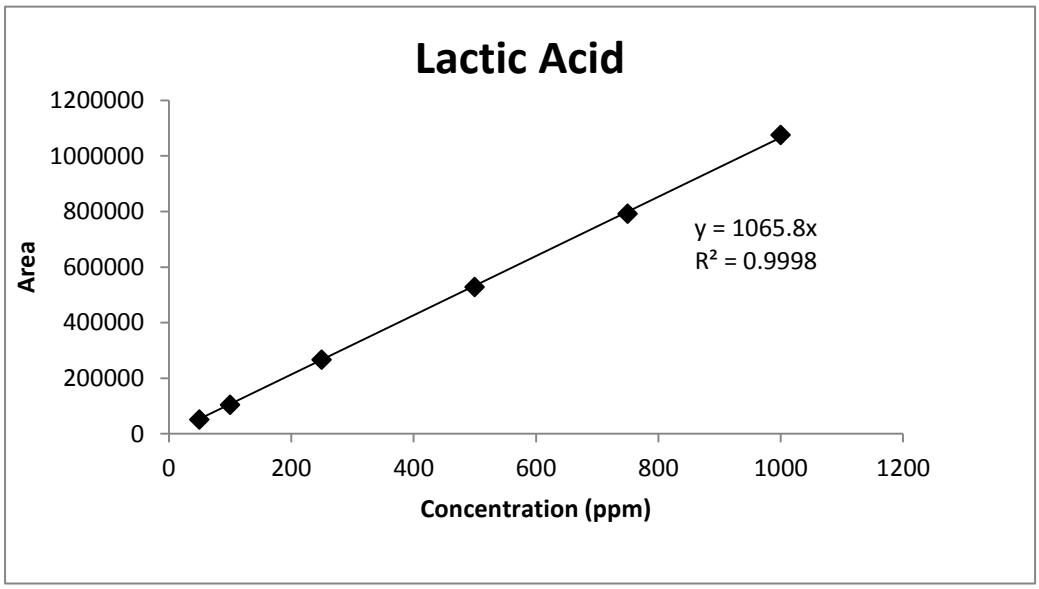

Figure D.3 Sample lactic acid calibration curve.

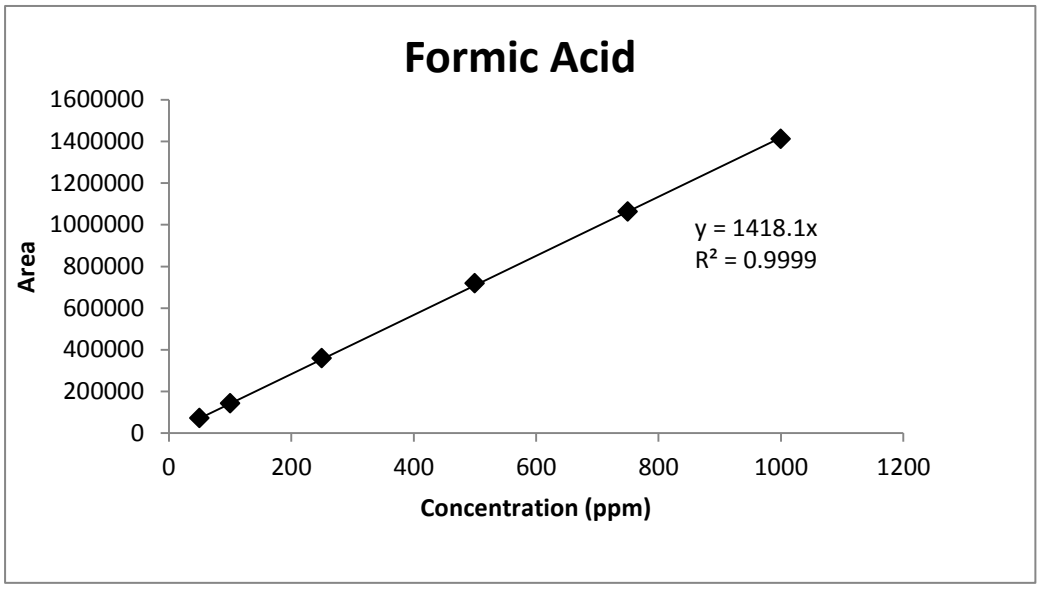

Figure D.4 Sample formic acid calibration curve.

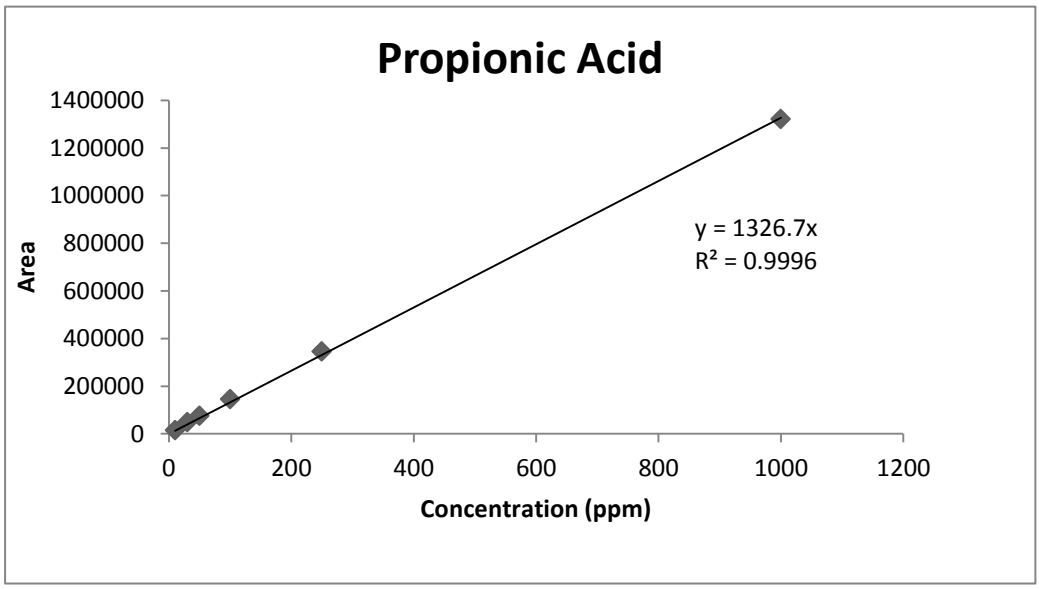

Figure D.5 Sample propionic acid calibration curve.

APPENDIX E

PHB MEASUREMENT

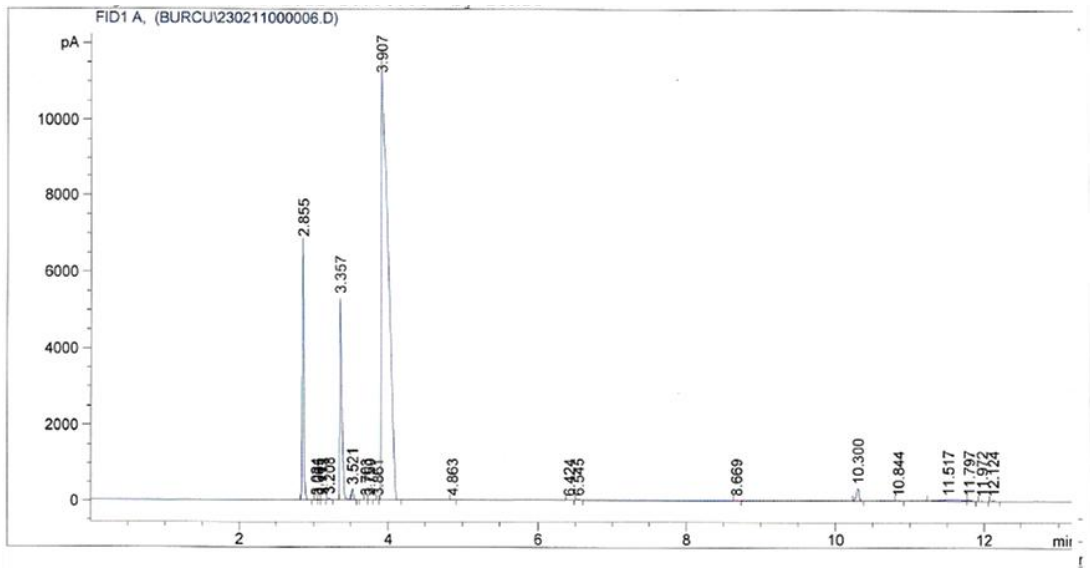

Figure E.1 Sample GC chromatogram for PHB analysis. Retention time of PHB is 10.3 minutes.

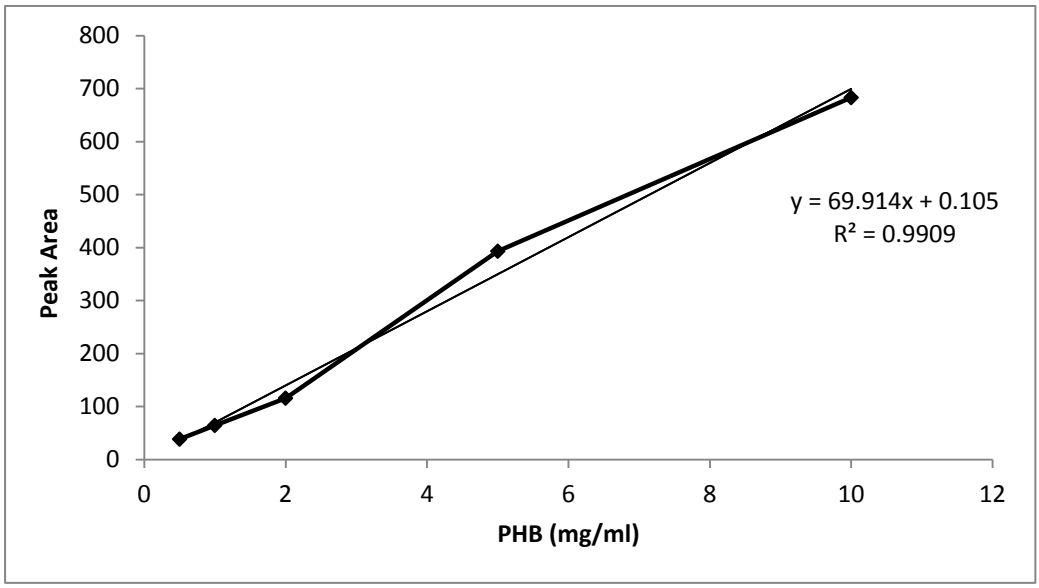

Figure E.2 Sample calibration curve for PHB measurement.

APPENDIX F

LOGISTIC MODEL

F1-F3. Curves fitted to the Logistic Model for growth of *R.capsulatus* at different acetate concentrations.

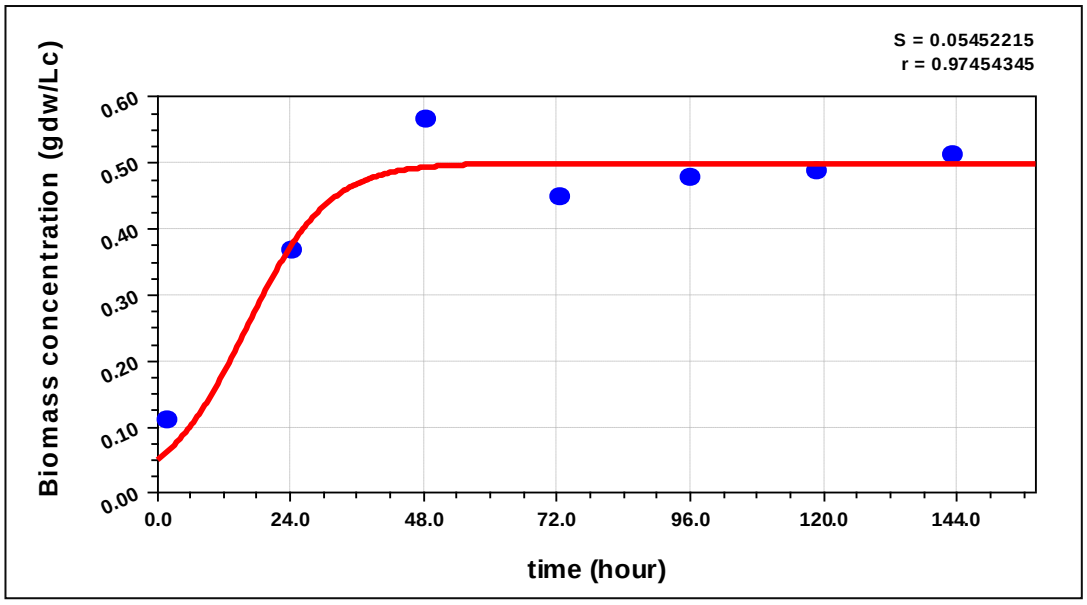

Figure F.1 The Logistic Growth Model of *R.capsulatus* at 10 mM initial acetate concentration.

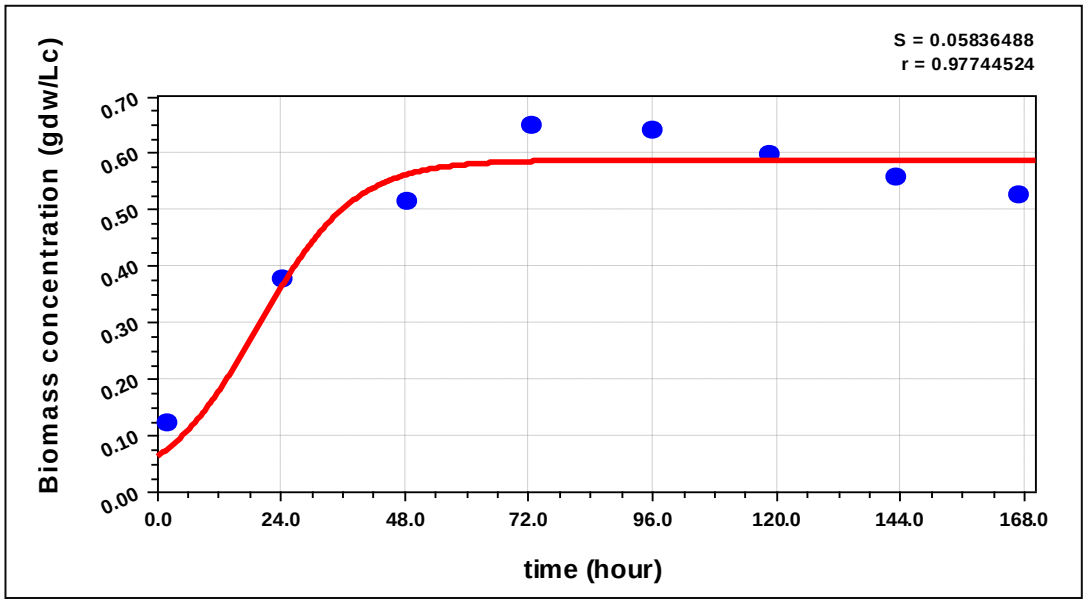

Figure F.2 The Logistic Growth Model of *R.capsulatus* at 25 mM initial acetate concentration.

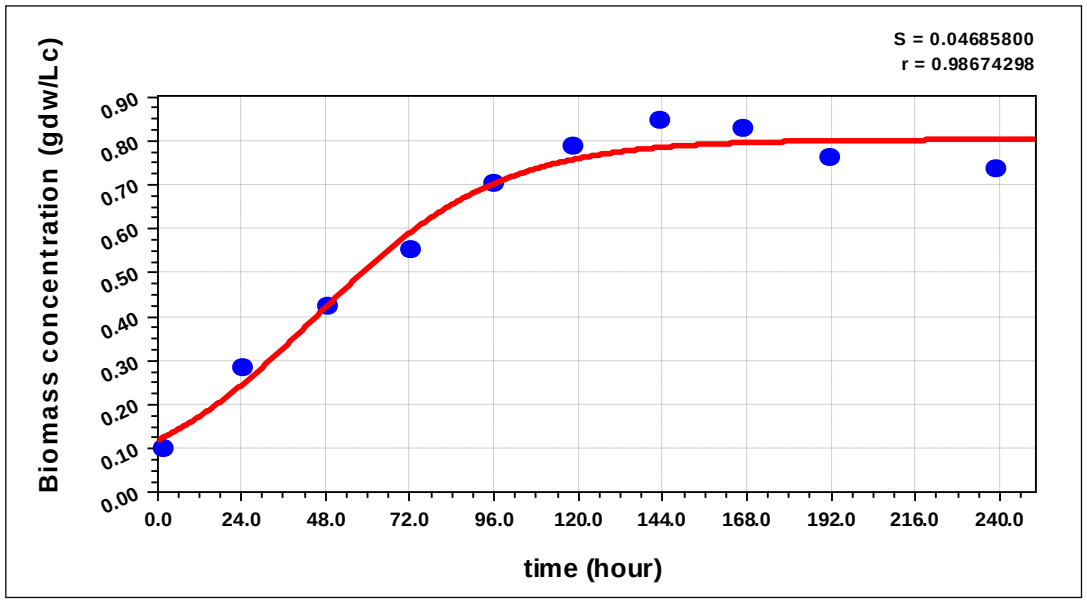

Figure F.3 The Logistic Growth Model of *R.capsulatus* at 65 mM initial acetate concentration.

APPENDIX G

MODIFIED GOMPERTZ MODEL

G1-G3. Curves fitted to the Modified Gompertz Model for hydrogen production of *R.capsulatus* at different acetate concentrations.

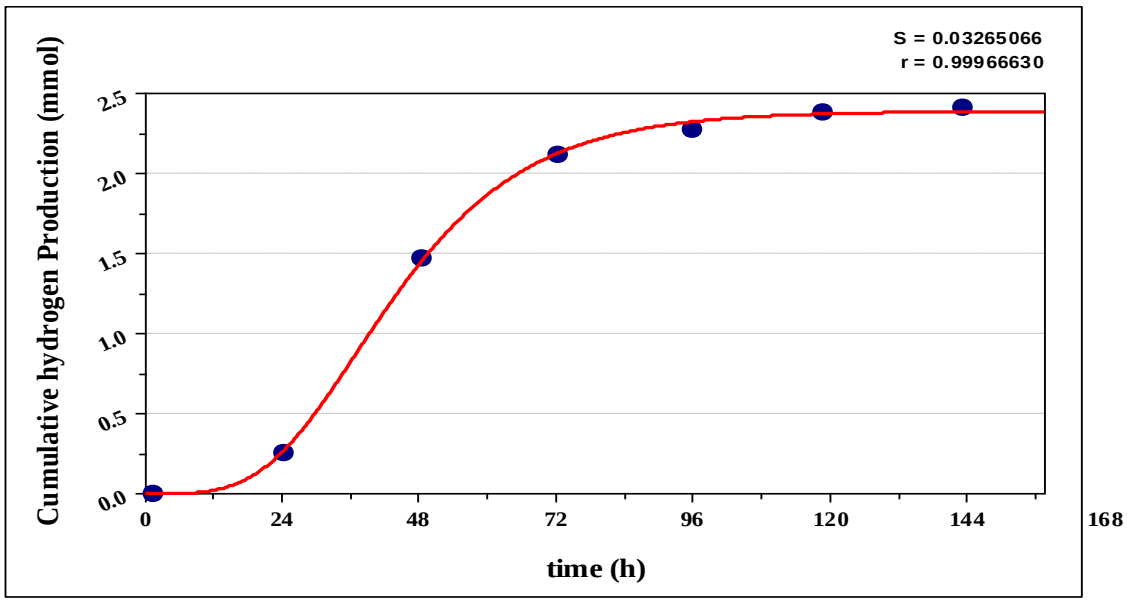

Figure G.1 The Modified Gompertz Model of *R.capsulatus* at 10 mM initial acetate concentration.

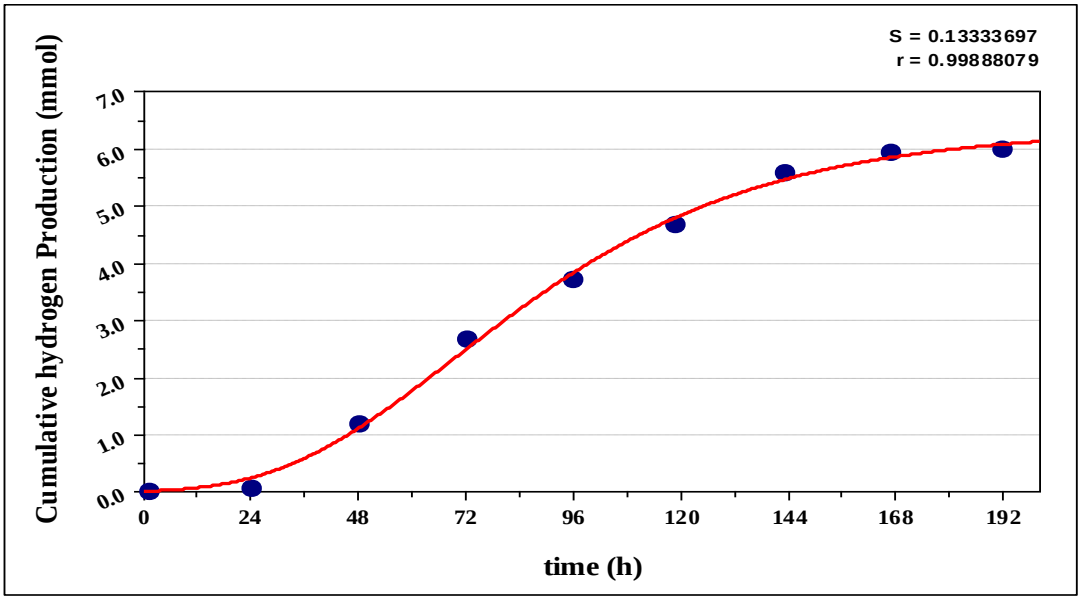

Figure G.2 The Modified Gompertz Model of *R.capsulatus* at 25 mM initial acetate concentration.

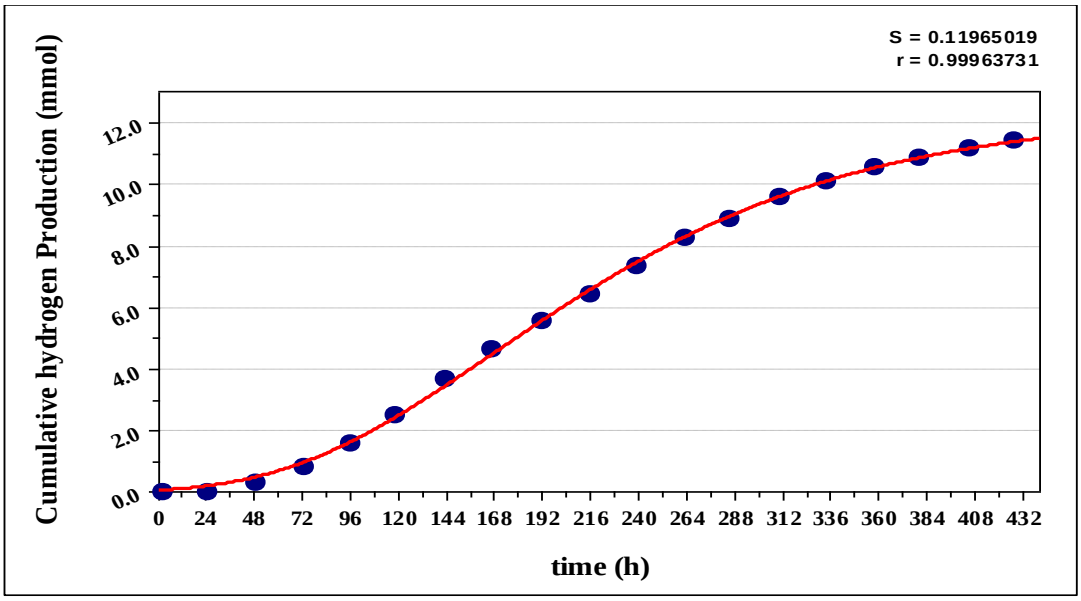

Figure G.3 The Modified Gompertz Model of *R.capsulatus* at 65 mM initial acetate concentration.

APPENDIX H

ACETIC ACID CONSUMPTION KINETICS

H1-H3. Acetic acid consumption kinetics of *R.capsulatus* at different acetate concentrations.

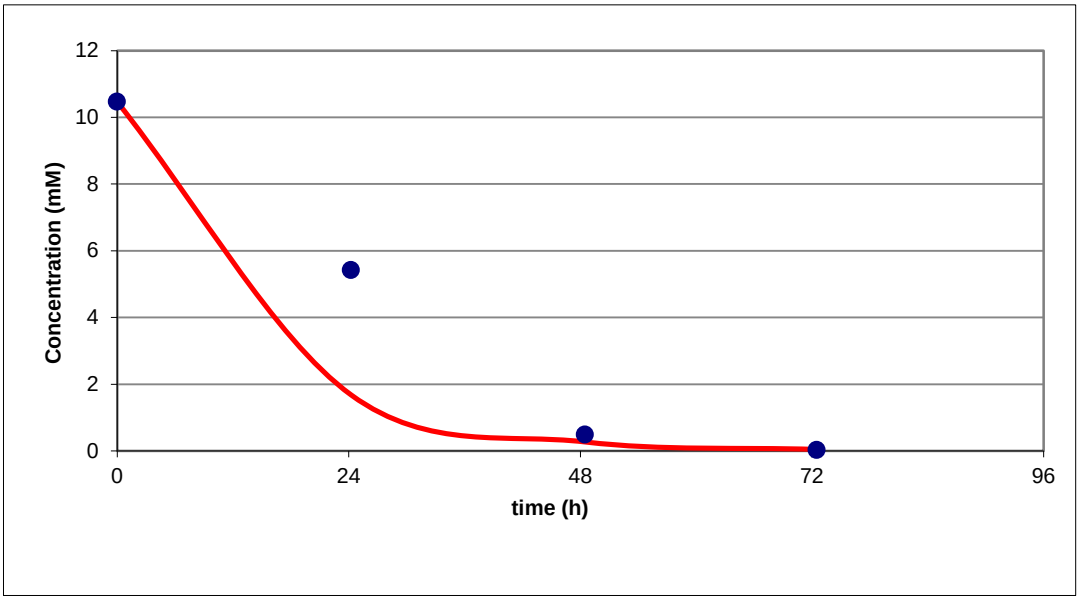

Figure H.1 First order kinetics for acetate consumption at 10 mM initial acetate concentration.

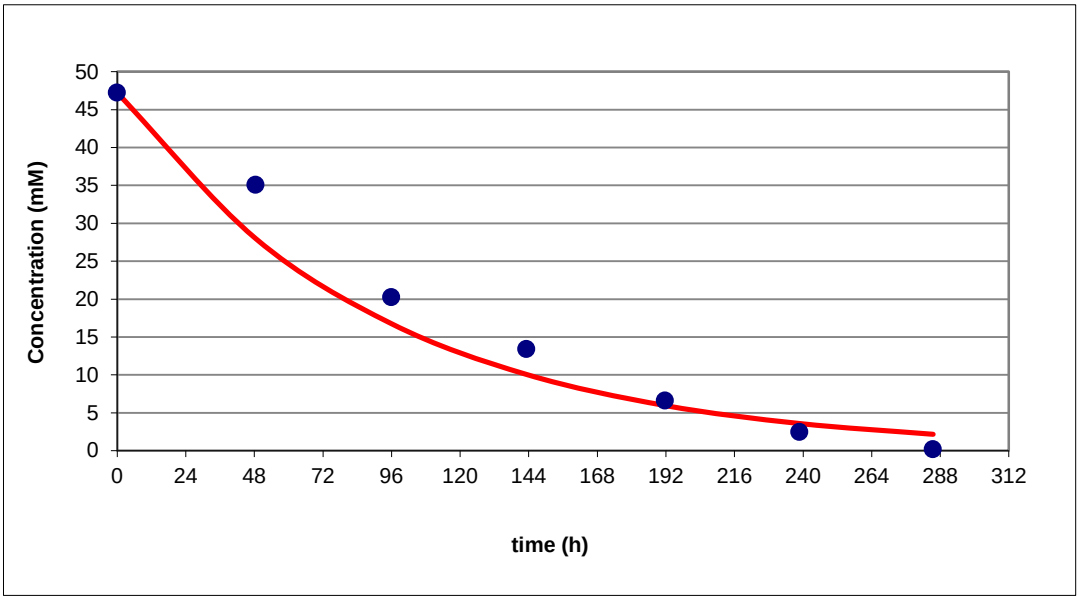

Figure H.2 First order kinetics for acetate consumption at 50 mM initial acetate concentration.

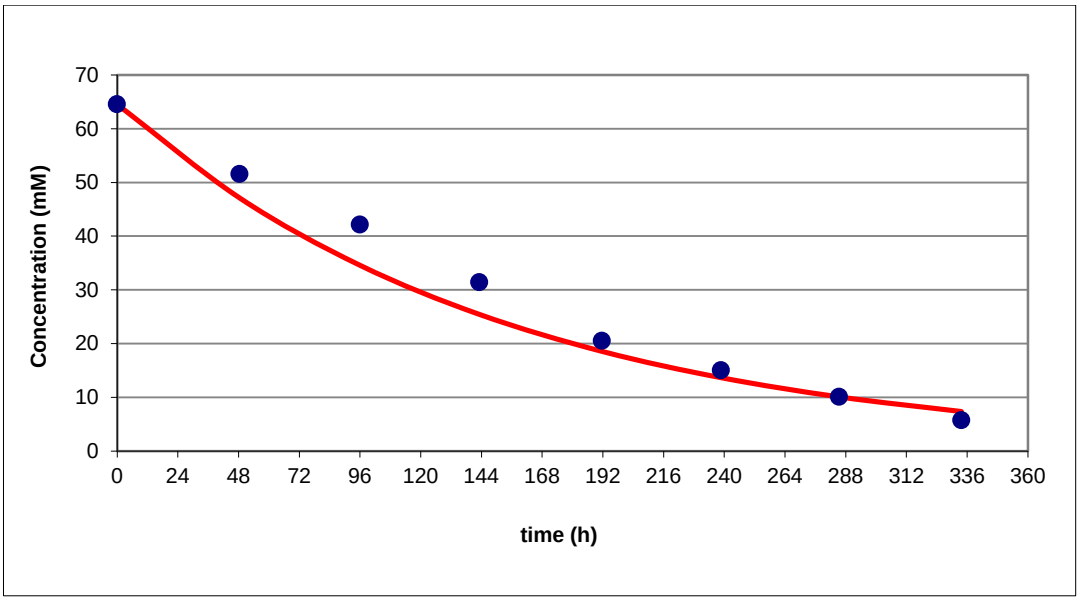

Figure H.3 First order kinetics for acetate consumption at 65 mM initial acetate concentration.

APPENDIX I

RNA ISOLATION

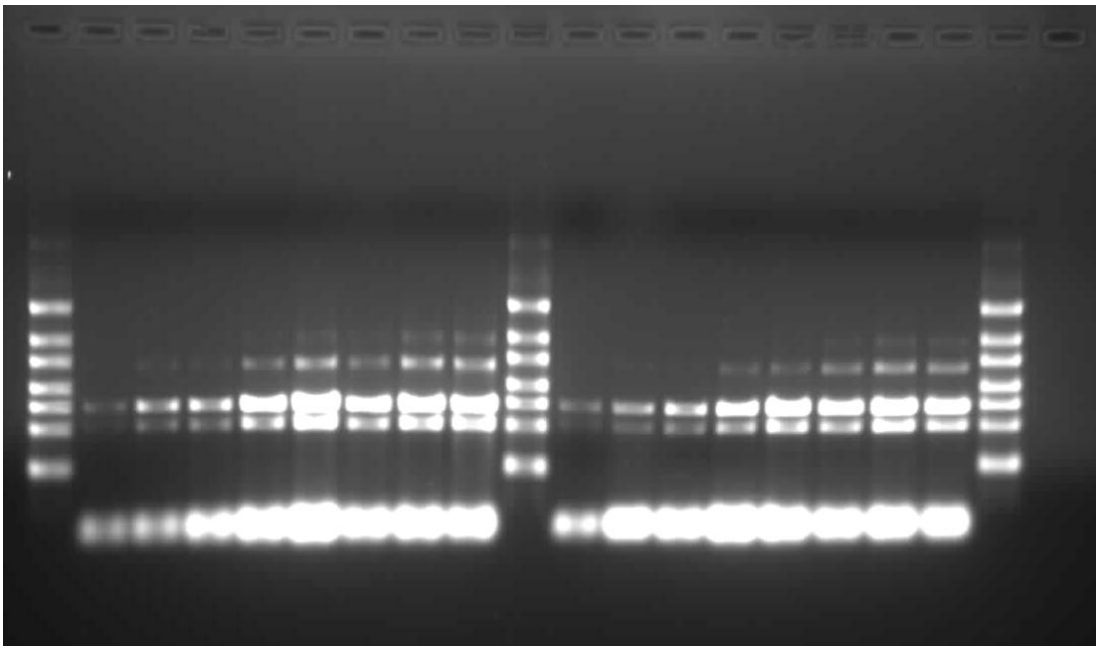

Figure I.1 Agarose gel electrophoresis (1 %) of isoaleted RNA samples.